Spring 2013

Molecular Insights into the Distinct Mechanisms Regulating the TLR4 Mediated Activation, Shut Down, and Endotoxin Tolerance of the IL1B and TNF Genes

Juraj Adamik

MOLECULAR INSIGHTS INTO THE DISTINCT MECHANISMS REGULATING THE TLR4 MEDIATED ACTIVATION, SHUT DOWN, AND ENDOTOXIN TOLERANCE OF THE *IL1B* AND *TNF* GENES

A Dissertation

Submitted to the Bayer School of Natural and Environmental Sciences

Duquesne University

In partial fulfillment of the requirements for

the degree of Doctor of Philosophy

By

Juraj Adamik

May 2013

MOLECULAR INSIGHTS INTO THE DISTINCT MECHANISMS REGULATING THE TLR4 MEDIATED ACTIVATION, SHUT DOWN, AND ENDOTOXIN TOLERANCE OF *IL1B* AND *TNF*

By

Juraj Adamik

Approved September 7, 2013

Philip E. Auron, Ph.D.
Professor, Dept. of Biological Sciences
(Committee Chair)

Rita Mihailescu, Ph.D.
Associate Professor, Dept. of Chemistry & Biochemistry
(Committee Member)

Joseph R. McCormick, Ph.D.
Associate Professor & Chair, Dept. of Biological Sciences
(Committee Member)

Karen Arndt, Ph.D.
Professor, Dept. of Biological Sciences
University of Pittsburgh
(External Committee Member)

David W. Seybert, Ph.D.
Dean, Bayer School of Natural and Environmental Sciences
Professor of Chemistry and Biochemistry

ABSTRACT

MOLECULAR INSIGHTS INTO THE DISTINCT MECHANISMS REGULATING THE TLR4 MEDIATED ACTIVATION, SHUT DOWN, AND ENDOTOXIN TOLERANCE OF *IL1B* AND *TNF*

By

Juraj Adamik

May 2013

Dissertation supervised by Philip. E. Auron, Ph.D.

The first wave of the inducible gene network up-regulated by pathogen-stimulated mononuclear cells encodes a variety of effector proteins with pleitropic biological activities. This class of primary immediate early (IE) genes codes for potent pro-inflammatory cytokines and chemokines that play a prominent role during the manifestation of inflammatory response. In an attempt to better understand induction mechanisms for such genes, I have focused on those coding for human interleukin-1β (*IL1B*) and tumor necrosis factor α (*TNF*), which exhibit both transient IE induction as well as cell-type restriction. Employing a combined approach using cell lines and primary cells, reporter transient transfection, chromatin conformational capture and immunoprecipitation, evaluation of transcript integrity, ectopic expression in a non-competent cell type, and comparison to mouse orthologs, I have determined that a

complex array of mechanisms interplay in order to distinctly regulate the Toll-like receptor (TLR) signaling-dependent induction of these two important pro-inflammatory genes whose deregulation provides the etiology for numerous diseases. Prior to induction, *TNF* exhibited pre-bound TATA Binding Protein (TBP) and paused RNA Polymerase II (Pol II), which are the hallmarks of poised IE genes. In contrast, *IL1B* is stringently regulated by long-distance chromosome gyrations, multistep activation through a unique doubly-paused Pol II which, in association with the monocyte lineage factor Spi1/PU.1 (Spi1), maintains a low TBP and Pol II occupancy prior to activation. Activation and DNA binding of the transcription factors C/EBPβ and NF-κB resulted in *de novo* recruitment of TBP and Pol II to *IL1B* in concert with a permissive state for elongation mediated by the recruitment of the positive elongation factor b (P-TEFb). This Spi1-dependent mechanism for *IL1B* transcription, which is unique for a rapidly-induced/poised IE gene, was more dependent upon P-TEFb than was the case for the TNF gene. Nucleosome occupancy and chromatin modification analyses of the *IL1B* and *TNF* promoters, revealed activation-specific changes in chromatin marks that are supportive for nucleosome clearance and formation of nucleosome free regions (NFR). Furthermore, ectopic expression of Spi1, along with a TLR surrogate (over-expressed TNF receptor associated factor 6, TRAF6), in a cell line incompetent for *IL1B* transcription, is observed to prime the cell's endogenous genome for *IL1B* induction by appropriately phasing promoter nucleosomes and recruiting paused Pol II in a manner reminiscent of that observed in competent monocytes. Here I report a novel connection between the metabolic state of cells and HIF-1α in regulating murine *Il1b* gene expression. With regard to the lipopolysaccharide (LPS) unresponsive state known as

endotoxin tolerance, my data revealed that following transient induction, *IL1B* and *TNF* remained marked with paused Pol II complexes for up to 24 hours post-stimulation. Upon subsequent LPS exposure, tolerized *TNF* remained in an unresponsive paused state, while *IL1B* resumed transcription due to recruitment of positive elongation kinase P-TEFb. Emerging evidence suggests that inflammatory responses of LPS/TLR4 activated macrophages are interconnected with metabolic pathways, resulting in the shift of energy utilization by the cells. Here I report that inhibition of either phosphoinositide 3-kinase (PI3K) or glucose metabolism had a greater affect on the transcriptional response of *Il1b* than of *Tnf*. The differences between these two genes, especially for endotoxin tolerance, suggest that *il1b* may play a distinct role from *tnf* in chronic inflammation.

ACKNOWLEDGEMENTS

First of all I would like to express my sincere gratitude to my advisor Dr. Philip E. Auron for sharing his knowledge, guidance, enthusiasm, and continuous support throughout my graduate studies. It was my privilege to learn and work under his supervision and be a part of his research group. I would like to express my appreciation to my dissertation committee members, Dr. Karen Arndt, Dr. Rita Mihailescu, and Dr. Joseph R. McCormick for their insightful advice, critique, and discussions during our meetings and generation of this dissertation work. Many thanks go to the staff in the Dean's office and the faculty, staff, and graduate students in the Department of Biological Sciences for their help and friendships. I also thank my former and current lab colleagues An-Jey A. Su and Dr. Kent Z. Q. Wang for their great collaboration, support, and contributions to my research.

The journey in the Auron Lab was quite an experience in getting to know the world of molecular biology. I had the opportunity to attend and present my research in several conferences in the US and Europe (The American Society For Biochemistry and Molecular Biology (ASBMB) 2009-2012, Cytokine 2010, The IL-1 Family of Cytokines 2011, IL-1 Family Members and the Inflammasome 2012, Pittsburgh Science 2012), which greatly enhanced my scientific advancement and provided opportunity to meet with international collaborators. I would like to thank my collaborators Dr. Deborah L. Galson, Dr. Luke O' Neill, Dr. Gillian Tannahill, Dr. Tripp Barrie, and Mathew Henkel for their support and valuable scientific interactions. In addition to my dissertation project, I have expanded my research experience by studying the role of HIF-1α during the metabolic shift of LPS activated bone marrow derived macrophages in a collaborative

effort with the laboratory of professor Luke O' Neill at Trinity college of Dublin, which has resulted in recent acceptance of a publication in the journal Nature entitled "Succinate is a danger signal from mitochondria that induces IL-1β transcription *via* HIF-1α". My second collaboration with the laboratory of Dr. Tripp Barrie at the University of Pittsburgh ventured into the world of the regulation of the *IL17A* and *IL17F* genes in primary Th17 cells.

There is a long list of acknowledgements among my mentors and friends who have provided me with support over the years and helped me to obtain solid foundations for my achievements. I will not be able to acknowledge them here individually.

The last but certainly not the least, I would like to dedicate my dissertation to my families in Slovakia, parents Adriena and Marek, grandparents Anna, Adela, Anton, and Stefan and my brothers Marek and Danny, as well as in United States parents Linda, Duane, brothers Jonny and Chris, his wife Anina, and grandfather Jim. You have provided me with love, understanding, and support that have been carried through my studies and preparation of this work.

TABLE OF CONTENTS

LIST OF TABLES

Page

LIST OF FIGURES

Page

Page

Page

Page

Page

ABBREVIATIONS

α-KG ..... α-ketoglutarate

Bp ..... base pair (s)

C/EBPβ ..... CCAAT/enhancer-binding protein β

ChIP ..... chromatin immuno precipitation

CTD ..... carboxy terminal domain

DNA ..... deoxyribonucleic acid

HRE ..... hypoxia-response element

HIF-1α ..... hypoxia induced factor α

H3 ..... histone 3

IE ..... immediate early

IL1B ..... human Interleukin-1β gene

Il1b ..... murine Interleukin-1β gene

il1b ..... indicates both, human and murine Interleukin-1β gene

IRF8 ..... Interferon regulatory factor 8

LPS ..... lipopolysaccharide

mRNA ..... messenger ribonucleic acid

NELF ..... Negative elongation factor

NF-κB ..... nuclear factor (NF)-kappaB

NFR ..... nucleosome free region

PAMPs ..... pathogen-associated molecular patterns

Pol II ..... RNA Polymerase II

PRRs ..... pattern recognition receptors

P-TEFb ..... Positive elongation factor b

qPCR..... quantitative polymerase chain reaction

S2P .....serine 2 phosphorylation

S5P .....serine 5 phosphorylation

TBP..... TATA binding protein

TLR4.....Toll-like Receptor 4

TNF.....human Tumor necrosis factor α gene

Tnf ..... murine Tumor necrosis factor α gene

tnf ..... indicates both, human and murine Tumor necrosis factor α gene

2-DG..... 2-deoxyglucose

INTRODUCTION

Innate Immune System, Toll-like Receptors and LPS Sensing

The immune system is an integrative network of organs, cells and defensive molecules capable of mounting protective responses against invading microorganisms. The evolution of vertebrate immunity was driven by a continuous challenge from the external environment mediated by interactions with a surrounding microbial world. Such homeostasis between the host organism and pathogens provided a framework for the expansion of various defense mechanisms, which are inherently tuned to distinguish and eliminate the microbial pathogens (Iwasaki and Medzhitov, 2010). However not all microbes are harmful. Adaptation of the immune system also led to the development of a symbiotic homeostasis with the various types of microorganisms. Enterobacteria residing within selective segments of the vertebrate digestive tract are an example of a symbiotic relationship. A specialized branch of the immune system associated with fostering gut microbes has evolved to maintain their metabolic benefits to the host (Hooper et al., 2012). In addition to the recognition of foreign substances, immune-surveillance is also primed to detect various features associated with physiologically altered cancerous and/or virus-infected host cells.

Innate immunity, as the first line of host defense, consists of a series of anatomical, physiological and phagocytic barriers. These mechanisms are present prior to the onset of infection in order to effectively initiate a set of rapid responses mediating the clearance of pathogens. When activated, components of the innate immune system trigger the adaptive defense mechanisms consisting of the T cell and B cell mediated responses (Akira et al., 2001). The hallmarks of acquired immunity include the high

specificity against a diverse set of antigens, immunologic memory and the prevention from initiating detrimental autoimmune responses. The integration of the innate and adaptive branches during the immune response results in a precise recognition of the invading pathogen, its effective clearance, and a build up of long-term memory against it, enabling a protection during the subsequent exposures.

The hallmark of the innate immune defense involves a set of protective mechanisms activated during tissue injury collectively known as the inflammatory response, which provides "non-specific" destruction of microbes and prevents the spreading of infection throughout a host organism. Initiation of this response requires a detection of microbial components by phagocytic cells such as neutrophils, monocytes and macrophages. Upon the recognition of pro-inflammatory, metabolic or immune stimuli, monocytes, comprising 10% of leukocytes in blood (Auffray et al., 2009), migrate into various anatomical locations where they differentiate into various types of macrophages and dendritic cells. The specific microenvironments within the peripheral tissues induce specialization of the individual macrophages into various sub-populations. These include the interstitial and alveolar macrophages (lungs), Kupffer cells (liver), Langerhan cells (skin), pleural and peritoneal macrophages (serous cavities), microglial cells (brain), and osteoclasts (bone) (Auwerx, 1991; Gordon and Taylor, 2005). These scavenger phagocytes detect the conserved metabolites unique to the microbial world, known as the pathogen-associated molecular patterns (PAMPs), by means of distinct types of pattern recognition receptors (PRRs) situated on their membrane surface as well as within the intracellular compartments. These receptor sensors and their associated signaling pathways are evolutionarily conserved throughout the animal and plant

kingdoms (O'Neill, 2011). PAMPs (LPS, flagellin, bacterial and viral unmethylated CpG DNA, to name few) are constitutively expressed metabolic products that are central to microbial survival. Since they are highly conserved among the different classes of microbes, the innate immune system evolved various mechanisms to specifically target these molecular patterns (Medzhitov, 2001). The continuously scavenging PRRs are also responsive to a variety of common endogenous products that are abnormally released from damaged tissues and necrotic cells, commonly known as the "Damage or Danger" associated molecular patterns (DAMPs). For instance the heat shock proteins, uric acid, ATP, defensins, and HMGB1, are released from dying cells that are harmed during common tissue injury, or by the effects of catalytic enzymes and reactive nitric oxide species released non-specifically from the surrounded inflamed areas (Bianchi, 2007; Kono and Rock, 2008).

Short-term effects of the inflammation controlling the protection and healing activities associated with tissue damage have beneficial effects. However the sites of infection or injury can also lead to the chronic (long-term) inflammatory responses that are the basis for the etiology of numerous diseases. Emerging evidence also suggests that inflammation can contribute to cancerous malignancies, due to a presence of various proliferative growth factors and stimulatory molecules that are vastly present in the inflamed tissues. In addition, the use of various receptors and adhesion molecules utilized by the spreading metastatic cells closely resemble the mechanisms associated with a tissue invasion of inflammatory cells (Coussens and Werb, 2002).

The toll-like receptors (TLR) are a super-family of germ-line encoded PRRs, found in plants, invertebrates, and mammals, which are known to recognize the diverse

classes of bacterial, fungal and microbial components (Armant and Fenton, 2002). Initial studies of a *Drosophila melanogaster* plasma membrane protein, *Toll,* led to the identification of a highly conserved family of ten human and twelve murine TLRs (Takeda and Akira, 2005). Each member of the TLR family can recognize distinct classes of molecules that are unique to microbes. In addition, these membrane receptors can form dimers and expand their scavenger potential. For instance the heterodimeric combinations TLR2/TLR1 and TLR2/TLR6 recognize extracellular lipopeptides and lipoproteins that are part of the bacterial cell walls. On the other hand TLR members 3, 7, 8, and 9 are strategically positioned within the intracellular compartments recognizing single and double stranded microbial nucleic acids (Kang and Lee, 2011). Lipopolysaccharide (LPS) is a unique component of gram-negative bacterial cell walls recognized by the family member TLR4, which is present at the cell surface of monocytes and various tissue macrophages. Binding of this endotoxin to the receptor transduces information from the cell surface to the cytoplasm where it stimulates a cascade of events involving various cytoplasmic factors, many of which are pre-made in the resting cells. During the final steps of signaling, protein kinase cascades and various enzymes converge and modify (for instance by phosphorylation, or ubiquitylation) the inactive transcription factors and their regulators residing within the cytoplasm. The altered/activated transcription factors can then translocate to the nucleus where they act as transcription activators and/or repressors affecting the induction of specific genes.

NF-κB and C/EBPβ

A classical example of sub-cellular sequestration is represented by the nuclear factor (NF)-kappaB (NF-κB) family of transcription factors, which are complexed with IκB inhibitor proteins. In resting monocytes, the latent NF-κB residing in the cytoplasm is bound by a member of the inhibitory IκB family of proteins. TLR4 stimulation activates IKKβ kinase (*via* ubiquitin ligase TRAF6), which phosphorylates IκB. This modification causes IKKβ degradation and the subsequent release of the active form of NF-κB, which translocates to the nucleus (Chen and Greene, 2004). **Figure 1** illustrates this TRAF6 mediated activation pathway. The NF-κB family of proteins consists of the "NF-κB" proteins (NF-κB1 and NF-κB2) and the three "Rel" subfamily proteins (RelA (p65), RelB and c-Rel). Initially translated as long precursors, NF-κB1 (p105) and NF-κB2 (p100) are cleaved into functional transcription factors p50 and p52, respectively (Radisky and Bissell, 2007). These two precursor members possess an extended C-terminal IκB-like domain, which facilitates their auto-inhibition and cytoplasmic retention (Kawai and Akira, 2007). RelA (p65), RelB and c-Rel do not require proteolytic processing for activation. In contrast to NF-κB1 and NF-κB2, the C-terminal portion of the Rel members contains a transactivation domain (TAD), which supports gene activation. A highly conserved Rel-homology domain (RHD) is a shared feature among all family members. This domain mediates DNA binding as well as dimerization among the family members (Gilmore, 2006).

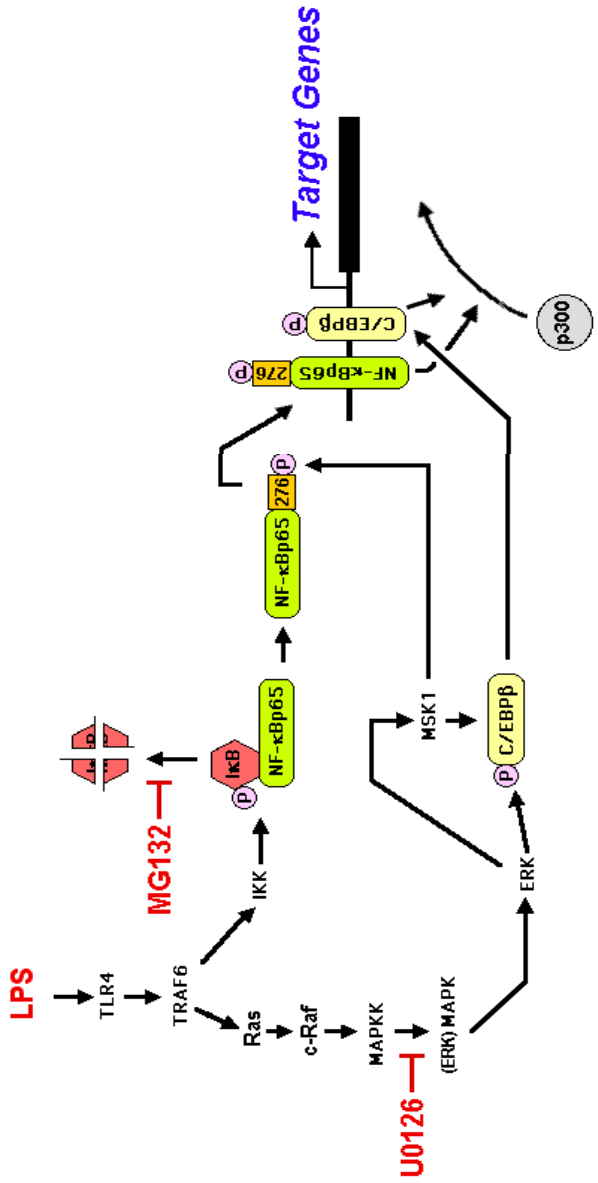

Figure1. The TLR4 meditated activation of NF-κB and C/EBPβ.

LPS binding causes the transmembrane pattern recognition receptor TLR4 to convey the activation signal into the cytoplasm through the signaling molecule TRAF6. Represented are two distinct signaling pathways downstream of TRAF6, which involve a cascade of adaptor proteins that activate transcription factors NF-κB and C/EBPβ. Shown are the target sites for inhibitors MG132 (NF-κB) and U0126 (C/EBPβ) used in this study. While MG132 blocks IKK induced proteosome degradation of the inhibitory IκB protein, U0126 strongly blocks the activation of ERK/MAPK phosphorylation pathway, and to a lesser degree the hyper-activation of NF-κB p65.

The most prominent form of activated NF-κB during TLR4 mediated signaling is a heterodimeric complex p65/p50 (Kawai and Akira, 2007). Upon translocation to the nucleus, the activated dimer binds to DNA sequences located within the regulatory regions of numerous pro-inflammatory genes and influences their transcription (Radisky and Bissell, 2007). An additional regulatory layer associated with NF-κB mediated transcriptional activation resides within its TAD. The NF-κB p65 TAD was shown to associate with the general transcription factor TATA-binding protein (TBP), transcription factor IIB (TFIIB) as well as the coactivators histone acetyl transferase (HAT) p300 and cyclic-AMP-response element (CREB) binding protein (CBP) (Chen and Greene, 2004). Deregulation of NF-κB signaling is often associated with the etiology of various forms of inflammatory diseases and malignancies due to its pleiotropic effects influencing several aspects of cell physiology, such as apoptosis and proliferation (Naugler and Karin, 2008).

The CCAAT/enhancer-binding protein (C/EBP) family of basic leucine zipper (bZIP) transcription factors plays an important role in regulating gene expression during immune responses, proliferation, and cell differentiation. The six members of C/EBP family include C/EBPα, C/EBPβ, C/EBPγ, C/EBPδ, C/EBPε and C/EBPζ. While C/EBPα, C/EBPβ and C/EBPγ are virtually universally expressed, the others are either inducible (C/EBPδ), or their expression is confined to selected cell types of the hematopoietic system (C/EBPε) (Johnson, 2005). LPS signaling in monoctyes initiates several mitogen activated protein kinase (MAPK) pathways, which ultimately converge to activate C/EBPβ. Both, the DNA binding and homotypic dimerization domains of the C/EBP members are confined to their C-terminal bZIP domain. This highly conserved basic DNA binding module also functions as the nuclear localization signal. The amino

terminal portion of C/EBPβ contains the TAD, as well as a signal-responsive regulatory domain (Johnson, 2005; Tsukada et al., 2011). **Figure 1** depicts the activation of C/EBPβ during the TLR4 signaling pathway, initiated by the small GTPase Ras. This mediator induces c-Raf and stimulates the MEK1/ERK1 transduction cascade to phosphorylate C/EBPβ, which undergoes a conformational change (Guha and Mackman, 2001). The inducible activation of C/EBPβ plays an important role in triggering the expression of various cytokines during the inflammatory response and genes controlling the acute-phase response and differentiation of hematopoietic cells (Tsukada et al., 2011). In addition to interacting with transcription factors such as c-Myb (Tsukada et al., 2011), C/EBPβ can synergistically interact with the chromatin remodeling SWI/SNF complexes (Kowenz-Leutz and Leutz, 1999), as well as transcriptional coactivators such as HATs, CBP and p300. These protein associations induce gene expression by promoting transcription permissive histone modifications (acetylation), nucleosome remodeling and the recruitment of general transcription factors to gene promoters (Kovacs et al., 2003).

Monocyte/Macrophage Gene Networks, Nucleosome Positioning and Pol II Pausing

LPS-stimulated monocytes activate distinctive sets of genes responsible for the initiation of appropriate immune-physiological responses that are characteristic for these cells. These gene networks are activated sequentially in a time dependent fashion, producing waves of immediate-early, early, and late gene transcription. For instance, the pathogen activated dendritic cells (DCs) rapidly repress genes associated with phagocytosis and pathogen recognition. At the same time these cells up-regulate the transcription of genes encoding immune products responsible for the recruitment of

monocytes, DCs, and macrophages to infected body areas (Huang et al., 2001).

The first wave of the inducible gene network up-regulated by pathogen-stimulated mononuclear cells encodes a variety of effector proteins with pleitropic biological activities. This class of primary immediate early (IE) genes codes for potent pro-inflammatory cytokines and chemokines that play a prominent role during the manifestation of the inflammatory response. The transcription of these genes is highly regulated, as their products are associated with potent immune-stimulatory and cytotoxic properties. Locally they can induce vasodilation by altering endothelial cells and stimulate recruitment of neutrophils and macrophages to the site of infection. Additionally, they mediate various systemic responses such as fever (hypothalamus) and the acute phase response (liver) (Smale, 2010). If not properly contained, the prolonged expression of these toxic molecules has harmful and destructive effects associated with chronic inflammation. The stimulus selective and inducible expression of the IE genes is often restricted to a specific cell type, and their expression does not require *de novo* protein synthesis (Herschman, 1991). Efficient activation of the IE responders requires a collaborative endeavor of transcription factors, coactivators, and chromatin modifiers, targeted to the regulatory sequences residing within gene promoters and enhancers. Various combinations of these factors are recruited to the regulatory regions of IE genes to establish favorable chromatin architecture and mediate recruitment of the transcription machinery. Often being separated by thousands of base pairs, the transcription factors mediate physical associations between distant promoters and enhancers to serve as an additional regulatory step controlling gene expression. In resting cells, IE genes are maintained in a repressed/poised state ready for a rapid induction in response to stimulus.

Eukaryotes package their DNA into a higher order structure known as the chromatin fiber. The basic units of chromatin are nucleosomes, which are comprised of 2 copies of 4 core histone proteins H2A, H2B, H3, and H4. The central H3/H4 tetramer is surrounded by the H2A/H2B dimers (Henikoff, 2008). The 147 bp of DNA wrapped 1.65 turns around each of these octameric structures represent the fundamental unit of the chromatin fiber (Radman-Livaja and Rando, 2010). An average distance between the midpoints of two nuclesosmes compacting the human genome is approximately 185 bp. Nucleosome positioning throughout the genome plays a major role in controlling the accessibility of DNA regulatory regions and influencing gene expression. Nucleosome positioning often corresponds to the transcriptional activity of a particular gene. For instance, the promoters of active genes are usually associated with a nucleosome free region (NFR), which facilitates the formation of pre-initiation complex formation (PIC) and RNA Polymerase II (Pol II) entry. The first, and usually most prominent, phased nucleosome (non-randomly positioned nucleosome along DNA) downstream of the TSS is referred to as +1. Contrary to yeast, in humans the nucleosome positioned within the NFR is defined as -1 and the first most prominent nucleosome upstream of the TSS is designated as -2. An additional aspect of gene packaging lies within the nature of covalent modifications associated with the N-terminal nucleosome histone tails that are subjected to the binding of various histone modifiers and transcriptional activators and repressors (Jiang and Pugh, 2009). **Figure 2** illustrates the nucleosome positions, Pol II occupancy, and the spatial distribution of several chromatin marks used in literature and this study as common indicators of transcriptional competency.

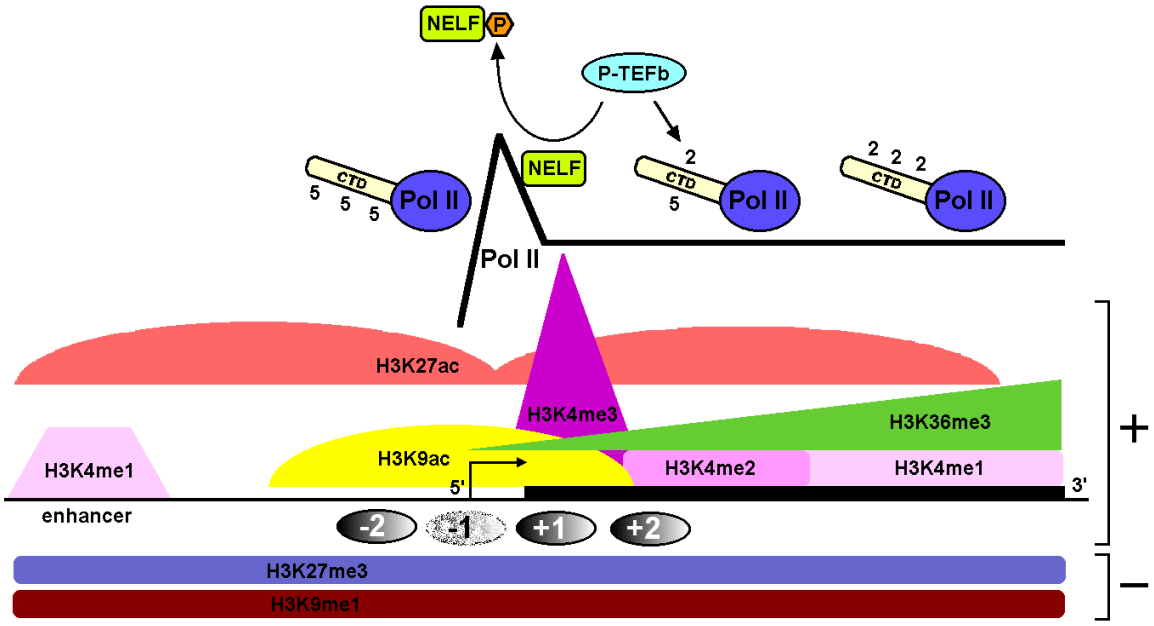

Figure 2. Illustration of the paused Pol II dynamics and chromatin landscape along a typical gene. Shown here are the various transcriptional permissive (+) and repressive (-) chromatin marks as well as their reported distribution throughout a typical gene locus (Henikoff and Shilatifard, 2011; Owen-Hughes and Gkikopoulos, 2012). Transcriptionally permissive modifications include H3K9ac, H3K4me3, H3K36me3, H3K4me1, and H3K27ac. H3K9ac is present at the promoter, H3K4me3 is most abundant in the vicinity of the +1 nucleosome, H3K36me3 increases towards the 3' end of the structural gene, and H3K27ac is distributed upstream and throughout the gene locus (Henikoff and Shilatifard, 2011; Owen-Hughes and Gkikopoulos, 2012). H3K4me1 marks enhancers of LPS inducible genes within the setting of a macrophage genome (Ghisletti et al., 2010; Heinz et al., 2010). Transcriptionally inactive genes are enriched for modifications such as H3K9me1 and H3K27me3. Typically phased nucleosomes are labeled according to their position relative to the transcription start site (TSS). Illustrated is also the Pol II progression throughout the locus. The paused Pol II complex is represented as a peak, located 50bp beyond TSS. Paused Pol II is associated with the C-terminal domain phosphorylation at serine 5 and the presence of negative elongation factor (NELF). The interplay between NELF and positive elongation factor b (P-TEFb) regulates the Pol II transition into the elongation state.

Recent reports from *Drosophila* and human genome studies revealed a new regulatory step within the transcriptional cycle of Pol II. These observations changed the way we think about transcriptional control of primary response genes. Pol II is pre-loaded at the 5' regions of many genes that are inactive or minimally expressed (Gilchrist et al., 2008; Guenther et al., 2007; Kininis et al., 2009; Muse et al., 2007; Rahl et al., 2010; Zeitlinger et al., 2007). In addition, TBP appears to be constitutively present on these genes (Donner, 2010). As shown by *in vitro* studies, these complexes are poised for rapid transcription, and will resume elongation upon the addition of nucleotides (Fish and Kane, 2002; Greive and von Hippel, 2005). Activation of the paused genes by an exposure of cells to developmental and environmental stimuli is dependent on the release of Pol II from its paused state (Wu and Snyder, 2008). The interplay of several elongation factors and chromatin modifiers is responsible for maintaining and liberating the paused Pol II. One of the proteins that induces Pol II stalling is the negative elongation factor (NELF), composed of four subunits, NELF-A, NELF-B, NELF-C/D, and NELF-E, which was proposed to interact with the nascent RNA emerging from Pol II, using its RNA recognition motif (RRM) (Gilchrist et al., 2008; Wu et al., 2003; Yamaguchi et al., 2002). Positive transcription-elongation factor-b (P-TEFb) has been shown to rescue the paused Pol II by simultaneously phosphorylating NELF as well as the Pol II C-terminal domain at serine 2 (S2P CTD), causing its transition into the state of elongation (Bres et al., 2008; Ni et al., 2008; Price, 2000). The differential modifications of Pol II CTD, as well as its interactions with the components of the splicing machinery, play a crucial role during the regulation of transcriptional dynamics. The mammalian CTD is a part of the largest Pol II subunit (RPB1) and contains 52 tandem repeats of a heptapeptide with the consensus

sequence Tyr-Ser-Pro-Thr-Ser-Pro-Ser (Buratowski, 2009). It has been postulated that the differential phosphorylation states of the CTD correspond to either a paused or an actively elongating Pol II. The phospho-serine 5 modified CTD (S5P CTD) is located primarily at the upstream regions of the genes as part of the engaged but stalled Pol II complex. Cyclin-dependent kinase 7 (CDK7), a subunit of the general transcription factor TFIIH, has been shown to mediate this S5P phosphorylation event, since the newly recruited Pol II is in a hypo-phosphorylated state (Brookes and Pombo, 2009). This modification aids in the process of the methylguanosine cap addition to the 5' end of the nascent mRNAs. ChIP experiments have shown that serine 2 phosphorylation by P-TEFb (which contains a CDK9 subunit) increases towards the 3' end of the actively transcribed genes. The serine 7 phosphorylation (S7P) serves as an additional site for Pol II CTD phosphorylation at a subset of genes encoding small nuclear (sn) RNAs in mammalian genomes (Egloff, 2012). This S7P modification is recognized by the RNA Pol II-associated protein 2 (RPAP2), which recruits the Integrator complex responsible for the RNA 3' end processing (Egloff et al., 2012). The spatial alteration of the CTD phosphorylation pattern corresponds to the recruitment of various factors responsible for proper pre-mRNA co-transcriptional processing including splicing and addition of the poly-A tail (Buratowski, 2003; Egloff and Murphy, 2008). In addition, the sequentially phospho-modified CTD serves as a landing pad for the recruitment of chromatin remodeling and modifying factors including the histone methyltransferases Set1 and Set2, as well as the histone acetyltransferases CBP/p300 and PCAF (Brookes and Pombo, 2009; Munoz et al., 2010; Weake and Workman, 2010). In fact, a specific set of chromatin marks, which are differentially distributed throughout the gene coding and

regulatory regions, have also been associated with Pol II transcription dynamics. For instance, tri-methylation of lysine 4 at histone 3 (H3K4me3) and the acetylation of lysine 9 at histone 3 (H3K9ac) are present at the promoter proximal regions of either actively transcribed or paused genes. In contrast, the tri-methylated lysine 36 of histone 3 (H3K36me3) downstream of the gene promoters is associated with actively elongating Pol II complexes (Brookes and Pombo, 2009; Wu and Snyder, 2008).

The phenomenon of Pol II pausing is thought to contribute to gene regulation in a variety of ways. Some reports indicate that the paused Pol II complexes provide a means for a rapid transcriptional response, as well as the coordinate induction of multiple genes (Fuda et al., 2009). Evidence suggests that Pol II pausing ensures the proper assembly of capping factors at the 5' end of genes, as well as the accurate formation of a Pol II elongation complex. Additional reports indicate that Pol II also pauses at the 3' end of genes, where it associates with protein machineries that direct the final steps of mRNA processing, including cleavage and polyadenylation (Glover-Cutter et al., 2008). Lastly, studies in *Drosophila* showed that the stalled Pol II serves as a physical barrier by preventing promoter-proximal nucleosome assembly (Gilchrist et al., 2008). This mechanism contributes to the accessibility of the core promoter for subsequent recruitment of Pol II and proper gene activation (Gilchrist et al., 2008). Pol II pausing is also associated with the negative regulation of gene expression. As recently reported, the NELF-induced paused Pol II complex at the *JunB* promoter is present prior to induction and persists during the transcription of the gene. According to the report, the gene is not activated to the full extent, because of the attenuating effects of paused Pol II (Aida et al., 2006). Additional studies investigating Pol II pausing will be required in order to better

resolve the role played by this regulatory step that influences the transcription of eukaryotic genes.

A signal (LPS) inducible enhancer and a cell type specific promoter constitute the main regulatory regions of the human *IL1B* gene.

Interleukin-1β (IL-1β) is a potent mediator of inflammatory responses with diverse biological activities affecting the endocrine, nervous, and immune systems. IL-1β has been shown to cause fever, activate acute-phase responses, modulate lymphocyte function, as well as induce both destructive and reparative changes in mesenchymal tissues (cartilage, bode, muscle) (Dinarello, 1986; Dinarello, 1994). The gene encoding IL-1β is located on human chromosome 2 within the homologous IL-1 family gene cluster, which contains 8 additional IL-1-like genes whose products have also been associated with diverse pro- and anti-inflammatory activities. The primary sources of this molecule in humans and mouse are activated monocytes/macrophages as well as related cells of the myeloid lineage. The transcriptional profile of *IL1B* in stimulated monocytes is reflected by rapid induction followed by a decreased sustained expression that lasts for several hours (Fenton et al., 1987). The past work in our and other groups has revealed numerous regulatory sequences upstream of the *IL1B* coding region that bind an array of transcription factors, including Spi1/PU.1 (Spi1), C/EBPβ, NF-κB p65, IRF4/8, and CREB, some of which are restricted to the monocytic-cell lineage, such as Spi1, and IRF4/8. Transcription factor interactions and binding to different positions along the *IL1B* regulatory regions likely account for the stringent regulation of this IE gene. In the past, the study of *IL1B* regulatory regions focused primarily on defining the specific DNA

sequences and their capabilities for binding various transcriptional activators. The past collection of studies resulted in the comprehensive dissection of the complex regulatory elements within the *IL1B* locus. **Figure 3** depicts the schematic representation of *IL1B* regulatory regions as well as the associated binding of transcription factors controlling *IL1B* transcription. Transient transfection studies using selected fragments of the *IL1B* trans-gene into murine RAW 264.7 (RAW) monocytes, revealed important regulatory sequences 3kb upstream of the TSS between -3134 and -2729 (Shirakawa et al., 1993). This stimulus-specific enhancer, termed the upstream induction sequence (UIS), is divided into 9 distinct regions (A through I) some of which contain collections of binding sites for an array of constitutively bound, as well as inducible, transcription factors. The C/EBPβ, a critical myeloid gene regulator (Pham et al., 2007), binds to the enhancer E and I regions following LPS stimulation. Mutation of these binding sites reduces the activity of *IL1B* promoter driven CAT plasmids transfected into monocyte cell lines, suggesting its functional role in the gene activation (Shirakawa et al., 1993; Tsukada et al., 1994b).

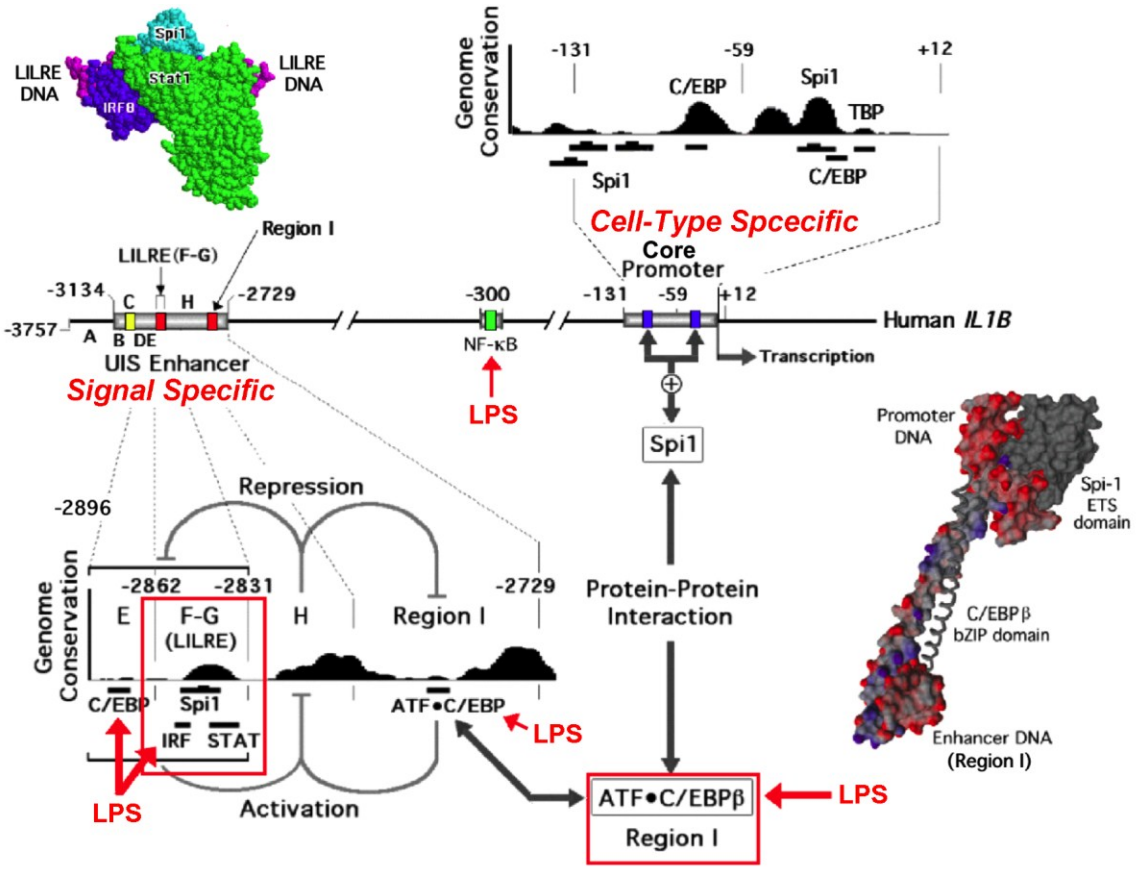

Figure 3. Depiction of the *IL1B* gene regulatory region.

Shown are the various regulatory regions that are known to affect *IL1B* induction. Magnified on the bottom left are the enhancer regions and top right the promoter transcription factor binding sites. LPS induced binding of the effector proteins is highlighted with red boxes and arrows. Illustrated is also the enhancer specific protein complex binding to the LILRE, as well as the looping mediated by the association of constitutive Spi1 (promoter) and LPS induced C/EBPβ (enhancer). Figure was provided by the courtesy of P.E. Auron.

In addition, these studies revealed an important role of the interferon stimulation response element (NF-β1) binding site within the enhancer F region during *IL1B* regulation. Chromatin immuno-precipitation (ChIP) studies showed cooperative association of non-tyrosine phosphorylated (NTP)-Stat1, IRF-8 and Spi1 bound to an

LPS/IL-1 Responsive Element (LILRE), located between the positions -2880 and -2849 in unstimulated monocytes. Upon LPS treatment, the trans-activation domain of IRF8 likely becomes phosphorylated at the tyrosine residue 727, possibly acting as a switch necessary for the rapid activation (up to 80%) of *IL1B* transcription (Unlu et al., 2007). Continuing with this mechanism, a recent study argued that LPS activates a casein kinase-2 (CK2)-dependent phosphorylation of the pre-associated Spi1 within the complex. This phosphorylation event of Spi1 at the serine 148 triggers the replacement of IRF-8 by its relative IRF4, which acts to enhance the recruitment of Pol II complex to the *IL1B* promoter (Zhang et al., 2008). Another site within the UIS that is necessary for proper *IL1B* gene activation is located within the enhancer I-region (-2768 to -2760), which contains the composite sequences recruiting competing heterodimeric complexes consisting of C/EBPβ and CREB and a CREB-like factor, possibly ATF4 (**Figure 3**) (Auron and Webb, 1994; Chandra et al., 1995; Tsukada et al., 1994). All of these activators and their modifications are needed for proper *IL1B* induction, in order to overcome the unknown nature of the potent suppressive effect of region H in the enhancer, which acts as a silencer for LPS induction (Tsukada et al., 1994b). Another feature likely enabling the observed rapid induction of *IL1B* is associated with the accessible/nucleosome-free promoter architecture, containing constitutively bound transcription factors and activators (Liang et al., 2006). One such protein, central to *IL1B* expression, is the previously mentioned Spi1, an ETS domain helix-turn-helix (HTH) DNA binding factor exclusively expressed in the monocytes/myelocytes, B cells, mast cells, and erythropoietic stem cells (Nishiyama et al., 2004; Pahl et al., 1993). It has been postulated that this lineage-determining factor facilitates the formation of a NFR,

exposing binding sites for the LPS-responsive transcription factors in activated monocytes (Natoli, 2012). Spi1 is a major factor involved in the genome-wide maintenance of the macrophage lineage (Lawrence and Natoli, 2011). In particular, recent genome-wide studies revealed a constitutive association of Spi1, often with other signal inducible factors such as NF-κB and C/EBPβ, at the LPS responsive enhancers in murine macrophages (Ghisletti et al., 2010; Heinz et al., 2010). It is speculated that the cell-type-restricted expression of *IL1B* is dependent on Spi1, which constitutively binds to the promoter at two distinct sites located between -50 to -39 and -115 to -97, relative to the TSS (**Figure 3**) (Kominato et al., 1995). In addition to its role as a pioneer factor, which is capable of binding nucleosome-wrapped DNA and facilitating chromatin accessibility (Marecki et al., 2004), Spi1 also recruits various activators such as the HMGB1 (Mouri et al., 2008), JunB (Grondin et al., 2007) and the general transcription factor TBP, involved in the pre-initiation complex (PIC) formation, responsible for Pol II recruitment to the promoter (Hagemeier et al., 1993). Our group proposed that C/EBPβ bound to the enhancer physically interacts with Spi1 located at the *IL1B* core promoter and cooperatively initiates *IL1B* gene induction. This protein-protein tethering would bring the *IL1B* enhancer and promoter into a close proximity resulting in a loop formation that enhances gene activation (Listman et al., 2005; Yang et al., 2000). In addition to the enhancer-binding sites, the *IL1B* promoter also contains two C/EBPβ binding sites positioned at -91 and -41 bp upstream of the TSS (Listman et al., 2005). Studies in mouse monocytes indicate that promoter bound (position -41) C/EBPβ undergoes p38 MAPK-dependent phosphorylation that is required for *IL1B* induction (Baldassare et al., 1999). Finally, *IL1B* transcription requires the recruitment of NF-κB p50-p65 hetero-dimer to a

putative binding site located 297 bp upstream of the TSS (**Figure 3**). Point mutations within this sequence significantly reduced *IL1B* activity (Hiscott et al., 1993). The proper activation of this inducible gene requires a series of combinatorial associations (often in protein complexes) and posttranslational modifications of these factors in a time-dependent fashion that are ultimately responsible for the recruitment of Pol II to the *IL1B* promoter.

IL-1 gene family members in human monocytes.

The human IL-1 family consists of 11 genes whose identity have been only recently identified and their biological relevance during the inflammatory responses is presently being investigated. The members include IL-1α (IL-1F1), IL-1β (IL-1F2), IL-1 receptor antagonist IL-1Ra (IL-1F3), IL-18 (IL-1F4), IL-36ra (IL-1F5), IL-36α (IL-1F6), IL-37 (IL-1F7), IL-36β (IL-1F8), IL-36γ (IL-1F9), IL-38 (IL-1F10), and the most recently added member IL-33 (IL-1F11). As **Figure 4** illustrates, all of the members are mapped to a cluster on the long arm of chromosome 2, except IL-18 and IL-33 (not included in the Figure), which reside on chromosomes 11 and 9, respectively (Liew et al., 2010). Emerging evidence suggests that IL-1α, IL-1β, IL-18, IL-36α, IL-36β, IL-36γ, and IL-33 have pro-inflammatory, while IL-1Ra, IL-36ra, and IL-37 have anti-inflammatory, functions. The role of IL-1F10 during the mediation of immune responses is not well understood (Dinarello; Dunn et al., 2001).

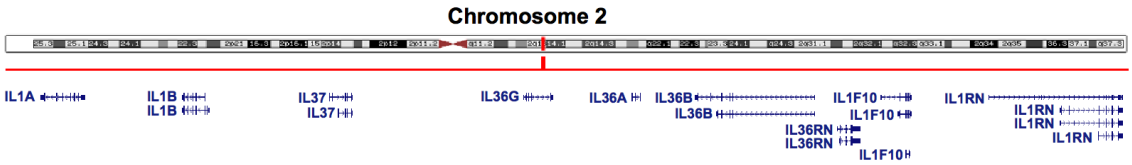

Figure 4. IL-1 family gene cluster on the long arm of chromosome 2.

Shown is a magnified section of the chromosome 2, which contains a gene cluster of 9 IL-1 family members. The arrows within the genes annotate their transcriptional direction. Certain genes show more then one predicted coding sequences of varying lengths. This figure was generated using the UCSC genome browser website.

Endotoxin Tolerance

Endotoxin tolerance, also known as desensitization, is defined as a decreased responsiveness of the host's (cells and organisms) to either repeated or prolonged LPS stimuli, after an initiation of the primary immune response (Fan and Cook, 2004). This state of immune-paralysis has been associated with a protective function, in preventing the excessive and uncontrolled onset of potentially harmful inflammatory responses to the host organism (Arbibe and Sansonetti, 2007). The first evidence suggesting endotoxin tolerance came from the 1947 reports by Beeson. His studies revealed decreased fever responses in rabbits repeatedly treated with bacterial pyrogens (Beeson, 1947a, b). Although some aspects of the endotoxin tolerance phenomenon have been elucidated, the mechanisms at the level of transcriptional regulation are still largely unknown. In the search for new answers, various laboratories often used a variable experimental set up in cell culturing and LPS treatment that resulted in some inconsistent results throughout the literature. A recent study using murine bone marrow-derived macrophages categorized the LPS responsive genes into two classes, *tolerant* and *non-tolerant*. The report argues that the protein products of the *tolerant* genes are associated with potent pro-inflammatory functions and therefore their expression is rapid and transient. They are refractory to an additional stimulus in order to prevent their harmful effects and potential tissue damage. On the other hand, the genes in the *non-tolerant* category encode various anti-microbial products whose expression remains inducible even after the repeated stimuli. These molecules are not associated with the harmful effects to the host. Instead, their re-activation is beneficial to the host by providing long-term protection form invading pathogens. The hypo-responsiveness of the *tolerant* genes was attributed to the

loss of histone modifications associated with gene activation (Foster et al., 2007). Both, *TNF* and *IL1B* were included in the list of genes that were unable to respond to the secondary LPS challenge. The issue of chromatin dynamics during endotoxin tolerance was explored by Gazzar et. al, indicating that increased repressive methylation at H3K9me1, induced binding of heterochromatin-binding protein 1α (HP1α) to *TNF* causing its transcriptional repression (El Gazzar et al., 2007). Additionally, a series of studies showed that the tolerant phenotype results form an increase in the nuclear concentration of NF-κB p50–p50 homodimer, which lacks a proper TAD, causing transcriptional deregulation of specific genes including *TNF* and *IL1B* (Kastenbauer and Ziegler-Heitbrock, 1999; Ziegler-Heitbrock et al., 1994). Two reports using human cell lines (LaRue and McCall, 1994) and a mouse model (Zuckerman et al., 1991) revealed two contradictory *tolerant* and *non-tolerant* properties, respectively, for the *il1b* gene, adding more dilemma to the endotoxin tolerance subject. Previous studies in our laboratory also showed a partial incomplete *IL1B* tolerance of LPS (Fenton et al., 1987) and a novel complete tolerant property for *IL1B* by using phorbol ester (PMA) as the secondary challenge (Fenton et al., 1987). Lastly, a recent study using non-monocytic cells showed that endotoxin tolerance manifests itself in a cell type specific manner (Wang et al., 2011). Collectively these reports suggest that the many aspects of endotoxin tolerance associated with transcriptional repression are still not well understood. Although the tolerant nature of *TNF* has been consistently reported, studies of *IL1B tolerance* are not yet conclusive. Since the effects of endotoxin tolerance are evident in various diseased states, including sepsis, non-infections systemic inflammatory responses, trauma, and hemorrhagic shock, the understating of the underlying

mechanisms associated with this phenomenon is significant for their treatment (Cavaillon et al., 2003).

The Role of HIF-1α in innate immunity and cancer

Hypoxia induced factor (HIF-1α) plays a major role as a regulator of oxygen homeostasis in cells. During the state of normal oxygen levels (normoxia), HIF-1α, a helix-loop-helix DNA binding factor, rapidly undergoes post-translational modification by the action of the enzyme prolyl hydroxylase (PHD), which causes the ubiquitin-mediated degradation of HIF-1α. The PHD activity is inhibited under conditions of oxygen deprivation (hypoxia), which induces HIF-1α stabilization and subsequent translocation to the nucleus, where it binds a DNA recognition motif known as the hypoxia-response element (HRE) and associates with co-activators such as p300/CBP, which activate target genes (Semenza, 2003) (**Figure 5**). Since hypoxia is a well-known feature of inflamed and cancerous tissues, the understanding of the homeostatic imbalance of HIF-1α activity has significant clinical implications.

Otto Warbug reported the first connection between malignant cells and metabolic activity in 1927 (Warburg et al., 1927). Today, it is well established that tumor cells undergo a metabolic shift resulting in the upregulation of the anaerobic glycolysis as a major source for their energy production. The alteration of mitochondrial physiology is due to mutations in the genes encoding succinate dehydrogenase (*SDH*) and fumarate hydratase (*FH*) enzymes associated with the TCA (Krebs) cycle, which links glucose utilization with oxidative phosphorylation (Gottlieb and Tomlinson, 2005). Often associated with the state of pseudo-hypoxia, the buildup of succinate and fumarate acts as

a direct inhibitor of PHD, causing activation of HIF-1α. HIF-1α, in turn, causes the up-regulation of genes involved in the anaerobic glycolysis, promoting neurovascularization and deregulation of cell apoptosis (Gottlieb and Tomlinson, 2005), contributing to the tumorigenesis. The metabolic changes associated with the upregulation of anaerobic glycolysis are also apparent in mononuclear cells residing within tumors and inflamed tissues (Tannahill and O'Neill, 2011). Several physiological processes controlling macrophage activity within inflamed and ischemic tissues are closely associated with HIF-1α mediated alterations in the transcription of a wide array of target genes.

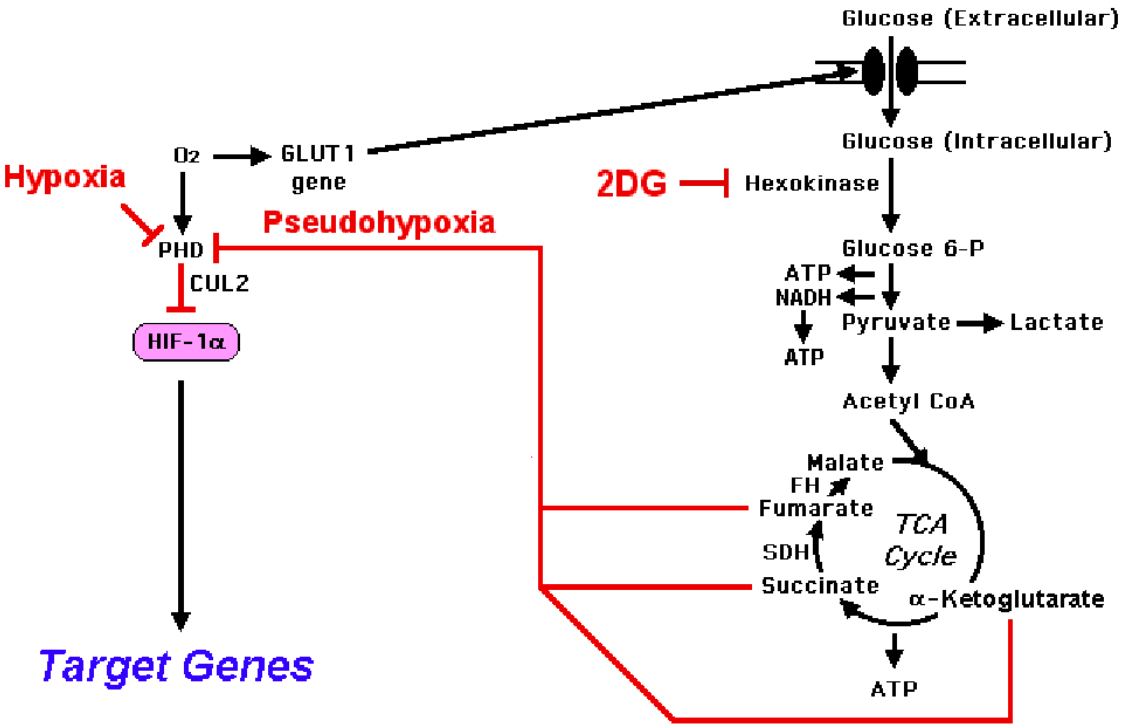

Figure 5. Glucose metabolism and regulation of HIF-1α.

Shown is a glycolysis pathway and the effects of various substrates (mediating a pseudo-hypoxia) whose build-up causes inhibition of prolyl hydroxylase (PHD) and the up-regulation of HIF-1α. Inhibitory pathways are marked with red colors. The effects associated with a drop in oxygen levels (hypoxia) are also depicted in the Figure.

The hypoxic microenvironment of inflamed tissues has been shown to trigger HIF-1α and alter the expression of proteins associated with macrophage survival, expression of cytokines/chemokines, and tissue angiogenesis (Murdoch et al., 2005). In addition to relieving the inhibitory effects of PHD, the TLR4 mediated activation of NF-κB was shown to augment the transcription of *Hif1α* and further amplify its regulatory potential (Nizet and Johnson, 2009).

HYPOTHESIS AND SPECIFIC AIMS

IL1B and *TNF* are immediate early genes induced in response to TLR4 activation of monocytes. Upon monocyte stimulation, *TNF* undergoes rapid induction and complete transcriptional shut down within a few hours. *IL1B* is expressed with similar initial kinetics, but in contrast to *TNF* its expression is not completely inhibited and remains sustained for many hours post-stimulation. In addition, *TNF* is refractory to subsequent LPS stimulation. In contrast, *IL1B* is less sensitive to endotoxin tolerance and can be re-activated when exposed to a secondary LPS challenge. One primary transcription factor NF-κB has been reported to regulate the expression of these IE genes (Collart et al., 1990; Hiscott et al., 1993). Since the expression profiles of *IL1B* and *TNF* are quite distinct, I hypothesize that additional regulatory mechanisms control the expression of *IL1B*. A series of kinetic ChIP experiments analyzing various transcription factors and nucleosome positioning and modification was performed in order to clarify the mechanisms responsible for the decreased, but sustained, transcriptional activity of *IL1B,* as well as its ability to escape endotoxin tolerance. In order to precisely define the importance of selected transcription factors, I performed transient transfection experiments using HEK 293 cells, as a "surrogate-monocyte" cell system. By adding combinations of signaling activators and transcription factors, an LPS stimulated monocyte environment can be mimicked within these cells with concomitant induction of developmentally quiescent *IL1B*. On the basis of *in vitro* studies, functional cooperation between enhancer bound C/EBPβ and promoter bound Spi1 *via* DNA looping has previously been proposed by our laboratory as a mechanism for *IL1B* induction (Listman et al., 2005; Yang et al., 2000). To validate the possible LPS induced chromatin looping

as a regulatory step for *IL1B* gene induction, chromatin conformation capture analysis was performed. Lastly, I investigated the expression of IL-1 family members at the primary IL1 locus on chromosome 2 and two of its distant members on chromosomes 9 and 11 in resting and activated human monocytes. According to my preliminary data, I hypothesize that this gene family will be coordinately expressed following LPS stimulation. The synchronous expression of the IL-1 gene family members suggests that they may be transcribed as a single structural-functional entity known as transcription factory. Since many transcriptional mechanisms are conserved among higher eukaryotes, the new information obtained from this research will be applicable to other rapidly induced genes. Because the regulation of gene expression is central to cell growth, differentiation, and physiological responses to environmental stress, it is important to understand the mechanisms underlying these processes. Especially important is the activation of pro-inflammatory genes such as *IL1B*, whose over-expressed bioactive products can be destructive to tissues. Given that extensive release of these homeostatic/immune-mediators is associated with numerous autoimmune diseases, an understanding of their transcriptional control can provide a means for developing new inhibitory therapeutics. Accordingly, the following specific aims were proposed in order to better understand the transcriptional regulation of *IL1B*:

Aim 1. Execution of positional-temporal ChIP studies of *IL1B* vs. *TNF* induction and transcriptional shut down.

Aim 2. Resolving the molecular nature of gene specific desensitization/immune-tolerance of *IL1B* and *TNF* genes.

Aim 3. Determining the role of Spi1 in induction of the *IL1B* gene and to characterize the relative importance of C/EBPβ and p65 during *IL1B* induction in monocytes and in HEK 293 cells supplemented by ectopic expression of monocyte-specific factor.

Aim 4. Investigation of the LPS inducible mRNA expression of IL-1 gene family members in human monocytes.

MATERIALS AND METHODS

Cell Culture

THP-1 cells were cultured in RPMI media (10-040-CV, Cellgro) supplemented with 10% heat-inactivated fetal bovine serum (FBS), 1% Penicillin/Streptomycin solution (30-002-CI, Cellgro) and 500 µl of 2ME (21985-023, Invitrogen). HEK 293 cells, MG 63 cells, grown in EMEM (10-010-CV, Cellgro) and HuT 102 cells grown in RPMI, containing 10% heat-inactivated FBS and 1% Penicillin/Streptomycin Solution, were obtained from American Type Culture Collection. RAW 264.3 were cultured in DMEM (10-013-CV, Cellgro) supplemented with 10% heat-inactivated fetal bovine serum (FBS), 1% Penicillin/Streptomycin Solution. Adult human elutriated monocytes were purchased from Advanced Biotechnologies (07-210-001). Monocytes were cultured in DMEM with 20% FBS (SH3007003N, Fisher), 1% Penicillin/Streptomycin, and 50 µg/ml Gentamicin (1676045, MP Biomedicals) for 7 days until macrophage monolayer was established. On day 7 and 8, 90% of the old media was replaced with 10 ml of fresh media to remove all non-adherent cells. Kinetic LPS stimulations were conducted on day 9 of cell culture. Bone marrow from C57BL/6 mice (Harlan Laboratories, UK) was differentiated for 10 d in granulocyte-macrophage colony-stimulating factor (4% (vol/vol) J588 myeloma cell supernatant) or for 7 d in M-CSF (20% (vol/vol) L929 mouse fibroblast supernatant) in typical media preparations for the preparation of BMDMs.

Reagents and Treatment Conditions

In all experiments, monocytes were stimulated with 1 µg/ml of *E. coli* 055:B5 Lipopolysaccharide (LPS) (Sigma) for indicated time periods. In the case of re-stimulation experiments, cells were initially stimulated with 1µg/ml of LPS and then re-

stimulated with additional 1μg/ml of LPS without washing the media. All inhibitors used in the study were applied one hour prior to LPS treatments in following concentrations; 1 μM/ml MG132 (474790, Calbiochem), 10μM/ml U0126 (V1121, Promega), 10 μM/ml SB 202190 (152121-30-7, Sigma), 50 μM/ml 5,6-Dichlorobenzimidazole 1-β-D-ribofuranoside (DRB) (D1916-10MG, Sigma) 10 μM/ml of IKK Inhibitor III (BMS-345541, Calbiochem), and 25 μM LY294002 (440202, Calbiochem).

Chromatin Immuno-precipitation (ChIP)

ChIP was performed using a modification of the Millipore/Upstate protocol (MCPROTO407). In brief, a total of $1x10^7$ cells were fixed in 1% formaldehyde (F79-500, Fisher) for 10 min at room temperature. Cross-linking was inhibited by addition of glycine to a final concentration 0.125 M. Cell pellets were washed twice with ice cold PBS and resuspended in SDS Lysis Buffer (1% SDS, 10 mM EDTA, 50 mM Tris, pH 8.1) supplemented with 1 μg/ml Aprotinin (A6279-5MG, Sigma), 1μM phenylmethylsulfonyl fluoride (PMSF) (93482, Fluka), and 1 μg/ml Leupeptin (L9783-5MG). Samples were sonicated (to generate DNA fragments of 250 base pairs (bp) average length) on ice using a Fisher Scientific Sonic Dismembrator (Model 100), as follows: 325 strokes at 100% power followed by 75 stokes at 50% power and centrifuged at 12000 RPM for 10 min. Chromatin from $5x10^6$ cells was diluted 7-fold in ChIP Dilution Buffer (0.01% SDS, 1.1% Triton X-100, 1.2 mM EDTA, 16.7 mM Tris-HCl, pH8.1, 167 mM NaCl), pre-cleared with protein Agarose/Salmon Sperm DNA beads (Protein G Agarose, 16-201 Millipore, Protein A Agarose 16-157 Millipore; IgM A4540 Sigma-Aldrich) for 30 min at 4°C, and centrifuged at 10,000 RPM for 2 min. Chromatin supernatants were incubated at 4°C overnight with respective antibodies (**Table 1**).

Aliquots for INPUT and non-specific IgG control samples were included with each experiment. Samples were precipitated using 40 µl of protein agarose beads, depending upon specific antibody requirements (**Table 1**) at 4°C for 2 hours, and subsequently washed with following solutions: once with Low-Salt Buffer (0.1% SDS, 1% Triton X-100, 2mM EDTA, 20 mM Tris-HCl, pH 8.1, 150 mM NaCl), once with High-Salt Buffer (0.1% SDS, 1% Triton X-100, 2mM EDTA, 20 mM Tris-HCl, pH 8.1, 550 mM NaCl), once with LiCl Wash Buffer (0.25 M LiCl, 1% IGEPAL-CA630, 1% deoxycholic acid, 1mM EDTA, 10 mM Tris, pH 8.1), and twice with TE Buffer (10 mM Tris-HCl, 1 mM EDTA, pH 8.0). Immunocomplexes were eluted in two stages for 30 min and 15 min at 65°C with 260 µl and 140 µl of ChIP Elution Buffer (1% SDS, 0.1M $NaHCO_3$), respectively. To reverse the cross-linking, eluted samples were treated with 16 µl of 5 M NaCl and subsequently incubated at 65°C for ≥4 hours. DNA was purified using a GeneJET PCR Purification kit (Fermentas, #K0702). Primer pairs against various regions of human and murine genes were designed using the PrimerQuest software available at the Integrated DNA technologies website (**Tables 2-4**). The size of the PCR products range between 80 and 150 bp. Twenty microliter qPCR reactions containing 2x Maxima SYBR Green/ROX qPCR Master Mix (K0223, Fermentas), 250 nM of primers, and 3 µl of precipitated DNA were set up in Fast 96-Well Reaction Plates (4346907, Applied Biosystems). qPCR reactions were carried out in a StepOnePlus Applied Biosystems Real Time Instrument. Fold enrichment was calculated based on Ct as $2^{(\Delta Ct)}$, where $\Delta Ct = (Ct_{Input} - Ct_{IP})$. Final enrichment values were adjusted by subtraction of the nonspecific IgG antibody binding.

Table 1. Antibodies used for ChIP and Western Blot Analyses

EPITOPE	SOURCE	CATALOG NUMBER	AGAROSE IP
RNA Pol II (N-20)	Santa Cruz Biotechnology, Inc.	sc-899	Protein A
RNA Pol II CTD Ser5	Babco-Covance	MMS-134R	Protein M
RNA Pol II CTD Ser2	Babco-Covance	MMS-129R	Protein M
RNA Pol II 8WG16	Babco-Covance	MMS-126R	Protein M
Cdk9 (H-169)	Santa Cruz Biotechnology, Inc.	sc-8338	Protein A
NELF-A (A-20)	Santa Cruz Biotechnology, Inc.	sc-23599	Protein G
PU.1 (H-135)	Santa Cruz Biotechnology, Inc.	sc-22805	Protein A
PU.1/Spi-1 (T-21)	Santa Cruz Biotechnology, Inc.	sc-352	Protein A
TFIID (TBP) (SI-1)	Santa Cruz Biotechnology, Inc.	sc-273	Protein G
TBP	Abcam, Inc.	ab28175	Protein A
C/EBPβ (47A1)	Santa Cruz Biotechnology, Inc.	sc-56637	Protein G
H3 (tri methyl K36)	Abcam, Inc.	ab9050	Protein A
H3 (tri methyl K27)	Active Motif	39156	Protein G
H3 (tri acetyl K27)	Abcam, Inc.	ab4729	Protein A
H3 (mono methyl K9)	Millipore	07-450	Protein A
H3 (acetyl K9)	Upstate	07-352	Protein A
H3 (mono methyl K4)	Active Motif	39635	Protein G
H3 (tri methyl K4)	Active Motif	39915	Protein A
Histone H3 (FL-136)	Abcam, Inc.	ab1791	Protein A
BRD4	Abcam, Inc.	ab84776	Protein A
P300 (N15)	Santa Cruz Biotechnology, Inc.	Sc-584	Protein A/G^{+}
NFκB p65	Abcam, Inc.	ab7970	Protein A
Anti-proIL-1β	R&D Systems	MAB6964	(Western Blot)

Table 2. Human *IL1B* ChIP primer sequences

IL1B

Position*	Forward	Reverse
-3000	CCAAGGAAGTGGAACAAGCAGAGA	CCAAGGAAGTGGAACAAGCAGAGA
-2876	TCTCCTTGGGAAGACAGGATCTGA	ACCTGGACCCAAATCTGCTACCAT
-2790	ACATGGCAGAACTGTGGAGACTGT	ATAGCACAGTGTGGTTGAAGCAGC
-2329	TCCCTTCCTGTCACTGGCTTTGAT	TGCATGATCACAGCAGCCTCAAAC
-1520	ATCAGAAGGCTGCTTGGAGAGCAA	TGCATTATCCAAGGGAGTGAGCCT
-800	TAGGCAGAGCTCATCTGGCATTGA	ATTGCAGGAGCCTCTGAGGAGAAA
-279	TGTGTGTCTTCCACTTTGTCCCAC	CCTGACAATCGTTGTGCAGTTGATG
-223	TGTGGACATCAACTGCACAACG	TTCATGGAAGGGCAAGGAGTAGCA
-155	TTGCTACTCCTTGCCCTTCCATGA	GAGTATTGGTGGAAGCTTCTTAGGG
-91	CCCTAAGAAGCTTCCACCAATACTC	GCAGAAGTAGGAGGCTGAGAAA
-19	CCCTAAGAAGCTTCCACCAATACTC	GCAGAAGTAGGAGGCTGAGAAA
+36	AAACCTCTTCGAGGCACAAG	GAGCAATGAAGATTGGCTGA
+98	CAGCCAATCTTCATTGCTCA	GCATACACACAAAGAGGCAGAG
+160	CTCTGCCTCTTTGTGTGTATGC	GAGGGAAGGAGAGGGAGAGA
+223	TCTCCCTCTCCTTCCCTCTC	TTCCCAGAATATTTCCCGAGT
+271	GCCAGGTGTAATATAATGCTTATGACTCGG	GACACTAACCTTTAGGGTGTCAGC
+505	TGCACTGGATGCTGAGAGAAA	GGCTGCTTCAGACACCTGTG
+1031	AATCTGCCTTCTGGACTGTTCTGC	AAGAAACTGCAAACAGCCTGCCTC
+3325	AATCTCCGACCACCACTACAGCAA	AAGGGAAAGAAGGTGCTCAGGTCA
+4000	TCGACACATGGGATAACGAGGCTT	TGGAGGTGGAGAGCTTTCAGTTCA
+5389	ACTGCTGTGTCCCTAACCACAAGA	TTCAACACGCAGGACAGGTACAGA
+6268	TCGCTGCAGAGTGTAGATCCCAAA	TGCTTGAGAGGTGCTGATGTACCA
+7192	CCTCATTGCTGAGTGCTGCAAAGT	AGTGCTTCAGCTGATCCTGTTCCA

* Numbers indicate the midpoint of amplicons in relation to the TSS

Table 3. Human *TNF* ChIP primer sequences

TNF

Position *	Forward	Reverse
-243	CACAAATCAGTCAGTGGCCCAGAA	GGACACACAAGCATCAAGGATACC
-181	GGTATCCTTGATGCTTGTGTGTCC	CTGCACCTTCTGTCTCGGTTTCTT
-128	GGAGAAGAAACCGAGACAGAAGGT	CTTCCTTGGTGGAGAAACCCATGA
-98	ACTACCGCTTCCTCCAGATGAG	GGGAAAGAATCATTCAACCAGCGG
-50	CCGCTGGTTGAATGATTCTT	TGTGCCAACAACTGCCTTTA
-15	CCCAGGGACATATAAAGGCAGTTG	TGTCCTTGCTGAGGGAGCGT
+18	TTGGCACACCCAGCCAGCAGA	GGTCTGTAGTTGCTTCTCTCCCTCTT
+57	CCAGCTAAGAGGGAGAGAAGCAACTA	ATGTGGCGTCTGAGGGTTGTTT
+97	AAACAACCCTCAGACGCCACAT	TATGTGAGAGGAAGAGAACCTGCC
+145	AGGCAGGTTCTCTTCCTCTCACAT	TGCTTTCAGTGCTCATGGTGTCCT
+214	TGGAAAGGACACCATGAGCACTGA	TGAGGAACAAGCACCGCCT
+293	AGGCGGTGCTTGTTCCTCA	TCCAAAGTGCAGCAGGCAGAAGA
+473	TGGGTGAAAGATGTGCGCTGATAG	TTGCCACATCTCTTTCTGCATCCC
+1326	ATGTGTCTTGGAACTTGGAGGGCT	TATCCCACTAAGGCCTGTGCTGTT
+1806	TCAACCTCCTCTCTGCCATCAAGA	ATAGATGGGCTCATACCAGGGCTT
+2014	AGGACGAACATCCAACCTTCCCAA	TTTGAGCCAGAAGAGGTTGAGGGT

* Numbers indicate the midpoint of amplicons in relation to the TSS

Table 4. Human *JUNB* and *HIST1H4K* ChIP primer sequences

JUNB

Position *	Forward	Reverse
-96	CCGCTGTTTACAAGGACACG	GGAAGTGCGCTCCGATTG
+33	GGCTGGGACCTTGAGAGC	GTGCGCAAAAGCCCTGTC
+78	TGACTAGCGCGGTATAAAGGCGT	CGATAGCTTTCCTGGCGTCGTTT
+793	GGACGATCTGCACAAGATGA	TGCTGAGGTTGGTGTAAACG
+1157	CATCAAAGTGGAGCGCAA	TTGAGCGTCTTCACCTTGTC
+1969	CCAGCTCAGTGCTGTTGGT	ATCCAACCCTGGAGATCTGG

HIST1H4K

Position *	Forward	Reverse
+35	GACTCCTCTTGCTCGTCATGTCTG	CGCCTTTGCCAAGACCCT
+237	GGTGCTGAAGGTGTTCCTGG	CGCTTGGCGTGCTCTGTA
+382	GGTTGAGCGTCCCTTTCTATCAACA	TGGGCAAACAAGCATCACGG

* Numbers indicate the midpoint of amplicons in relation to the TSS

Table 5. Murine *Il1b* and *Tnf* ChIP primer sequences

Il1b

Position *	Forward	Reverse
-408	TGATGGAGAGCACAGAAGCACCAT	ACGTAGATGCACACCCAGAAGTGT
+ 31	ACAAGTTGGACAACAAACCCTGC	TACTTGCACAAGGAAGCTTGGCTGGA
+1126	AGGGACTCCTACAGATGCAATGGT	TGCTCTGGTTGCTCTCTGTTGACT
+ 3627	AAATCCAATGTTCTTGCCCAGCCC	TGCAAGCACTGTGAAGTGAAGCAG
+5169	GCCTTGGGCCTCAAAGGAAAGAAT	TAAAGGCAGAGTCTTCGGTGAGCA
+6478	ATAGCCCGCACTGAGGTCTTTCAT	CTCATCAAAGCAATGTGCTGGTGC

Tnf

Position *	Forward	Reverse
-404	TATGCACCCAGCTTTCAGAAGCAC	AGGACCCTGAGAACTGAAACCCAT
- 79	ACTACCGCTTCCTCCACATGAGAT	AGACGGCCGCCTTTATAGCCCTT
+ 15	CTCTTCCCCAAGGGCTATAAAGG	CTTGCTTTTCTGGGAGCTATTTCC
+ 71	ACTAGCCAGGAGGGAGAACAGAAA	AGTGAGTGAAAGGGACAGAACCTG
+ 797	AAAGAAGCCGTGGGTTGGACAGAT	AGAACTGATGAGAGGGAGGCCATT
+ 1585	AGCCGATGGGTTGTACCTTGTCTA	TGAGATAGCAAATCGGCTGACGGT
+2106	TCTCATGCACCACCATCAAGGACT	ACCACTCTCCCTTTGCAGAACTCA
+2937	GTACTGCAGTTCTTTCCGGCTGTT	TCTGTCTGTTCAGAGGCAGGTTGA

* Numbers indicate the midpoint of amplicons in relation to the TSS

RNA Expression Analyses

$1x10^6$ cells were plated into 6-well plates (353846, FALCON). Following treatments cells were transferred into 1.5 ml tubes and centrifuged at 3500 RPM for 3 min at room temperature. The cell pellets were resuspended in 500 µl of TRIzol reagent (15596-026, Invitrogen). After addition of 170 µl of Chloroform (C606-1, Fisher) samples were vortexed, incubated at room temperature for 15 min, and centrifuged for 15 min at 13000

RPM in 4°C chilled centrifuge. Aqueous layer was removed, combined with equal volume of Isopropanol (BP2632-4, Fisher), 1 µl of Glycogen (9510, Ambion), and centrifuged for 10 min 13000 RPM at 4°C. Sample pellets were washed with 500 µl of 75% Ethanol (111ACS200, Pharmaco-AAPER) and centrifuged for 10 min in room temperature at 14000 RPM. Air-dried pellets were resuspended in 30 µl of RNAse free water and subjected to DNAse treatments using Turbo DNA-*free* reagents (AM1907, Ambion) according to the manufacturer instructions in order to eliminate genomic DNA contamination. RNA was converted to cDNA using GoScript Reverse Transcription System (A5001, Promega). Relative expression levels were calculated using ΔΔCt method using *B2M* and *18srRNA* as an endogenous controls. In certain experiments RNA was directly subjected to an RT-PCR utilizing the Access RT-PCR system (A1250, Promega).

Transfection Constructs

Luciferase reporter XT-Luc *IL1B*, wild type IRF8 and mutant IRF8Y211F were as described (Unlu et al., 2007). Expression plasmids for wild-type C/EBPβ and the truncated C/EBPβΔSPL, were constructed and characterized as reported (Tsukada et al., 1994). Expression plasmids expressing wild-type Spi1 and the dnSpi1 deletion mutant were constructed as described (Galson et al., 1993; Kominato et al., 1995). The MHCκB-Luc reporter is as described (Mitchell and Sugden, 1995; Yoshida et al., 2004).

Table 6. mRNA analyses and qPCR primer sequences

Gene	Forward	Reverse
18srRNA	TAGAGGGACAAGTGGCGTTC	TCCTCGTTCATGGGGAATAA
hB2M	TGCTGTCTCCATGTTTGATGTATC	TCTCTGCTCCCCACCTCTAAGT
mB2M	GGCCTGTATGCTATCCAGAA	GAAAGACCAGTCCTTGCTGA
hIL1B	AATCTCCGACCACCACTACAGCAA	AAGGGAAAGAAGGTGCTCAGGTCA
Splice IL1B	TCTGTACCTGCTCTGCGTGTTGAA	GGGCAGACTCAAATTCCAGCTTGT
mIL1B	CCCAACTGGTACATCAGCAC	TCTGCTCATTCACGAAAAGG
hTNF	AAGCCCTGGTATGAGCCCATCTAT	ATGATCCCAAAGTAGACCTGCCCA
Splice TNF	AGTGACAAGCCTGTAGCCCATGTT	GTTATCTCTCAGCTCCACGCCATT
mTNF	CCCACTCTGACCCCTTTACT	TTTGAGTCCTTGATGGTGGT
hSPI1	CCAGCTCAGATGAGGAGGAG	GCTTGGACGAGAACTGGAAG
hC/EBPA	TGGCCAACTTCTACTACGAGG	AGAGGAAGTCGTGGTGCTGC
hC/EBPB	TACTACGAGGCGGACTGCTT	CGTAGTCGTCGGAGAAGAGG
p65	GGCGAGAGGAGCACAGATAC	CACTGTCACCTGGAAGCAGA
hIRF8	ACGAGGTTACGCTGTGCTTT	CCAGTCTGGAAGGAGCTGAC

Transient Transfections

293 cells were seeded into 24 well plates to 60-70% confluency. Reporter and expression plasmids were transfected into 293 cells with FUGENE 6 Transfection Reagent (11814443001, Roche) at 3 µl of reagent per µg of DNA, according to the manufacturer's instructions. Individual expression vectors were transfected as follows: 0.05 µg of Spi1 and 0.1 ug of TRAF6, IRF8, C/EBPβ, and NF-κB into 24 well plates containing 500 µl of media. Total amount of transfected DNA was maintained constant for each experiment by addition of empty vector. Endogenous *IL1B* studies were conducted in 6 well culture plates with the amount of transfected material adjusted 3 fold.

Luciferase Assays

At 24 hours after transfection, cells were lysed with 60 µl of 1X cell lysis buffer in each well (24 well plate) and shaken for 20 min at RT. 20 µl of supernatant from each well was used for luciferase assay using Luciferase Assay System (Promega E1501) and analyzed by Veritas Microplate Luminometer and Software.

Chromatin Conformation Capture (3C)

In brief, a total of $1.5x10^6$ cells were fixed in 2% formaldehyde (F79-500, Fisher) for 10 min at room temperature. Cross-linking was inhibited by addition of glycine to a final concentration 0.125 M. Cell pellets were collected into 15 ml Falcon tubes and washed twice with ice cold PBS and resuspended in Lysis Buffer (10mM Tris-HCl pH 8.0, 10 mM NaCl, 0.2% NP-40, supplemented with 1 mM PMSF, and protease inhibitor cocktail (Sigma) in 1:500 dilution) on ice for 90 min. Samples were centrifuged at 1800 rpm for 5 min, resuspended in 900 µl of 1.2xNEB4 (diluted with 0.3% SDS), and transferred into 1.5 ml Eppendorf tubes. Nuclear lysates were incubated for 1 hr at 37°C with moderate vortexing. 180 µl of Triton X-100 (final concentration of 1.8%) was added and samples were incubated for additional 1 hr at 37°C. Portion of chromatin (1 ug) was removed and treated overnight with MfeI (40 Unit) at 37°C. Lysates were treated with 1.6% SDS and incubated 60°C for 20 min. 47.5 µl of Lysates were used for ligation reaction (40 µl 10% Triton X-100, 40 µl ligase buffer (10x), 270 µl H2O, 2.5 µl T4 DNA ligase) that was carried out for 16 hours at 16°C. Next, 100 µg/ml of proteinase K was added to samples that were subsequently incubated overnight at 65°C. Next day, samples were treated with RNase A (0.5 µg/ml) for 30 min at 37°C and DNA was extracted. PCR products were amplified using following primers 1': 5'-GGG GCC TCC AAA TCA CTA AGC-3', 2:

5’-GCA TTG CCC CAT GGC TCC AAA AT-3’, 3’: 5’-TCT CTA CCT TGG GTG CTG TTC TC-3’, 4: 5’-CCG CTG TAA CGG GCA AAA GTT TC-3’. GoTaq PCR Core System I (M7660, Promega) was used for PCR analyses.

Site Directed Mutagenesis

XT-Luc binding site mutation reporter constructs: C/EBPβ I region binding site (XT-I c/g-Luc), NF-KB site at position -300 (XT-300κB-Luc), and the double I(c/g)/-300κB were generated using QuickChange XL Site-Directed Mutagenesis Kit (Stratagene 200516) using appropriately mutated primer sequences. Primer pairs listed in were used for site directed mutagenesis. The XT-I(c/g)-Luc plasmid was used as a template for generation of the double mutant (I region/-300 NF-κB site) construct. XT-300mut (F)/(R) were used as primers.

Table 7. Site-directed mutagenesis primer pairs

IL1B enhancer I region XT-I (c/g)-Luc primer pairs:	
I (c/g) F	5’CTGTGGAGACTGTTAGGTCAGGGGGCATTGC3’
I (c/g) R	5’GCAATGCCCCCTGACCTAACAGTCTCCACAG3’
NF-κB site (-300) mutation	
XT-300 F	5’AACATTCTTCTAACGTGTGAAAATACAGTATTTTAATGTGGACATC3’
XT-300 R	5’GATGTCCACATTAAAATACTGTATTTTCACACGTTAGAAGAATGTT3’

RESULTS

IL1B and *TNF* mRNA are Differentially Expressed in Monocytes

Steady-state mRNA kinetic profiles of the IE genes *IL1B* and *TNF* in a human cell line (THP-1) and human primary macrophages (hPBMCs), as well as a murine cell line (RAW 264.7), revealed differences in the transcriptional responses of these two genes. The expression profiles were assessed by various methods including agarose gel resolution of reverse transcribed (RT) PCR products (**Figure 6**) and Real Time Quantitative PCR (RT-qPCR) (**Figure 7**). *TNF* undergoes rapid induction and significant transcriptional shut down within a few hours of LPS treatment. In contrast, *IL1B* is also rapidly induced and then decreased, but is not completely switched off, continuing expression for many hours post-stimulation.

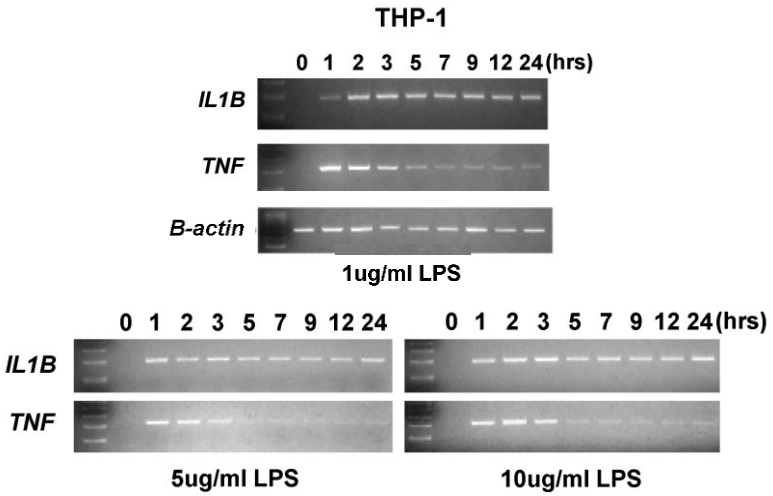

Figure 6. *IL1B* and *TNF* expression in LPS stimulated THP-1 cells.

THP-1 cells were stimulated with 1μg/ml of LPS for indicated time points and 3% agarose gels were used to resolve the band pattern of amplified products. Following a strong transient phase, the expression of *IL1B* decreases but is sustained for hours post stimulation. In contrast to *IL1B*, expression of *TNF* terminates 3 hours post stimulation after its initial transcriptional response. Increased dosage of LPS (5

μg/ml and 10 μg/ml) causes amplified and lengthened initial expression of the *IL1B* and *TNF* genes. The amplification of beta actin serves as a loading control.

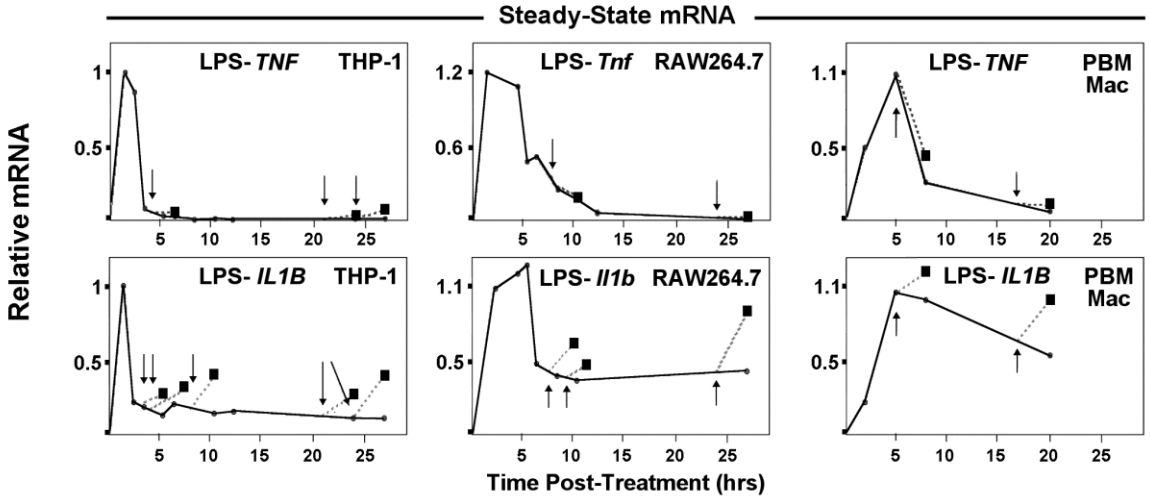

Figure 7. Comparison of *IL1B* and *TNF* Transcription in Monocytes.

Steady-state mRNA kinetics for *IL1B* and *TNF* transcripts in LPS stimulated THP-1, RAW264.7, and hPBMCs. Transcript levels were normalized to beta 2-microtubulin (*B2M*), and then as the ratio of amount in resting vs. LPS-treated cells. Circles denote mRNA levels for primary LPS challenge. Squares show transcript levels following re-stimulation as indicated by arrows. Data used for generation of this figure are presented in **Appendix A**.

Transient expression patterns for these two genes are reflective of their transcription status because of the short mRNA half-life mediated by AU-rich element (ARE) degradation (Chen et al., 1994; Fenton et al., 1988). ARE, localized within the 3' untranslated region of many pro-inflammatory genes influence their rapid degradation and/or repress their translation. Inhibitory properties of these elements are conveyed by the recruitment of ARE-binding proteins, which utilize various mechanisms for targeting and eliminating accumulating messages (Wu and Brewer, 2012). The stability of mRNA

is an important feature shaping the classical transient temporal pattern of the IE pro-inflammatory gene expression. As **Figure 6** reveals, an increased amount of LPS stimulus (from 5 to 10 μg/ml) caused a more robust and prolonged transient expression pattern of both genes.

Additional differences between these two genes were also apparent in resting human monocytes, in which basal levels of predominantly full-length unspliced *TNF,* but not *IL1B,* transcripts were detected (**Figure 8A**). Kinetic mRNA profiles within the first 3 hours revealed that *TNF* transcript production is 30 minutes faster than that of *IL1B* (**Figure 8B**).

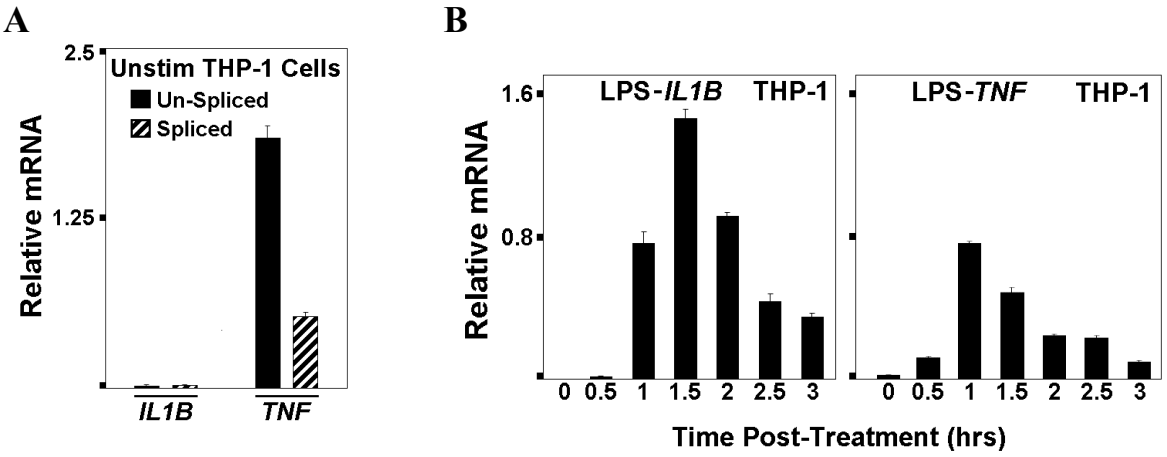

Figure 8. Analysis of *IL1B* and *TNF* mRNA splicing efficiency and expression kinetics in resting and stimulated THP-1 monocytes.

The *IL1B* and *TNF* gene expression data was normalized to the endogenous 18s ribosomal RNA (18s rRNA) gene expression. **(A)** qPCR data comparing the splicing efficiency of *IL1B* and *TNF* mRNA in resting THP-1 cells. cDNA samples were prepared using random primer directed reverse transcription. Selective amplicons were designed for the detection of un-spliced/primary (primers targeting sequence within a single intron) and spliced (spanning the last intron and splice site) transcripts. **(B)** qPCR analysis of LPS-treated human THP-1 monocytes (High resolution 0-3 h kinetics).

Semi-quantitative analysis revealed that approximately 20% of these rapidly accumulated *TNF* messages appear to be incompletely processed primary transcripts (**Figure 9A, B, C**).

A

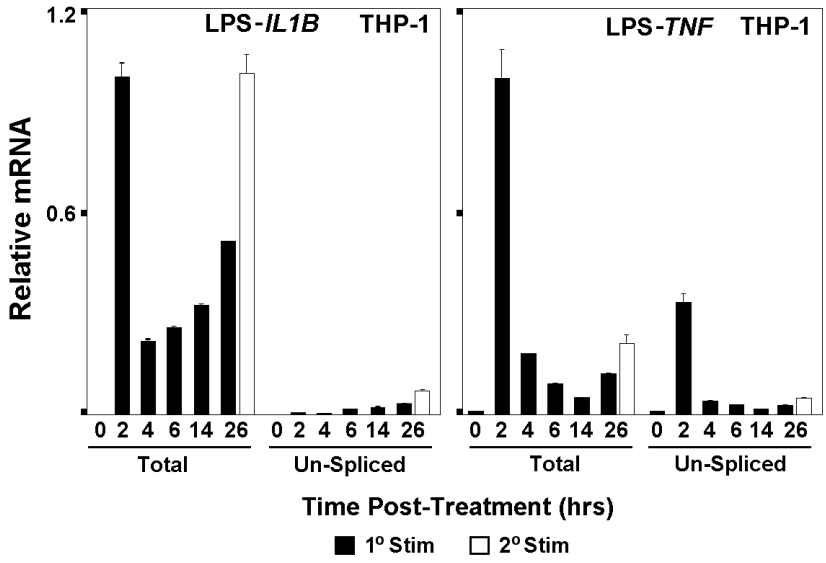

B

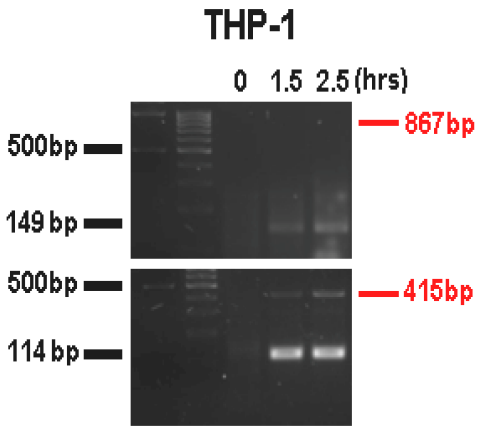

C

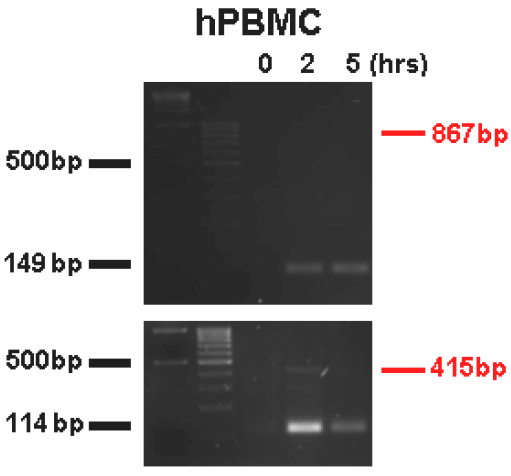

Figure 9. Un-spliced *TNF* transcripts in LPS treated THP-1 cells and hPBMC.

(A) *IL1B* and *TNF* mRNA splicing efficiency in LPS stimulated THP-1 cells and hPBMCs, as measured by comparing the total (amplicons designed within a single exon containing both spliced, and un-spliced products) vs. un-spliced/primary (within single intron) transcripts. The qPCR data are normalized to the endogenous 18srRNA levels. Shown are 3% agarose gels resolving the presence of spliced and/or un-spliced mRNAs of *IL1B* (top gel) and *TNF* (bottom gel) genes expressed in LPS treated THP-1 cells **(B)** and human primary macrophages **(C)**. Black labels indicate the 500 bp reference marks and the sizes of properly spliced mRNAs (149 for *IL1B*, and 114 for *TNF*). The red numbers denote the expected size of the intron-retaining unspliced transcripts (867bp for *IL1B* and 415bp for *TNF*). Retention of the intron sequence within the *TNF* gene causes a 301 bp shift and creates an additional lower intensity band at the 415 bp mark.

RNA polymerase II (Pol II) ChIP-qPCR was employed in order to directly measure the transcriptional status of *IL1B* and *TNF* in monocytes. Series of primer pairs scanning throughout the promoter proximal regions and structural parts of the genes were designed to accurately characterize the binding enrichment of Pol II and various factors at the *IL1B* and *TNF* loci (**Figure 10A)**.

A

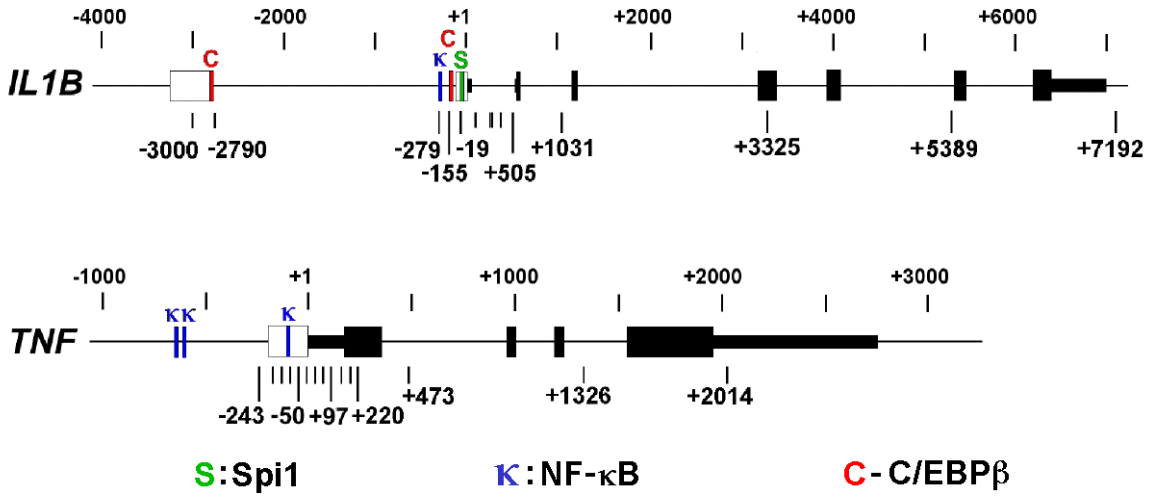

B

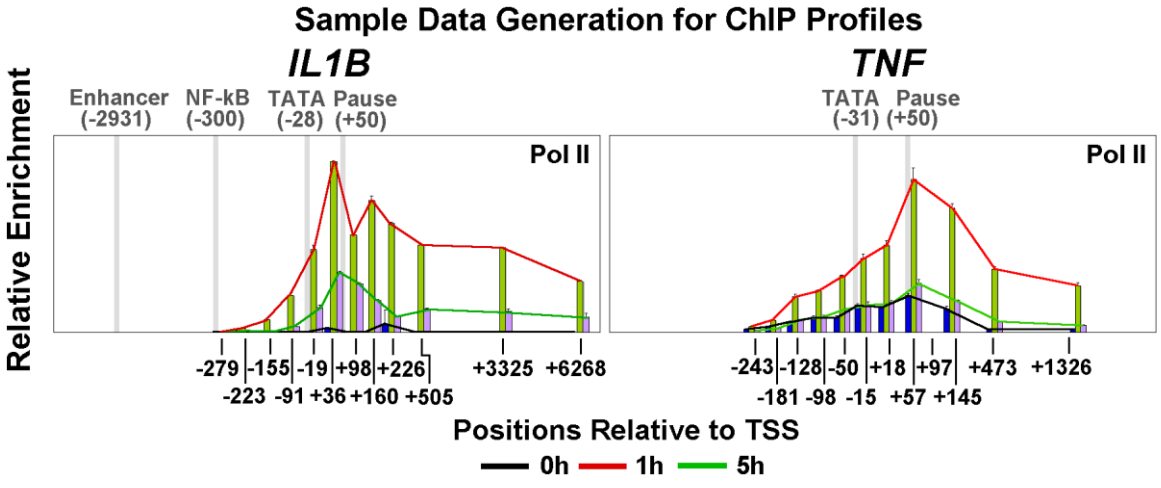

Figure 10. Schematic representation of ChIP-qPCR amplicons and generation of the data profiles for resting (0h), 1h, and 5h LPS treated THP-1 cells.

(A) Schematic of *IL1B* and *TNF* gene structures showing exons (solid boxes), positions of ChIP amplicons (midpoint relative to TSS), and important transcription factor binding sites (**C**: C/EBPβ, **κ**: NF-κB, and **S**: Spi1) within regulatory regions (open boxes). **(B)** Illustration of a sample Pol II ChIP used for generation of a representative diagram. Each colored line tracing the ChIP enrichment bars, represents a specific LPS treatment time point 0h (black), 1h (red), and 5h (green). This color-coding is used in all figures that contain similar kinetic ChIP data. The enrichment values were normalized to the input DNA in all ChIP experiments. ChIP data presented are representative of at least 2 independent experiments.

The bar graphs obtained from ChIP-qPCR experiments were used to generate the diagrams that represent the average enrichment data sets. **Figure 10B** illustrates a tracing pattern for a sample Pol II experiment. Pol II occupancy kinetics, particularly in the THP-1 cells (**Figure 11**), mimic the respective steady-state mRNA profiles confirming that the sustained expression of *IL1B* shown in **Figure 11** is a result of a continuous polymerase engagement and not necessarily an increase in mRNA stabilization.

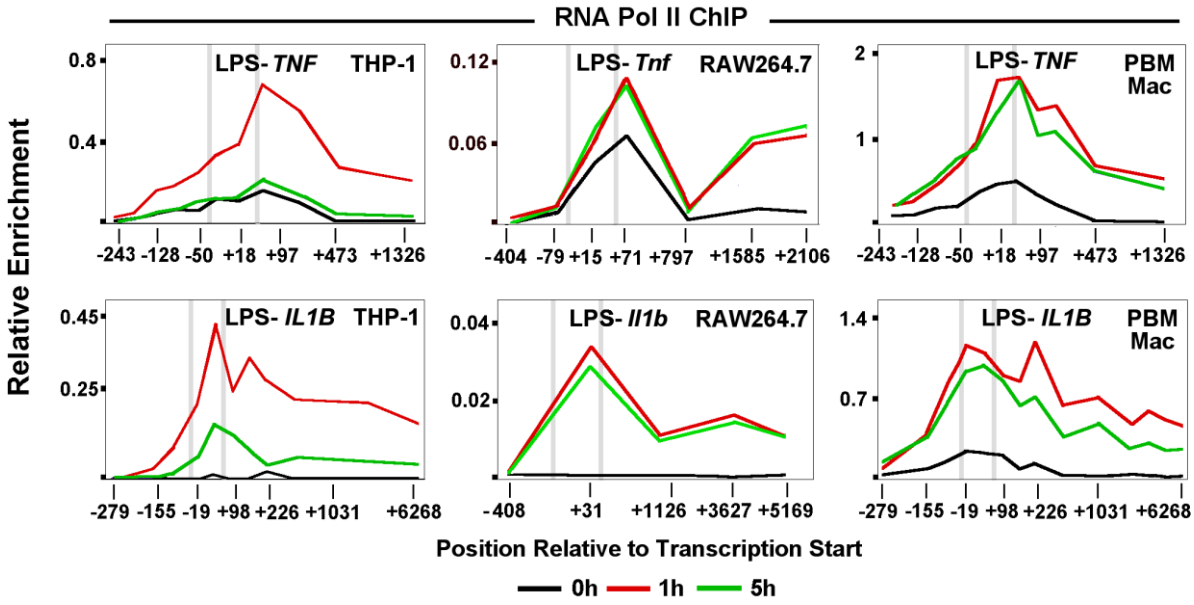

Figure 11. Pol II occupancy at the *il1b* and *tnf* loci.

Pol II ChIP throughout the *il1b* and *tnf* loci in resting (black), 1h (red), and 5h (green) LPS stimulated THP-1, RAW264.7, and hPBMC cells. Vertical gray bars locate the positions of important gene *landmarks*. These include TATA box and the canonical Pol II pause position (approximately 30 bp upstream and 50 bp downsteam of TSS, respectively). Data used for generation of this figure are presented in **Appendix B**.

Further kinetic analysis of the transient phase of THP-1 cell gene activation revealed a 15 minute delay in Pol II recruitment to *IL1B* (**Figure 12)**, consistent with the

observed 30 min delay seen in mRNA profiles (**Figure 8B**). Increased Pol II binding at the *TNF* promoter was detected as early as 15 min post-stimulation (**Figure 12)**. Of note, the transient nature of Pol II enrichment in RAW264.7 cells and human primary macrophages is less apparent due to the prolonged early phase of *IL1B* and *TNF* transcription in these cells (**Figure 7**).

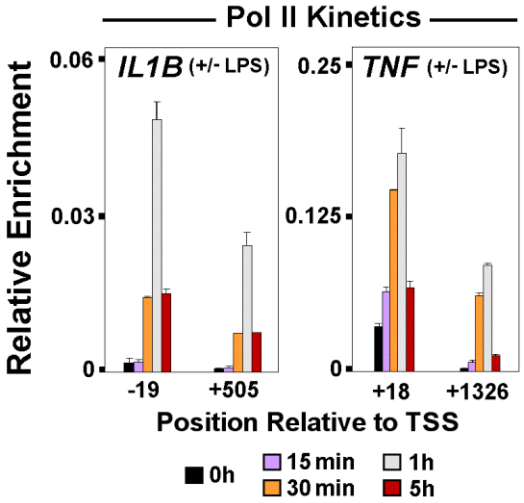

Figure12. Kinetic ChIP analysis of Pol II recruitment to the *IL1B* and *TNF* gene promoters.

Pol II recruitment was measured at the promoter region and a downstream site for *IL1B* and *TNF* in resting or LPS stimulated monocytes. The indicated time points underneath the graph correspond to the LPS treatment kinetics used for the ChIP assay.

I next asked, whether the observed differential shutdown of these two immune genes contributes to their ability to be resistant to reinduction (tolerized), when exposed to a secondary LPS stimulus. A previous report argued that murine *Ilib* and *Tnf* are refractory to reactivation due to a plethora of intrinsic immuno-protective mechanisms commonly recognized as endotoxin tolerance (Foster et al., 2007). Endotoxin tolerance results in a decreased responsiveness of certain rapidly-induced monocyte genes to

repeated LPS stimulation. In my reactivation experiments, cell cultures were stimulated with LPS for indicated times with an equal dose of secondary LPS (**Figure 7**, arrows and boxes) administered for 2.5 hours to unwashed cultures, prior to assay (**Figure 7**, dotted lines). In agreement with the earlier report, my data indicate that *tnf* genes are tolerized, so that once activated they cannot be re-expressed by additional LPS treatment. In contrast to that report, transcription of *il1b* remained significantly inducible after repeated LPS exposure, as shown in murine and human cell lines and human primary macrophages (**Figure 7**). Additional experiments revealed that increased LPS concentrations used for secondary stimulation (4.5 μg/ml and 9.5 μg/ml) did not affect the *tolerant* nature of *TNF*. **Figure 13** illustrates and further validates that *TNF* is rapidly shut down at 3 hours post stimulation and does not reactivate with subsequent LPS stimulus.

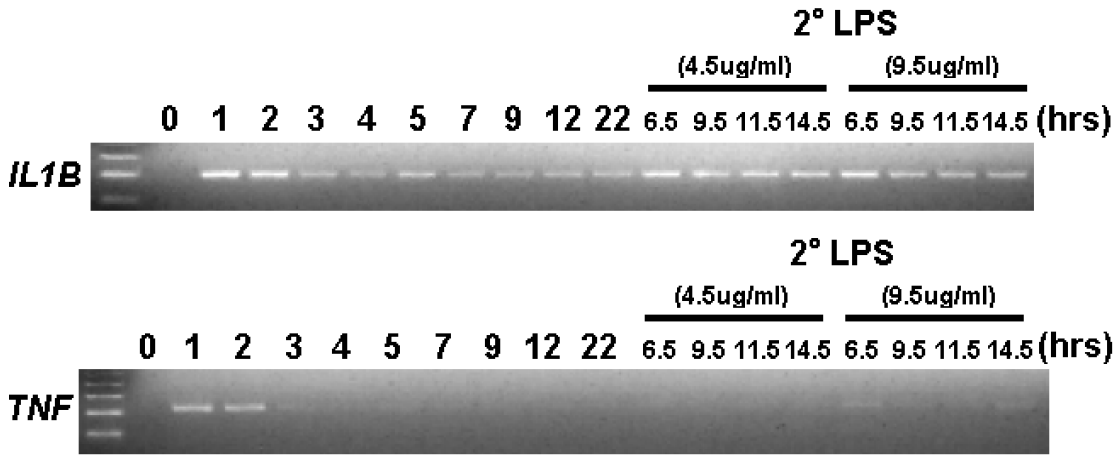

Figure 13. *TNF* expression is desensitized in THP-1 cells.

Cell cultures were initially stimulated with a low amount of LPS (0.5 μg/ml) for indicated times. Two increased doses of secondary LPS (4.5 μg/ml or 9.5 μg/ml as indicated) were administered for 2.5 hours to unwashed cultures, prior to assay. 3% agarose gel was used to resolve the RT-PCR products.

Pol II Pausing and the P-TEFb:NELF Axis Contribute to Differential Transcriptional Shutdown of *IL1B* and *TNF*

Pol II recruitment and pre-initiation complex assembly at IE gene promoters has recently been associated with the presence of pre-bound, paused, Pol II (Gilchrist et al., 2010; Gilchrist et al., 2008; Guenther et al., 2007; Kininis et al., 2009; Min et al., 2011; Muse et al., 2007; Rahl et al., 2010; Zeitlinger et al., 2007). These genes are associated with immediate responsiveness to stimuli, with rapid expression dependent on the release of Pol II from its pre-induced paused state (Wu and Snyder, 2008). In this way, pre-loaded polymerases likely facilitate synchronized and rapid transcription of IE genes. Since the *il1b* and *tnf* genes are transcribed almost instantly in activated monocytes, Pol II enrichment on their promoters was examined. In agreement with a previous report for murine macrophages (Adelman et al., 2009), *TNF* exhibited a significant Pol II presence approximately 50 bp downstream of the TSS in resting THP-1 cells and human primary macrophages (**Figure 11**). Surprisingly, less preloaded Pol II was detected on *IL1B* than on *TNF* in unstimulated monocytes. LPS activation caused increased levels of Pol II signal at the promoter proximal region and throughout the transcribed regions of both genes, consistent with elongating Pol II. Following cell activation, a large increase of paused Pol II at the *IL1B* promoter was evident in all three cell types (**Figure 11**). A more precise fragmentation of genomic DNA and appropriate design of qPCR amplicons are vital components of ChIP studies that influence the final resolution of the enrichment data. My initial ChIP experiments using a sparsely designed qPCR amplicons yielded useful and consistent information about the kinetic associations of various molecules but lacked the spatial resolution of their binding. **Figure 14** shows a few samples of low-

resolution ChIP experiments used to detect recruitment of various factors to the *IL1B* and *TNF* genes.

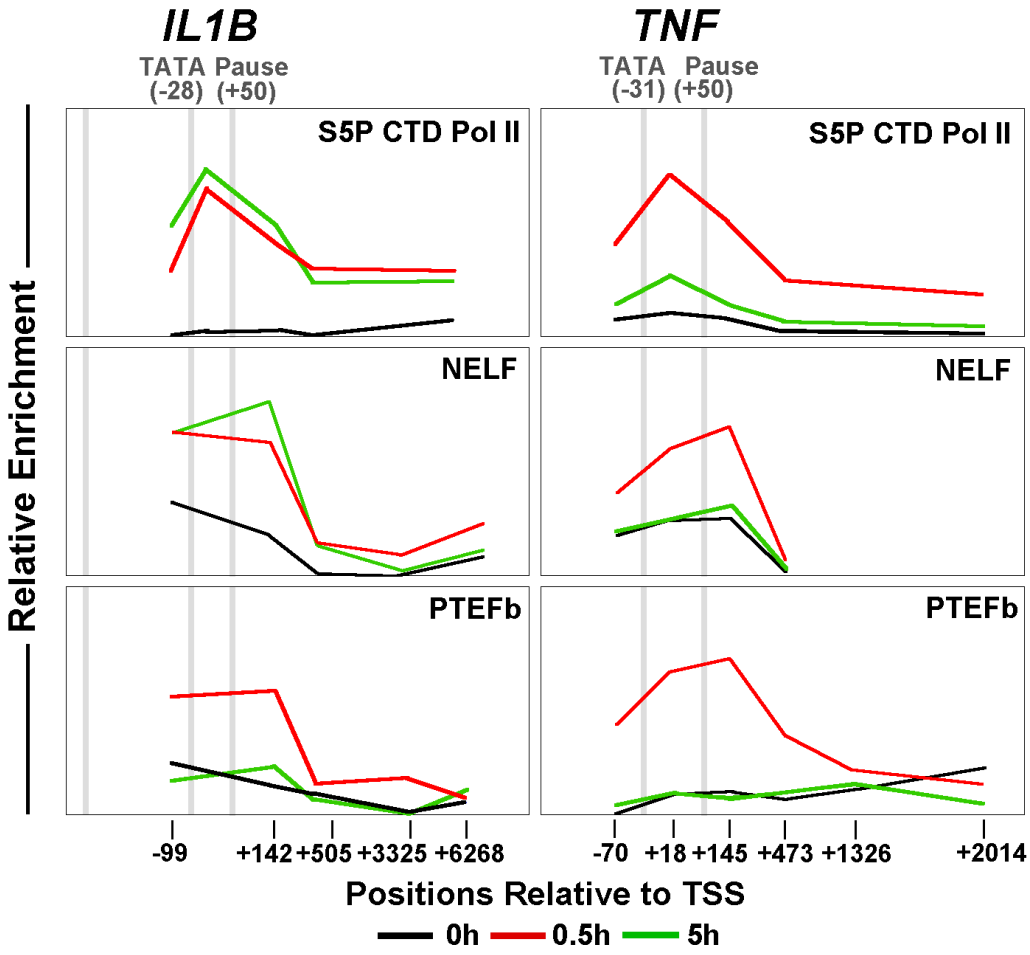

Figure 14. Low resolution ChIP profiles for *IL1B* and *TNF*.

Illustrated are low-resolution ChIP profiles for Pol II S5P CTD, and the transcription elongation factors NELF and P-TEFb. Association of these individual molecules with the *IL1B* and *TNF* was measured at indicated LPS treatment time points (0h-black, 0.5h-red, 5h-green). These data can be compared to another independent experiment (**Figure 17**) that was executed using high-resolution primers depicted in **Figure 15**.

In order to improve the spatial data quality I designed a new set of high-density qPCR amplicons that selectively target the promoter proximal region of *IL1B* and *TNF* genes (**Figure 15**). As **Figure 16** illustrates, the sonication method used in this study

yielded DNA fragments with average length of 250-300 bp. Statistical evidence, as well as experimental testing revealed that such fine chromatin fragmentation and appropriate size of qPCR amplicons provide sufficient resolution for qPCR-ChIP analysis used in this study (Xie et al., 2008).

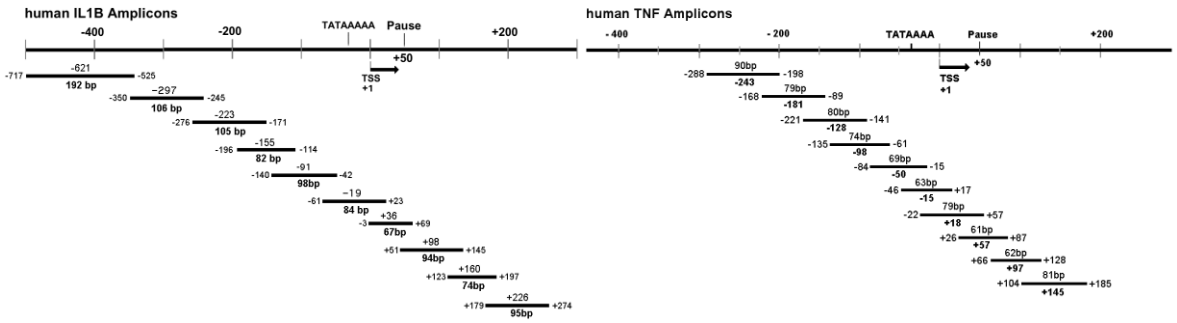

Figure 15. High-density qPCR-ChIP amplicons encompassing the promoters of the *IL1B* and *TNF* genes.

Illustrated is a series of qPCR amplicons, average length of 80 bp, designed for high resolution ChIP analyses.

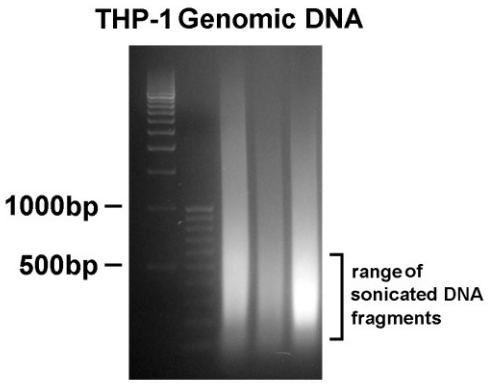

Figure 16. Analysis of the chromatin fragmentation.

Shown is a 1.5% agarose gel analysis of the sonicated genomic DNA isolated from THP-1 cells. The DNA fragments obtained by this sonication method have an average length of 250-300 bp.

Figure 11 revealed a differential spatial distribution of bound Pol II complexes for *IL1B vs. TNF*, represented by two promoter-proximal peaks located approximately 150 base pairs apart for *IL1B*, and a single peak for *TNF*. The single Pol II peak on *TNF* (centered at +57) and the first on *IL1B* (centered at +36) map near the TSS. This is consistent with a paused polymerase (Core and Lis, 2008). Analysis of TBP revealed an expected peak upstream of the Pol II complexes located to the TATA box of both genes. Differential amounts of TBP binding between *IL1B* and *TNF* in resting and induced cells agrees with and further supports differential Pol II pre-association for these genes (**Figure 17**). *TNF* contains significant amount of pre-bound TBP in resting monocytes and its levels further increase upon LPS stimulation. On the other hand *IL1B* lacks pre-bound TBP and its *de novo* recruitment is primarily dependent upon LPS stimulus (**Figure 17**).

JunB, an IE gene known to have pre-associated promoter-proximal Pol II (Aida et al., 2006; Fujita et al., 2009; Muse et al., 2007) and *HIST1H4K*, encoding a constitutively expressed "housekeeping" gene, Histone 4, whose Pol II levels remain constant in resting and LPS treated THP-1 cells serve as controls (**Figure 18**).

During induction of IE genes, Pol II transitions from paused into an elongating polymerase in order to generate mRNA intermediates. An actively elongating Pol II is associated with characteristic post-translational modifications and a presence of unique proteins. I have analyzed several of the distinguishing features in order to define changes that correspond to the LPS induced release of paused Pol II in stimulated monocytes.

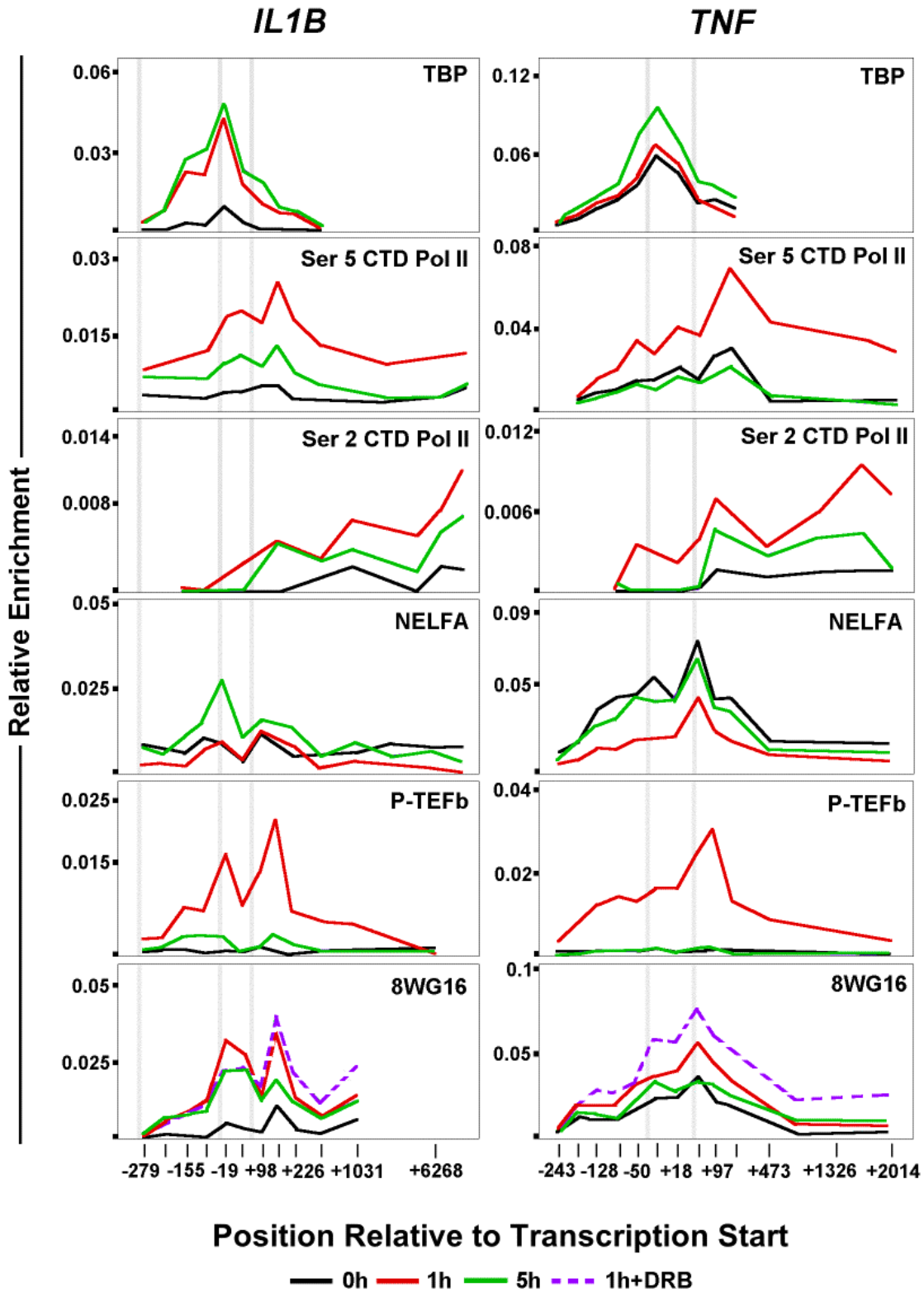
IL1B
TNF
TBP
Ser 5 CTD Pol II
Ser 2 CTD Pol II
NELFA
P-TEFb
8WG16
Relative Enrichment
0.06
0.03
0.12
0.08
0.04
0.015
0.014
0.008
0.012
0.006
0.05
0.025
0.09
0.1
-279 -155 -19 +98 +226 +1031 +6268
-243 -128 -50 +18 +97 +473 +1326 +2014
Position Relative to Transcription Start
0h
1h
5h
1h+DRB

Figure 17. Distribution of factors relevant to differential transcriptional regulation.

ChIP for factors related to Pol II initiation and elongation at *IL1B* and *TNF* loci in THP-1 cells was measured at distinct time points in resting (black), 1h (red) and 5h (green) LPS stimulated THP-1 cells. Enrichment profiles for TBP, S5P CTD Pol II, S2P CTD Pol II, NELF, P-TEFb and Pol II (using alternative 8WG16 antibody) are shown. A purple dotted line in the 8WG16 (bottom panels) experiment represents a 1-hour time point, in which THP-1 cells were pre-treated with the P-TEFb inhibitor 5,6-dichloro-1-beta-D-ribofuranosylbenzimidazol (DRB) prior to stimulation with LPS. Data used for generation of this figure are presented in **Appendix C**.

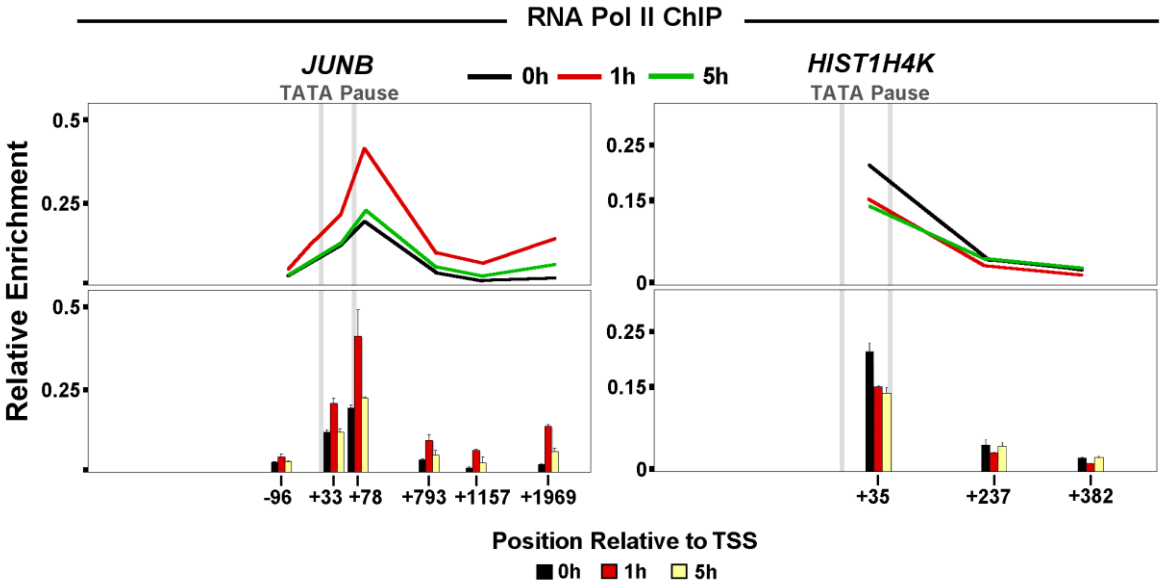

Figure 18. ChIP analysis for Pol II enrichment at control genes *JUNB* and *HIST1H4K*.

Pol II occupancy kinetics on *JUNB* and *HIST1H4K* genes in resting (black), 1h (red), and 5h (green) LPS stimulated THP-1 cells. Data (*upper panels*) used to generate Pol II kinetic profiles are shown in the lower panels.

The carboxy-terminal domain (CTD) of the RPB1 subunit of mammalian Pol II containing 52 tandem heptapeptide repeats with the consensus sequence YSPTSPS, was demonstrated to be differentially phosphorylated in paused *vs.* actively elongating Pol II. Phospho-serine 5-modified CTD (S5P) locates primarily to the upstream regions of genes as part of engaged, but stalled, Pol II. The cyclin-dependent kinase 7 (CDK7) component of the general transcription factor TFIIH mediates this phosphorylation (Egloff and Murphy, 2008), which aids in the process of methylguanosine cap addition to the 5' end of nascent mRNAs (Brookes and Pombo, 2009). I observed that the enrichment of S5P polymerase is confined to the 5' promoter proximal regions and decreases throughout the gene bodies of *IL1B* and *TNF* (**Figure 17**). S5P Pol II ChIP also revealed two 5' proximal

peaks, supporting the presence of two Pol II complexes at the *IL1B* promoter. Phosphorylated CTD serine 2 (S2P) marks elongating polymerases and mediates the recruitment of various factors responsible for proper mRNA co-transcriptional processing, including splicing and 3' poly-A addition (Buratowski, 2003). Pol II S2P ChIP confirmed the presence of elongating polymerase in LPS stimulated monoctyes, having a characteristic enrichment profile in which the signals increased towards the 3' end of both genes. Negative elongation factor (NELF) interacts with paused polymerases and contributes to stalling by a proposed interaction with nascent RNA emerging from Pol II *via* its RNA recognition motif (Gilchrist et al., 2008; Wu et al., 2003; Yamaguchi et al., 2002). The negative effects of NELF are relieved by positive transcription-elongation factor-b (P-TEFb), a complex of CDK9 and cyclin T1. By simultaneously phosphorylating NELF and the S2P CTD, signal dependent recruitment of PTEF-b leads to Pol II release from a paused state into one of elongation during pro-inflammatory responses in murine macrophages (Hargreaves et al., 2009). **Figure 17** shows kinetic profiles for various indicators of transcription elongation following LPS treatment of THP-1 cells. Increased binding of NELF to paused Pol II at the *TNF* promoter is diminished within an hour of LPS stimulation. As induced transcription concludes, around five hours post stimulation, NELF binding to *TNF* returns to pre-stimulation levels. NELF ChIP for the *IL1B* promoter revealed a distinct binding pattern with increased enrichment values at later time points. I did not see significant NELF enrichment in unstimulated cells. Although surprising at first, this supports the low level of paused Pol II in resting cells, and its existence in LPS stimulated monocytes. P-TEFb is coordinately recruited to the promoters of both genes. Treatment of cells with the

P-TEFb inhibitor 5,6-dichloro-1-beta-D-ribofuranosylbenzimidazol (DRB) caused an increase in Pol II at the proposed pause sites, as confirmed by an alternative Pol II antibody (8WG16), confirming the significance of P-TEFb in inducible control of *IL1B* and *TNF* (**Figure 17**). It has been reported that the 8WG16 antibody was specifically designed for detection of non-S2P phosphorylated CTD tail of Pol II (Brookes and Pombo, 2009). My data correspond to an expected 8WG16 ChIP enrichment profile for the paused genes with a peak at the promoter proximal region, which drops off towards the 3' end (**Figure 17**). Kinetic differences in P-TEFb recruitment to *IL1B* vs. *TNF* were also observed in LPS treated monocytes. In contrast to *TNF*, a rapid P-TEFb recruitment is prolonged (although decreased) on *IL1B* at 5 hours post stimulation. This provides an explanation for the delayed/sustained phase of *IL1B* expression as compared to that of *TNF*. The data argue for a kinetic interplay between positive (P-TEFb) and negative (NELF) pausing factors that may contribute to the differential post-induction decrease and shutdown of these two immediate-early genes. ChIP analysis of Pol II dynamics was also expanded to the murine *il1b* and *Tnf* genes. Similar profiles of positive and negative elongation factors and the Pol II modifications were observed for RAW264.7 cells (**Figure 19**) as well as bone marrow derived macrophages (BMDM) (**Figure 20**). As revealed in steady state mRNA analysis, the initial phase of *Il1b* and *Tnf* transcription is prolonged (**Figure 7**). Since the Pol II binding profiles mimic this transcriptional phenomenon, the transient nature of Pol II enrichment in these cells is less apparent (**Figure 19, 20**). I observed that Pol II is pre-loaded on *Tnf* in similar fashion as in its human counterpart. Following LPS treatment, rapidly recruited P-TEFb induces *Tnf* elongation by inducing NELF discharge and S2P of Pol II CTD.

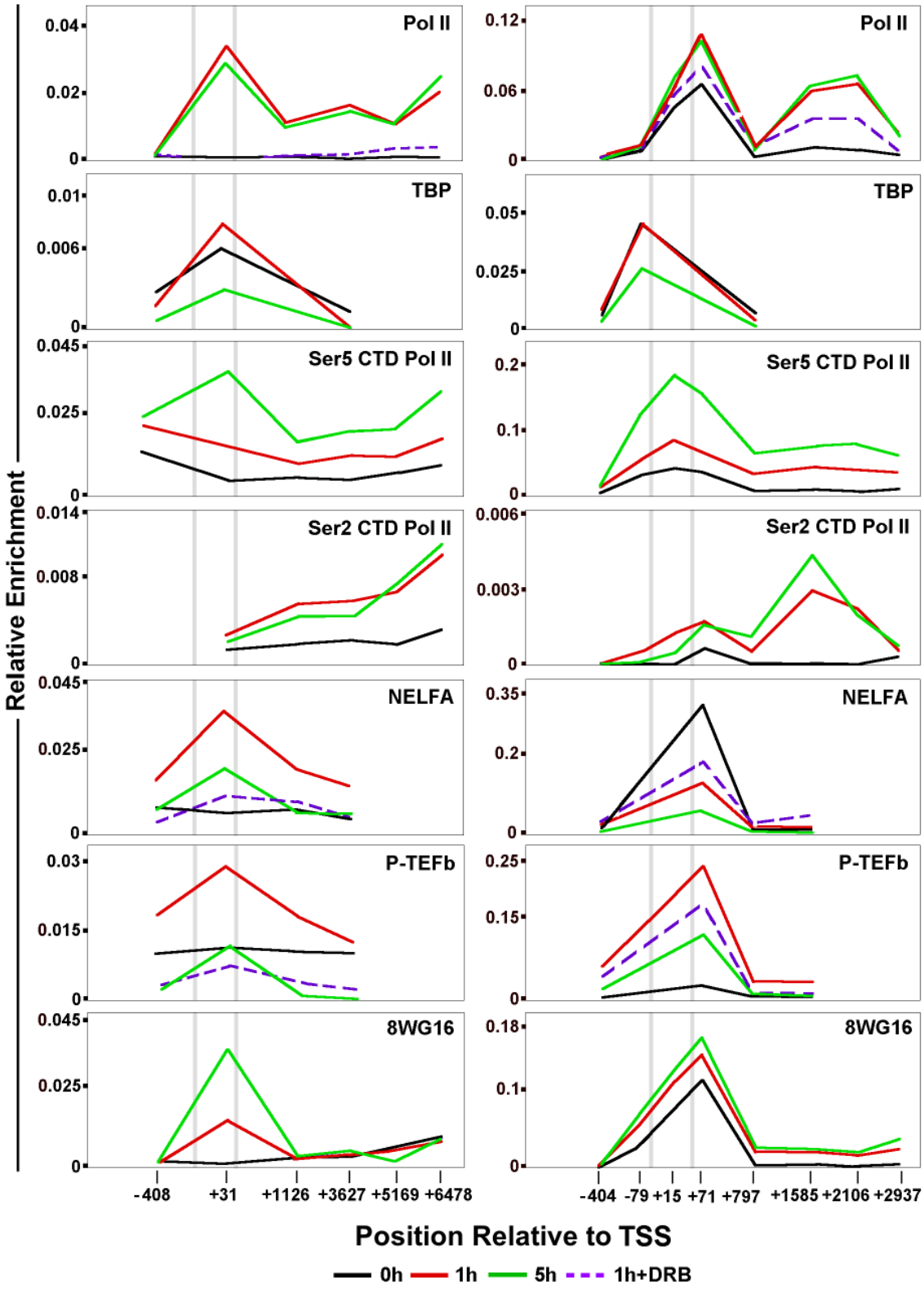
Relative Enrichment
Pol II
TBP
Ser5 CTD Pol II
Ser2 CTD Pol II
NELFA
P-TEFb
8WG16
0.04
0.02
0
0.12
0.06
0.01
0.006
0.05
0.025
0.045
0.2
0.1
0.014
0.008
0.003
0.35
0.03
0.015
0.25
0.15
0.18
-408
+31
+1126
+3627
+5169
+6478
-404
-79
+15
+71
+797
+1585
+2106
+2937
Position Relative to TSS
0h
1h
5h
1h+DRB

Figure 19. Average profiles of factors relevant to differential transcriptional regulation in LPS-treated RAW264.7 cells.

ChIP for factors related to Pol II initiation and elongation at *Il1b* and *Tnf* loci in RAW264.7 cells was measured at distinct time points in resting (black), 1h (red) and 5h (green) LPS stimulated THP-1, cells. Enrichment profiles for Pol II, TBP, S5P CTD Pol II, S2P CTD Pol II, NELF, P-TEFb and Pol II (using alternative 8WG16 antibody) are shown. A purple dotted line in the 8WG16 (bottom-most panels) experiment represents a 1-hour time point, in which RAW264.7 cells were pre-treated with the P-TEFb inhibitor 5,6-dichloro-1-beta-D-ribofuranosylbenzimidazol (DRB) prior to stimulation with LPS. Data used for generation of this figure are presented in **Appendix D**.

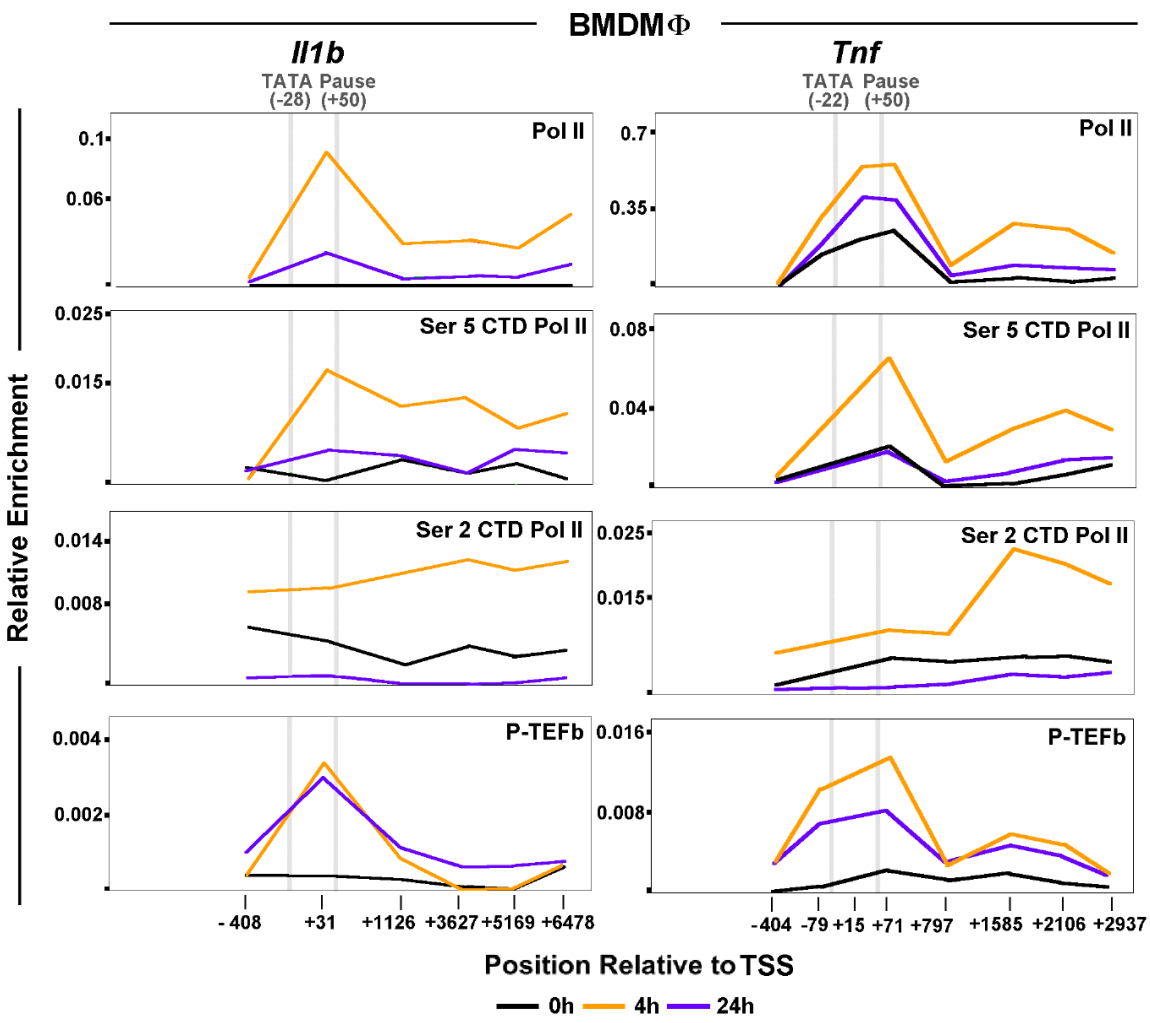

Figure 20. Average profiles of various factors relevant to differential transcriptional regulation in *ex vivo*-differentiated LPS-treated BMDM.

ChIP for factors related to Pol II initiation and elongation at *Il1b* and *Tnf* loci in RAW264.7 cells was measured at distinct time points in resting (black), 4h (yellow) and 24h (blue) LPS stimulated *ex vivo*-differentiated BMDM. Enrichment profiles for Pol II, S5P CTD Pol II, S2P CTD Pol II, and P-TEFb are shown. The bar graph ChIP enrichment data used for generation of this figure are presented in **Figure 60**.

Consistent with the THP-1 study, murine *Il1b* does not contain NELF-mediated paused Pol II complex in resting monocytes, and its induction relies on the *de novo* recruitment of Pol II. The characteristic peak of Pol II enrichment in the vicinity of TSS in LPS stimulated cells indicates a presence of rate limiting step controlling the release of stalled polymerase. As reported for THP-1 cells, P-TEFb mediates this transition in murine monocyte/macrophages (**Figure 19, 20**).

LPS Triggers a Double Pol II Pause on *IL1B*

Various ChIP binding profiles including total Pol II, S5P CTD Pol II, NELF and P-TEFb collectively revealed two pausing sites near the *IL1B* gene promoter. This prompted investigation of whether these two complexes are associated with either short aborted transcripts, or Pol II dwelling. High-density amplicons designed for ChIP (**Figure 15**) were used for RT-qPCR amplification of random primer-generated cDNA samples from resting and stimulated monocytes. Genomic DNA was used for the analysis of primer pair PCR efficiency (**Figure 21)**. This technique provided sufficient resolution for measuring transcriptional activity of Pol II within the observed Pol II ChIP peaks. Amplicons specific for the DNA upstream of the TSS served as controls, registering negligible signals. Semi-quantitative transcription profiles revealed peaks of short transcripts corresponding to the sites of engaged, but stalled, Pol II (**Figure 22**). These data represent appropriate measurements of nascent transcript production by Pol II, as they convey consistent inducible and temporal expression patterns (**Figure 22***, upper panels*). Production of these RNA intermediates is sensitive to inhibitor treatments (**Figure 22***, lower panels*).

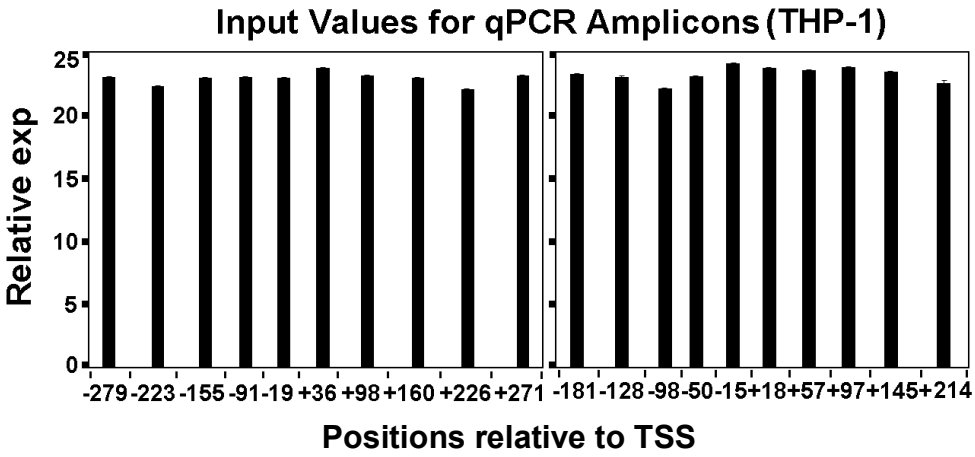

Figure 21. Analysis of promoter proximal qPCR amplicon efficiency.

Genomic DNA from THP-1 cells was used to determine the amplification efficiency of a series of primers designed for ChIP-qPCR analysis as well as random primer generated cDNA analysis. For this analysis 10% of chromatin used for antibody precipitation, equal to $4x10^5$ THP-1 cells was used.

The inhibitors used for this experiment abolish activation of the transcription factors NF-κB (MG 132) and C/EBPβ (U0126). While NF-κB is the primary activator of *TNF*, both NF-κB and C/EBPβ are required for efficient transcription of the *IL1B* gene, which is consistent with the inhibitor effects on mRNA levels shown in **Figure 22**. In agreement with observed Pol II ChIP data, the presence of basal transcription for *TNF* in unstimulated monocytes was further confirmed utilizing this technique. Data sets for *TNF* closely resembled the classically paused *JunB* gene (**Figure 22**). Since the second Pol II peak on *IL1B* was not associated with a significant level of nascent RNA signal, it is possible that these Pol II complexes represent resting/dwelling polymerases, and not the presence of two transcription initiation sites. Contrary to the inducible *IL1B, TNF*, and *JunB* profiles, the control *HIST1H4K* gene transcript amplification shows constitutive expression (**Figure 22**).

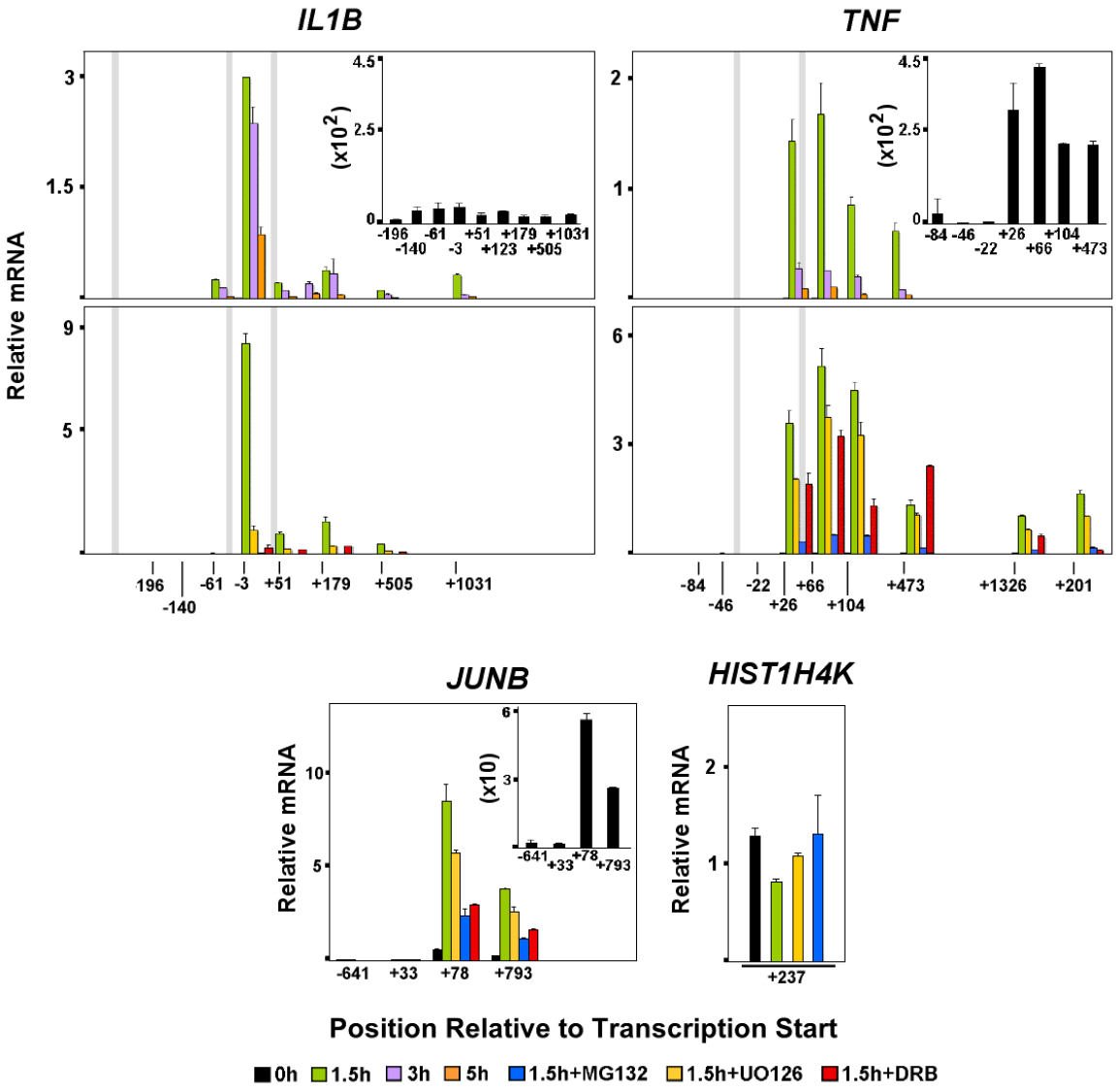
IL1B
TNF
JUNB
HIST1H4K
Relative mRNA
(x10^2)
(x10)
Position Relative to Transcription Start
0h
1.5h
3h
5h
1.5h+MG132
1.5h+UO126
1.5h+DRB

Figure 22. Steady-state mRNA kinetics for *IL1B*, *TNF*, and control gene transcripts in LPS stimulated THP-1 cells.

cDNA prepared form THP-1 cells, stimulated with LPS at different time points and/or pre-treated with various inhibitors was subjected to qPCR analysis using high-resolution primers spanning the promoter proximal regions of *IL1B* and *TNF*. Transiently induced *JUNB* and constitutively expressed *HIST1H4K* were used as controls for this experiment. Black bar graphs located in the upper corners of the diagrams represent magnification of mRNA in unstimulated THP-1 cells due to the fact that their levels are extremely low (*TNF*) or absent (*IL1B*) in comparison to the 1.5h LPS activated monocytes. The inhibitors MG132 (blue bars) and U0126 (yellow bars) were used to inhibit the activation of transcription factors NF-κB and C/EBPβ. While NF-κB is the primary activator of *TNF*, both NF-κB and C/EBPβ are required for efficient induction of the *IL1B* gene. The red bars represent samples that were pre-treated with the P-TEFb inhibitor DRB, which interferes with the transition of Pol II into transcription elongation.

Pol II S2P CTD Differentially Influences *IL1B* and *TNF* Endotoxin Tolerance

Some IE cytokines have been associated with inhibitory mechanisms that prevent re-expression upon secondary endotoxin stimulus (Foster et al., 2007). Prior attempts to explain this phenomenon by transcription suppression have failed to note that the expression profiles for these genes are highly transient. If transcription following secondary stimulation is not analyzed within a short time frame, the re-stimulation properties can be overlooked. In addition, usage of inconsistent doses of secondary LPS and washing of cells between primary and secondary endotoxin challenge may result in experimental variability and induce physiological stress to highly sensitive cells, respectively. In my experiments, Western blot analysis demonstrated that secondary stimulation of *IL1B* resulted in expression of 30 KDa proIL-1β precursor protein (**Figure 23**). Strikingly, these results recapitulate an earlier report that *in vivo* injection of a sublethal dose of LPS into mice resulted in TNF, but not IL-1 tolerance, as assayed by kinetic protein analysis of serum (Zuckerman et al., 1991).

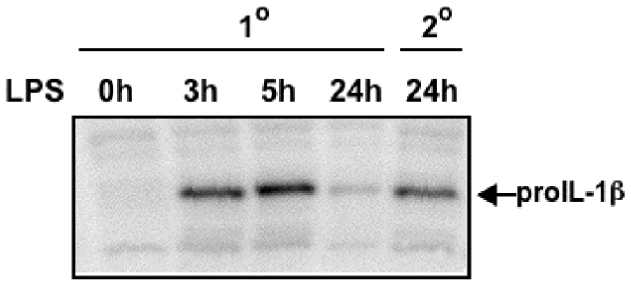

Figure 23. Western blot depiction of the 30 KDa proIL-1β precursor protein.

THP-1 cell were initially stimulated with 1 μg/ml of LPS for indicated times and an equal dose of secondary LPS was administered for 3 hours to unwashed THP-1 cultures, prior to cell harvest and analysis of the proIL-1β expression. The chemiluminescent detection of secondary antibody was assayed using a molecular dynamics Typhoon 8600 phosphor/fluorescence imager.

Similarly, steady-state kinetic mRNA secondary stimulation revealed that *IL1B* transcription is not completely desensitized/tolerized (**Figure 7**). ChIP revealed a somewhat decreased, but significant, amount of Pol II at the promoter-proximal regions of both genes in 13 and 25 hour stimulated monocytes, with decreased signal downstream of the pause sites (**Figure 24, 25**). At 25 hours, Pol II occupancy within the gene body was slightly higher for *IL1B*, likely explaining the sustained transcriptional profile of the gene. NELF was co-localized with promoter bound Pol II on both genes (**Figure 24**). My data reveal that upon secondary stimulation, P-TEFb is re-recruited to the *IL1B* promoter, resulting in resumption and maintenance of transcriptional elongation by Pol II. This is in contrast to tolerized *TNF*, in which P-TEFb recruitment and S2P CTD levels are not increased in LPS re-stimulated cells (**Figure 24**).

Re-stimulation experiments carried out at 13 hours revealed a similar but decreased response to a secondary LPS stimulus. This suggests that *IL1B* undergoes a degree of decreased LPS responsiveness within the first 13 hours of initial stimulation (**Figure 25**). As described in the Introduction, P-TEFb mediated phosphorylation of serine 2 within the CTD of elongating Pol II promotes recruitment of various splicing factors to ensure proper nascent mRNA processing. The fact that P-TEFb is recruited to *IL1B* and not *TNF* during secondary LPS exposures, prompted us to examine the integrity of transcripts produced in the reactivated THP-1 cells.

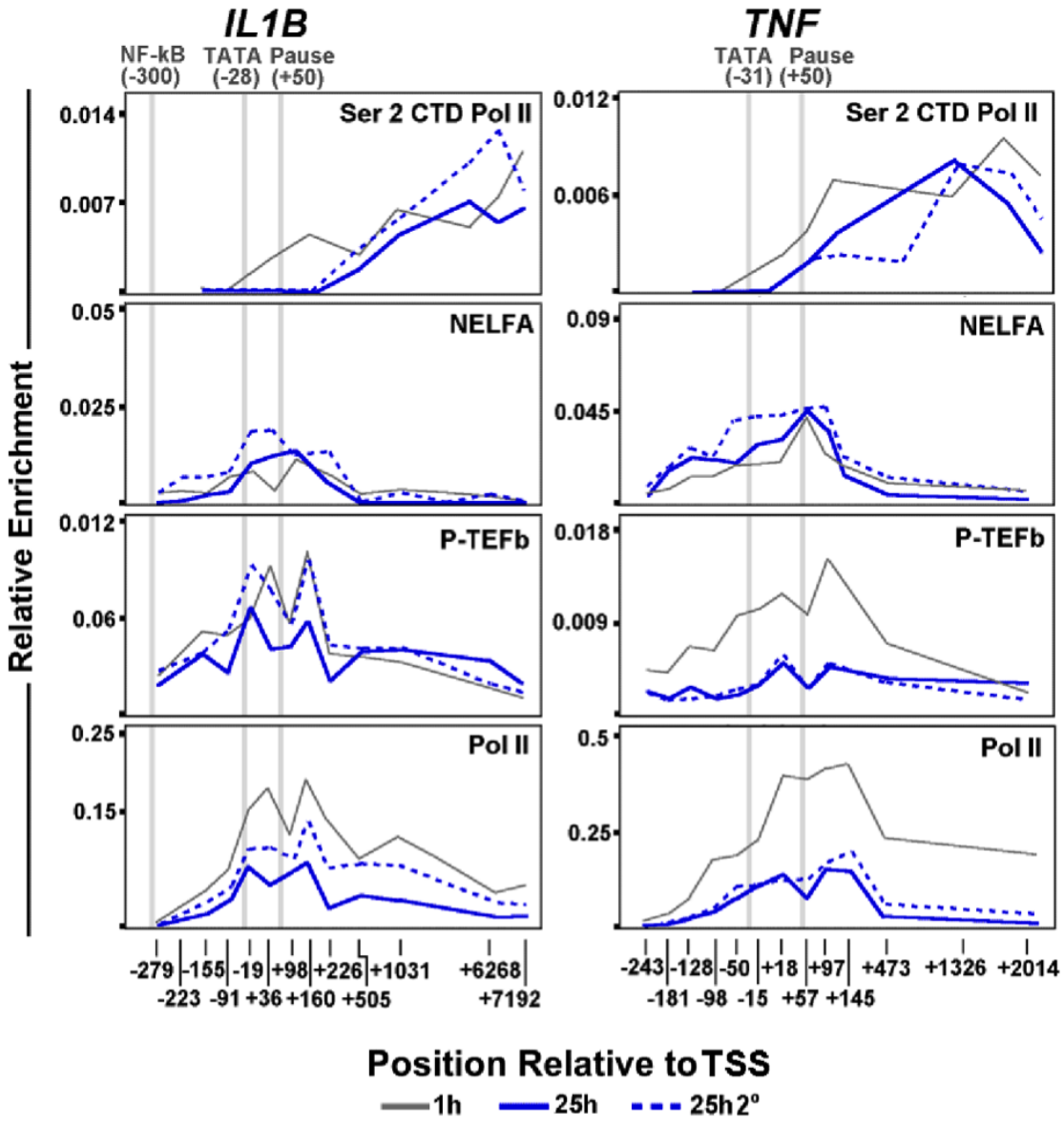
IL1B
TNF
NF-kB (-300)
TATA (-28)
Pause (+50)
TATA (-31)
Pause (+50)
Ser 2 CTD Pol II
NELFA
P-TEFb
Pol II
Relative Enrichment
0.014
0.007
0.012
0.006
0.05
0.025
0.09
0.045
0.012
0.06
0.018
0.009
0.25
0.15
0.5
0.25
-279 -155 -19 +98 +226 +1031 +6268
-223 -91 +36 +160 +505 +7192
-243 -128 -50 +18 +97 +473 +1326 +2014
-181 -98 -15 +57 +145
Position Relative to TSS
1h
25h
25h 2°

Figure 24. ChIP re-stimulation experiments at 25 hours.

ChIP for S2P CTD Pol II, NELF, P-TEFb, and Pol II on *IL1B* and *TNF* during secondary LPS stimulation of THP-1 cells. The solid lines represent primary and dotted lines secondary LPS treatment of THP-1 cells at indicated times. Thin gray lines denote 1h LPS reference. Gene *landmarks* (gray bars) reveal the location of an additional important NF-κB binding site (-300 bp) for *IL1B*. Solid blue lines denote ChIP data for primary LPS challenge harvested at 25 hours post simulation. Dotted blue lines show ChIP data for THP-1 cells that were initially treated for 24 hours with LPS, and subjected to a re-stimulation for an hour prior to their fixation and harvest. Equal dosage of LPS (1 μg/ml) was used in both, primary and secondary stimulation experiments. Data used for generation of this Figure are presented in **Appendix E**.

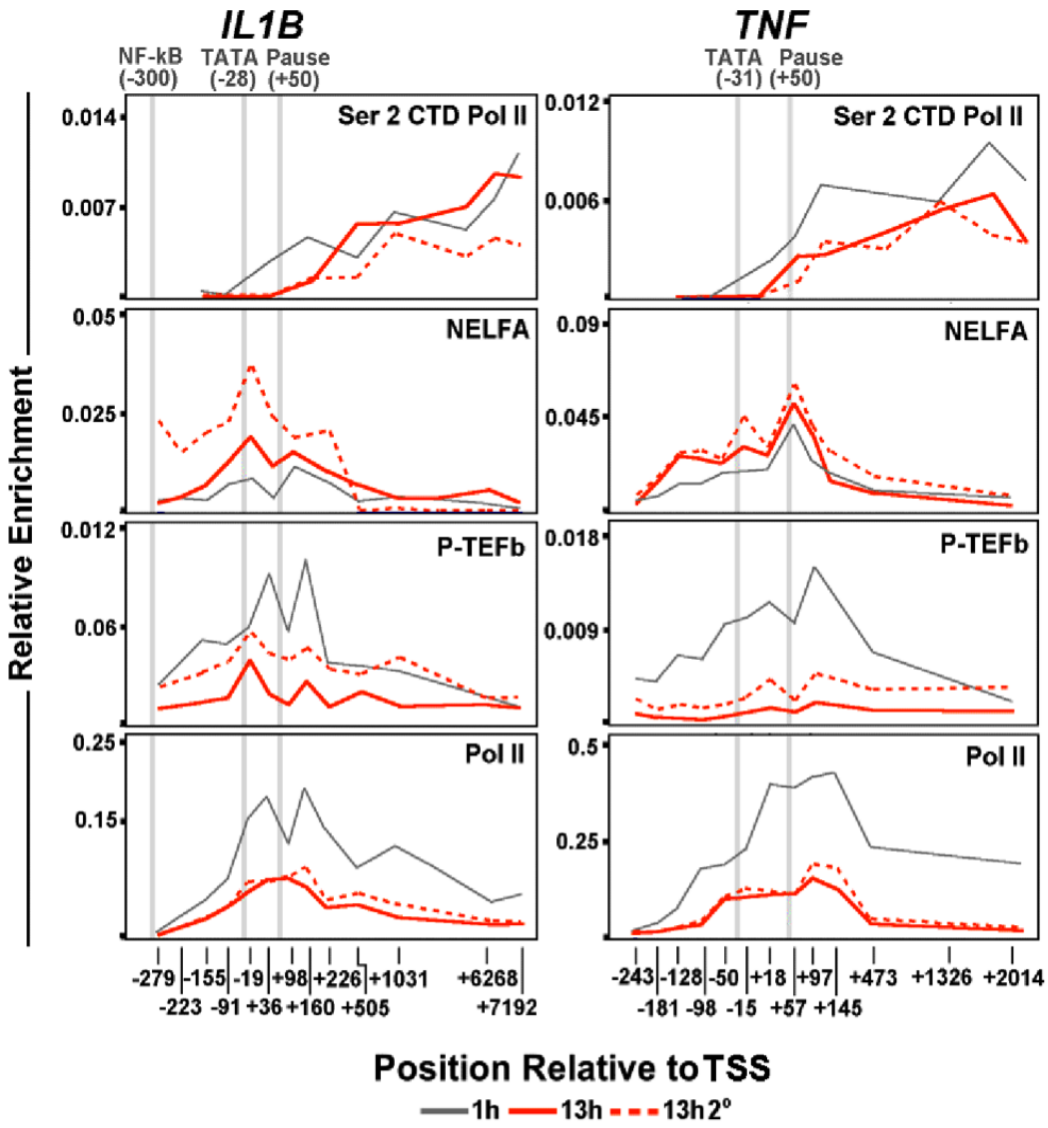

Figure 25. ChIP re-stimulation experiments at 13 hours.

ChIP for S2P CTD Pol II, NELF, P-TEFb, and Pol II on *IL1B* and *TNF* during secondary LPS stimulation of THP-1 cells. The solid lines represent primary and dotted lines secondary LPS treatment of THP-1 cells at indicated times. Thin gray lines denote 1h LPS reference. Gene *landmarks* (gray bars) reveal the location of an additional important NF-κB binding site (-300 bp) for *IL1B*. Solid blue lines denote ChIP data for primary LPS challenge harvested at 13 hours post simulation. Dotted blue lines show ChIP data for THP-1 cells that were initially treated for 12 hours with LPS, and subjected to a re-stimulation for an hour prior to their fixation and harvest. Data used for generation of this Figure are presented in **Appendix E**.

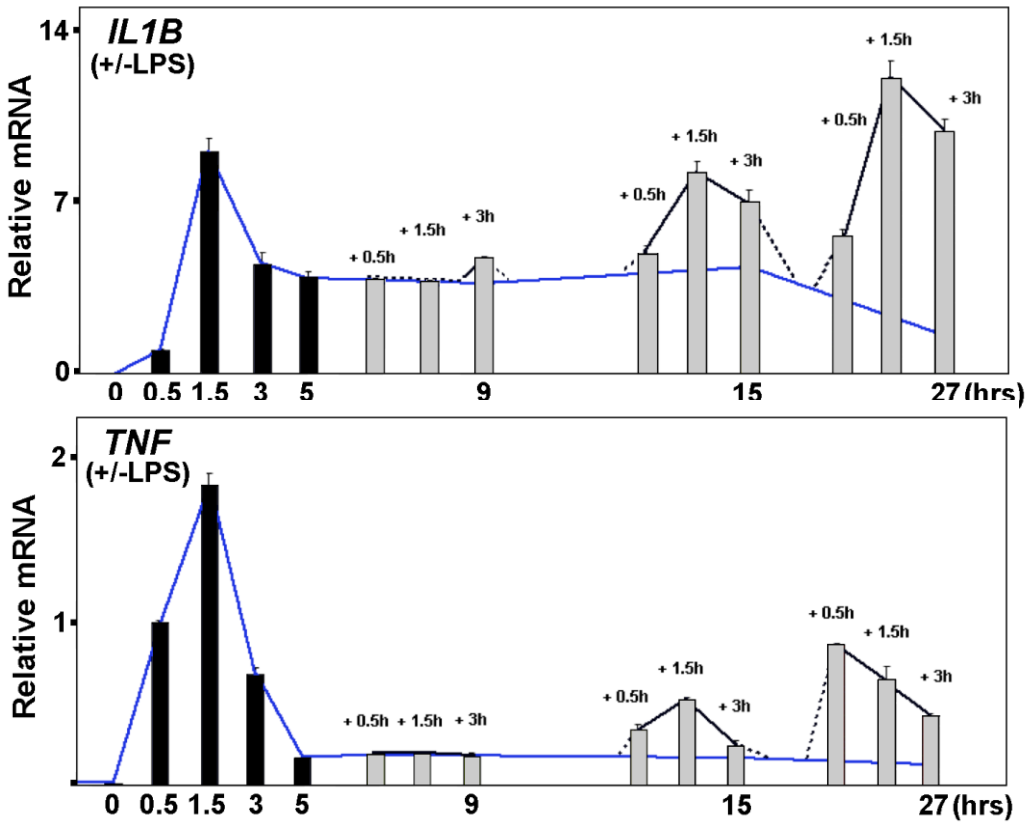

Figure 26. qPCR-amplified random primer generated cDNA levels for *IL1B* and *TNF* following re-stimulation.

Primary stimulations are labeled as black bars while secondary treatments are shown as gray bars. Re-stimulation time points are indicated above the respective gray bars (0.5h, 1.5h, and 3h). Equal dosage of LPS (1 μg/ml) was used in all treatments. The qPCR data are normalized to the endogenous 18srRNA levels.

The analysis of a random primer (instead of polyA) generated cDNA products revealed a minor increase of *TNF* mRNA in secondary stimulated monocytes (**Figure 26**). These messages are likely representing incompletely processed primary *TNF* transcripts that are generated by the low levels of P-TEFb deficient transcribing Pol II. I propose that the gene specific recruitment of P-TEFb serves as a regulatory step

mediating the escape form endotoxin tolerance. This mechanism ensures proper *IL1B* mRNA polyadenylation and processing, which is deficient during the re-stimulation of *TNF* gene. My results indicate that the low levels of sustained *IL1B* expression may maintain the gene sufficiently competent for secondary re-induction. These data argue that secondary induction of *IL1B* is a physiologically significant phenomenon that further distinguishes it from *TNF*.

Contrary to previous studies (Chan et al., 2005; Foster et al., 2007; Yoza et al., 2002) our re-stimulation experiments were conducted without washing of the monocytes between primary and secondary endotoxin challenge. Since some of these reports argued that both *TNF* and *IL1B* are incapable of re-activation, I decided to repeat their experimental set up and conduct a set of experiments in washed THP-1 cultures. As **Figure 27** demonstrates, washing of monocytes prior to the secondary LPS treatments decreased expression of *IL1B*. These experiments suggest that the washing step may impede function of cell surface TLR4-mediated receptor signaling.

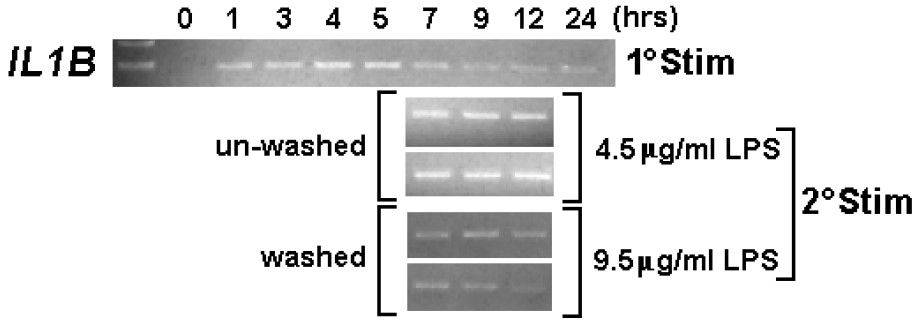

Figure 27. Washing of cells prior to re-stimulation abolishes *IL1B* expression.

Cell cultures were initially stimulated with a low amount of LPS (0.5 µg/ml) for indicated times. Two increased doses of secondary LPS (4.5 µg/ml or 9.5 µg/ml as indicated) were administered for 2.5 hours to washed or unwashed cultures, prior to assay. Three percent agarose gel was used to resolve the RT-PCR products.

LPS Stimulation of Monocytes Results in Dynamic Changes in Nucleosome Positioning and Modification on *IL1B* and *TNF*

Nucleosome positioning plays a critical role in controlling the accessibility of promoters for transcription machinery, and genome-wide studies have shown that *Drosophila* and human promoters are commonly devoid of nucleosomes (Mavrich et al., 2008; Schones et al., 2008). Stalled Pol II can serve as a physical barrier by preventing promoter-proximal nucleosome assembly and formation of repressive chromatin, thus enabling explicit gene regulation (Gilchrist et al., 2010). Additionally, it has been demonstrated that CpG-islands near gene promoters prevent nucleosome deposition and, therefore, can influence the competence of transcriptional responsiveness to TLR4 stimulus (Ramirez-Carrozzi et al., 2009). It is interesting to note that *IL1B* and *TNF* do not contain a significant presence of CpG-islands in the vicinity of their promoters. To address the question of chromatin influence on these two genes, promoter nucleosome occupancy in resting and stimulated THP-1 monocytes, as well as a cell line that fails to express either *IL1B* or *TNF* (HEK293 pre-neuronal (Shaw et al., 2002)) and one that constitutively expresses only TNF (HUT102 cutaneous T lymphocyte), were examined by core histone 3 (H3) ChIP (Gilchrist et al., 2008; Schones et al., 2008). This provided sufficient resolution to obtain enrichment profiles for phased nucleosomes (**Figure 28**). Here I report +1 nucleosomes on both genes approximately 200 bp downstream of TSS. A similar observation was reported for the *Hsp70* promoter in *Drosophila* (Petesch and Lis, 2008). The distribution of more weakly positioned nucleosomes, upstream of TSS was unique to each of the genes. I observed a significant depletion of promoter bound nucleosomes in 1 hour-stimulated monocytes, similar to that reported for activated genes

in yeast (Lee et al., 2004). The extent of nucleosome depletion was reduced in cells pretreated with the inhibitors selective for transcription factors associated with one or both of these genes (**Figure 28**).

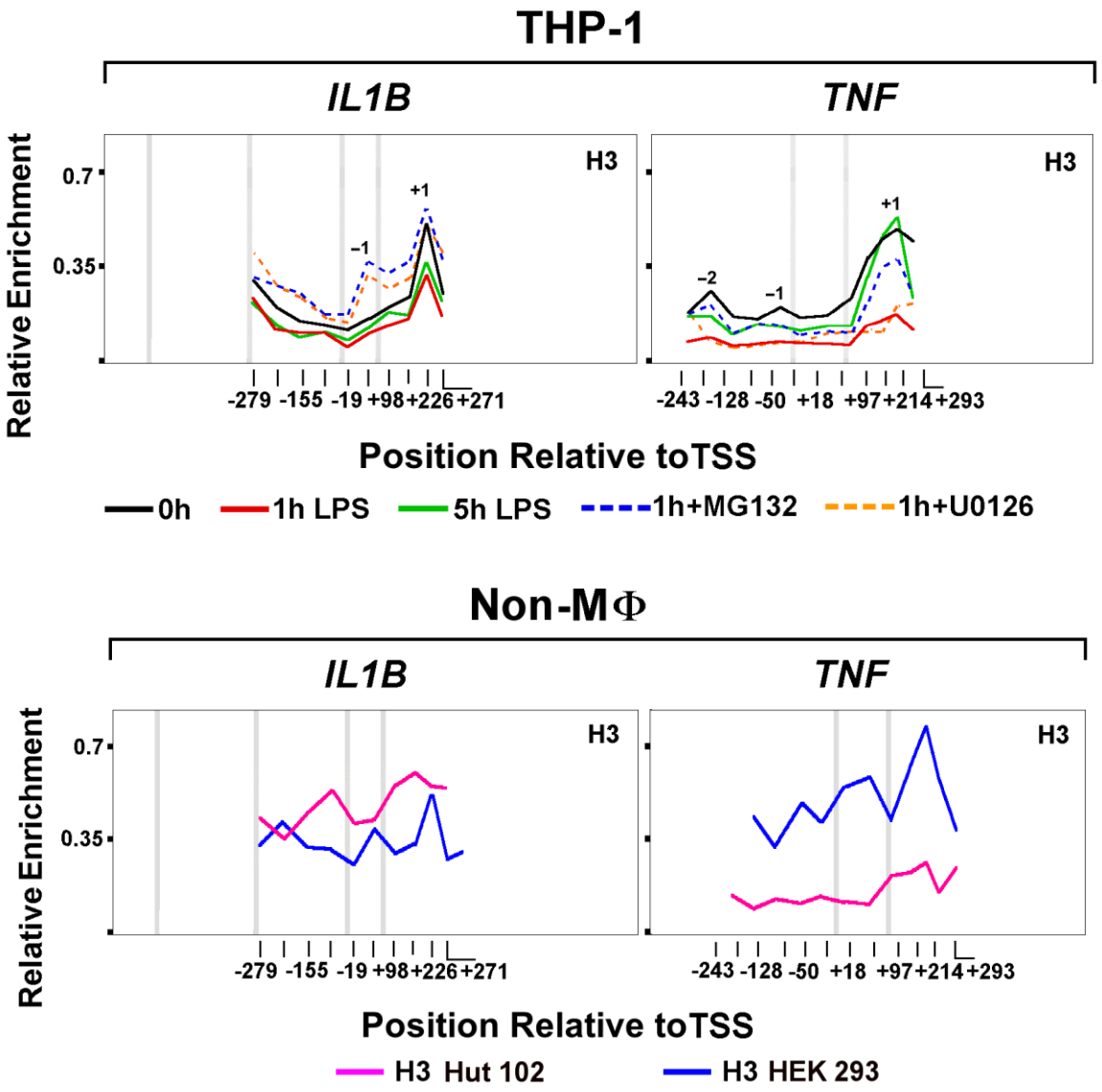

Figure 28. Nucleosome positioning dynamics during *IL1B* and *TNF* induction. Depicted are spatial and kinetic histone 3 (H3) ChIP data for *IL1B* and *TNF* in resting (black), 1h (red), and 5h (green) stimulated THP-1 cells, as well as control Hut102 (pink line) and HEK293 (blue line) cells. Key nucleosomes are designated by position relative to the TSS (-2, -1, +1). The blue dotted line represents H3 ChIP for THP-1 cells pre-treated with the NF-κB inhibitor MG132 and the yellow dotted line denotes the U0126 (C/EBPβ inhibitor) treated THP-1 cell samples. Data used for generation of this Figure are presented in **Appendix F**.

I argue that this process is stimulation dependent, requiring specific factor recruitment. It is noteworthy that the *IL1B* nucleosome displacement is sensitive to both inhibitors, whereas *TNF* is almost exclusively affected by MG132, suggesting that C/EBPβ is specific to *IL1B*. Five hours post-stimulation, as the Pol II recruitment levels decline, depleted nucleosomes recovered, approaching initial enrichment levels for the +1 nucleosome of *TNF*. In contrast, *IL1B* nucleosome depletion only exhibited a partial recovery. In addition, pre-treatment of cells with either inhibitor resulted in a striking increase in the -1 *IL1B* nucleosome, revealing an additional distinction from *TNF*. The presence of a uniquely phased -1 nucleosome within the NFR has been suggested to inhibit Pol II recruitment (Gilchrist and Adelman, 2012; Jiang and Pugh, 2009), but to our knowledge this is the first report indicating its role affecting inducible IE activation in human immune cells and may reflect loss of an important priming function for *TNF*. **Figure 29** illustrates that the nucleosome eviction at *IL1B* and *TNF* promoter regions is likely mediated by the ATP-dependent histone remodeler SNF2β/BRG1. ChIP data reveal a rapid recruitment of BRG1 to the promoters of both IE genes within 30 minutes of LPS treatment. The inducible BRG1 binding was prominent in vicinity of the *IL1B* and *TNF* promoters as compared to the structural part of the genes (**Figure 29**).

In HEK293, *IL1B* and *TNF* nucleosomes were similarly positioned to those in THP-1, exhibiting higher levels, especially for the -1 nucleosome. Nucleosomes were similarly more abundant than in THP-1 for *IL1B* in Hut102, with higher levels for -2 and +1 nucleosomes. The constitutive expression of TNF in Hut102 revealed a depleted profile almost identical, but slightly higher, than that for 1 h stimulated THP-1 cells.

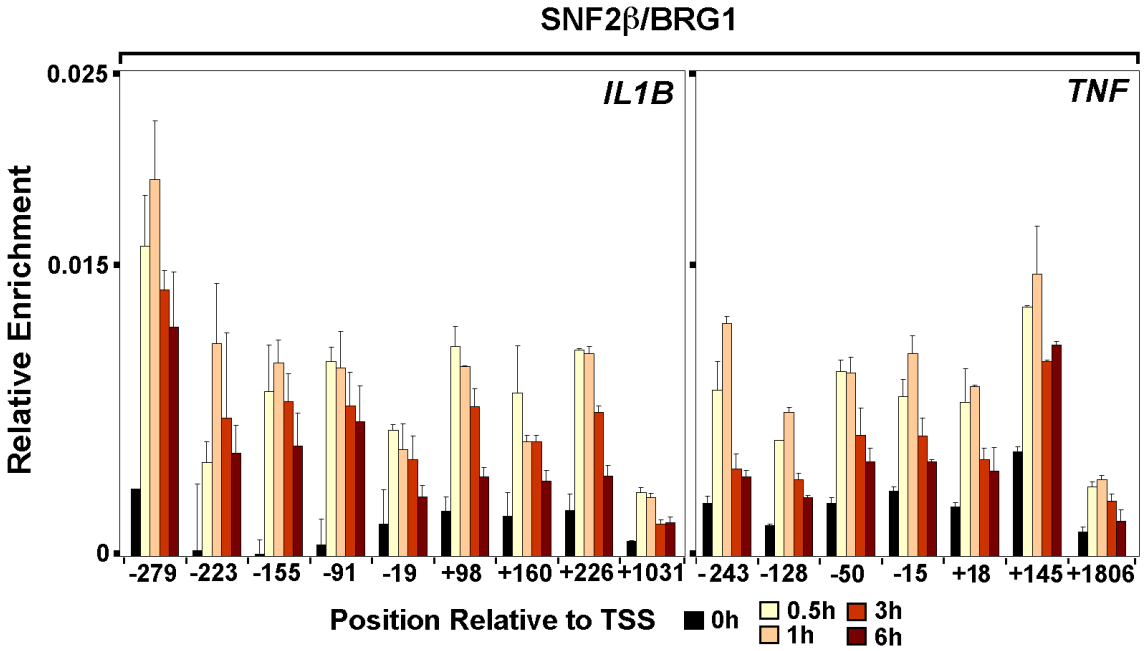

Figure 29. Nucleosome eviction at the *IL1B* and *TNF* promoter regions is likely mediated by the ATP-dependent histone remodeler SNF2β/BRG1.

Spatial and temporal occupancy of the SNF2β/BRG1 complex at the *IL1B* and *TNF* genes was analyzed at indicated time points (0h, 0.5h 1h, 3h, 6h) following LPS treatment.

To further understand the processes regulating the initially poised, but repressed, gene architectures and LPS induced transcriptional profiles, spatial-temporal distribution of several chromatin marks on *IL1B* and *TNF* was investigated (**Figure 30**). LPS activation induced changes in nucleosome marks on these two genes. I observed the presence of high levels of H3K4me3 and low levels of H3K27me3 (Akkers et al., 2009) in monocytes that likely contribute to activity.

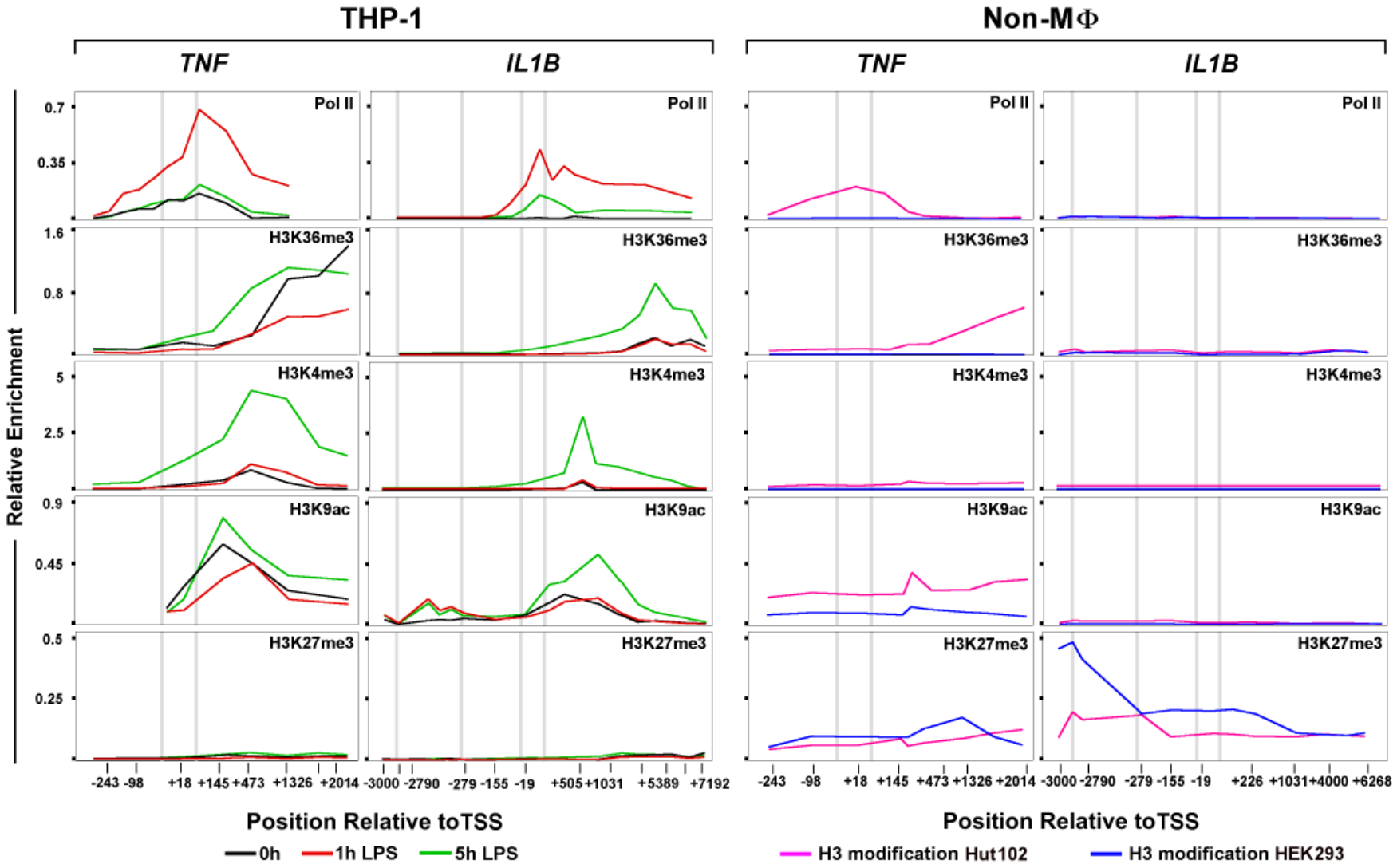
THP-1
Non-MΦ
TNF
IL1B
TNF
IL1B
Relative Enrichment
Pol II
H3K36me3
H3K4me3
H3K9ac
H3K27me3
0.7
0.35
1.6
0.8
5
2.5
0.9
0.45
0.5
0.25
-243 -98 +18 +145 +473 +1326 +2014 -3000 -2790 -279 -155 -19 +505 +1031 +5389 +7192
-243 -98 +18 +145 +473 +1326 +2014 -3000 -2790 -279 -155 -19 +226 +1031 +4000 +6268
Position Relative toTSS
Position Relative toTSS
0h
1h LPS
5h LPS
H3 modification Hut102
H3 modification HEK293

Figure 30. Histone modifications at *IL1B* and *TNF* in THP-1, Hut102, and HEK 293 cells.

Depicted are spatial and kinetic ChIP profiles for Pol II, H3K36me3, H3k4me3, H3K9ac, and H3K27me3 for *IL1B* and *TNF* in resting (black), 1h (red), and 5h (green) stimulated THP-1 cells, as well as control Hut102 (pink line) and HEK293 (blue line) cells. All panels are similarly scaled with respect to spatial distribution along each gene, permitting comparative localization. Data used for generation of this Figure are presented in **Appendix G**.

The initial permissive levels of H3K4me3 restricted to the vicinity of + 1 nucleosomes do not show a significant increase during the initial one hour LPS treatment. To our surprise, enrichment of this mark revealed delayed kinetics and follows Pol II recruitment as shown by an increase at 5 hours post-stimulation. Higher levels of H3K4me3 at 5 h remain mostly focused at the promoter for *IL1B*, but spread throughout the downstream coding region of *TNF*. The distinct positional effect of H3K4me3 at the promoter versus the downstream coding region of genes has previously been observed for other genes (Barski, et al., 2007), and may be critical for differences between *IL1B* and *TNF*. Examination of other nucleosome marks for these two genes revealed that the relative level of H3K9ac within the coding region is relatively higher for *IL1B* than *TNF* at 5 h post LPS. Taken together, the relative levels of H3K4me3 and H3K9ac downstream of the TSS suggest a possible association with post-stimulatory tolerance for *TNF*. It is important to note that prior to stimulation, both genes are associated with low levels of H3K9ac that might play an additional role in maintaining the *IL1B* and *TNF* promoters in a transcriptionally poised state. The suppressive effect of the polycomb group proteins mediated by H3K27me3 directed transcriptional silencing is reversed by the H3K27 specific demethylase JMJD3 during macrophage inflammatory responses (De Santa et al., 2007). Loss of this repressive chromatin mark in *Drosophila* and embryonic stem cells, was shown to result in an increase in H3K27 acetylation, which was mediated by the acetyltransferase (HAT) activity of p300 and CBP (Pasini et al., 2010; Tie et al., 2009). Our observations of depleted levels of H3K27Me3 encouraged us to examine the kinetic changes in H3K27Ac deposition and binding patterns of p300 on *IL1B* and *TNF*. As revealed in **Figure 31**, acetylation at lysine 27 was associated with an LPS-dependent

increase at the -2 nucleosomes, while a transient decrease was observed in H3K27Ac on downstream nucleosomes.

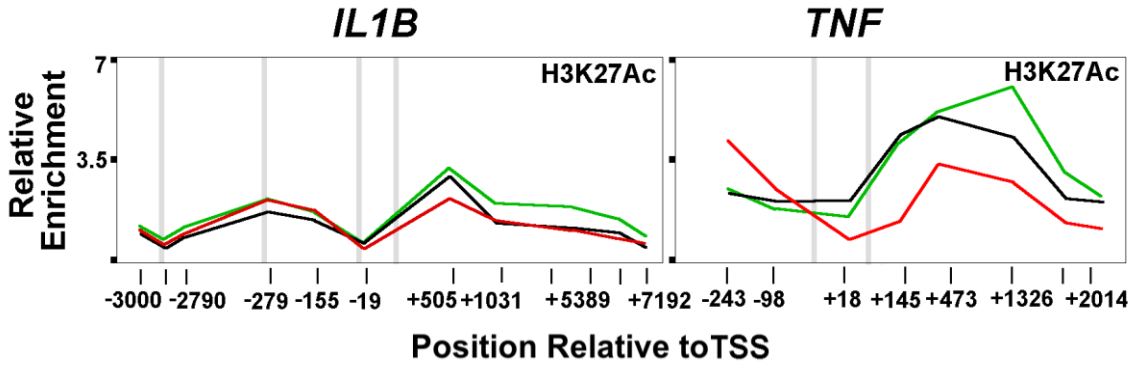

Figure 31. Spatial-temporal distribution of H3K4me1 at *IL1B* and *TNF* in THP-1 cells.

Depicted are spatial and kinetic ChIP profiles for H3K27ac for *IL1B* and *TNF* in resting (black), 1h (red), and 5h (green) stimulated THP-1 cells. The additional vertical gray bar located at the -3000 position upstream of TSS marks the *IL1B* enhancer region. Data used for generation of this Figure are presented in **Appendix G**.

In agreement with these changes, p300 was transiently recruited upstream of the *IL1B* and *TNF* promoters by LPS (**Figure 32**). The Pol II elongation footprint marked by H3K36me3 (Henikoff and Shilatifard, 2011) revealed a consistent LPS-induced transient enrichment pattern increasing towards the 3' end of both genes (**Figure 30**). In contrast to *IL1B*, significant levels of H3K36me3 were detected on the *TNF* locus in un-stimulated monocytes, further confirming constitutive basal activity. The spatial distribution of chromatin modifications at the *IL1B* and *TNF* loci were also assessed for Hut102 and HEK293 cells (**Figure 30**). Pol II levels and chromatin marks for *TNF* in Hut102 are consistent with the active transcription previously reported (Kronke et al., 1988), whereas *IL1B* is repressed in these cells and does not exhibit any positive indicators for either gene, while revealing inhibitory H3K27me3, absent in THP-1 (**Figure 30)**.

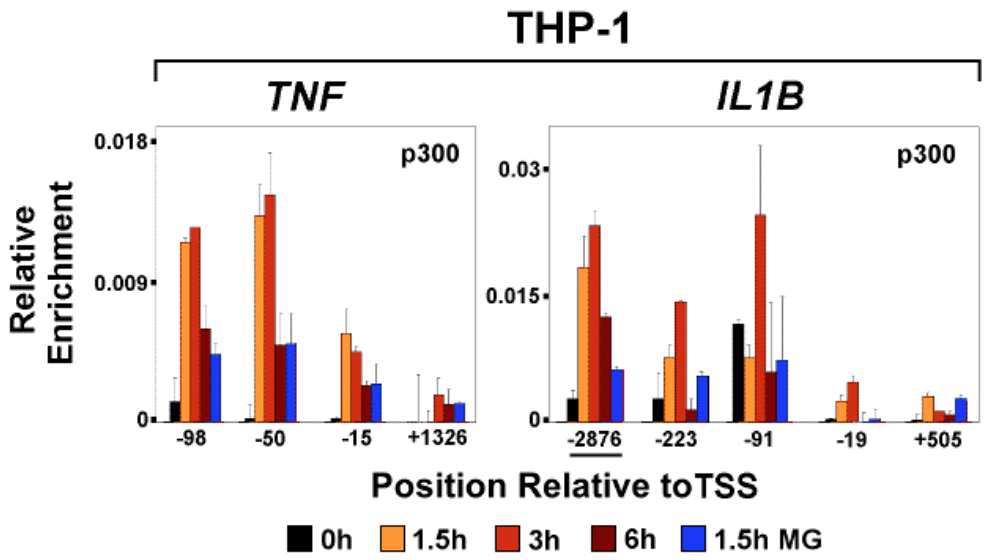

Figure 32. ChIP analysis of p300 association at the *IL1B* and *TNF* genes.

Shown is the LPS inducible association of p300 with the *TNF* and *IL1B* promoters as well as the *IL1B* enhancer. The NF-κB inhibition using inhibitor MG132 abolishes p300 recruitment to both IE genes.

TNF in Hut102 reveals significant levels of both H3K4me3 and H3K27me3, the so-called "bivalent" mark (Akkers et al., 2009), indicative of developmental, rather than transient IE induction, possibly responsible for the constitutive expression of this gene in these HTLV-1 infected malignant T cells. HEK293 does not show positive indicators for either gene, exhibiting non-bivalent inhibitory H3K27me3 on both. The inhibitory H3K27me3 extends throughout the entirety of both genes, but appears to be more focused over the coding region of TNF, while for IL1B, there is a greater level far upstream over the potent LPS enhancer near -3000, which binds C/EBPβ (Shirakawa et al., 1993). The analysis of spatial distribution of chromatin modifications at the *IL1B* and *TNF* locus was extended to the osteosarcoma MG 63 cell line. My data set (represented in the comprehensive **Figure 33**) reveals that MG 63 do not support expression of either one of the two IE genes.

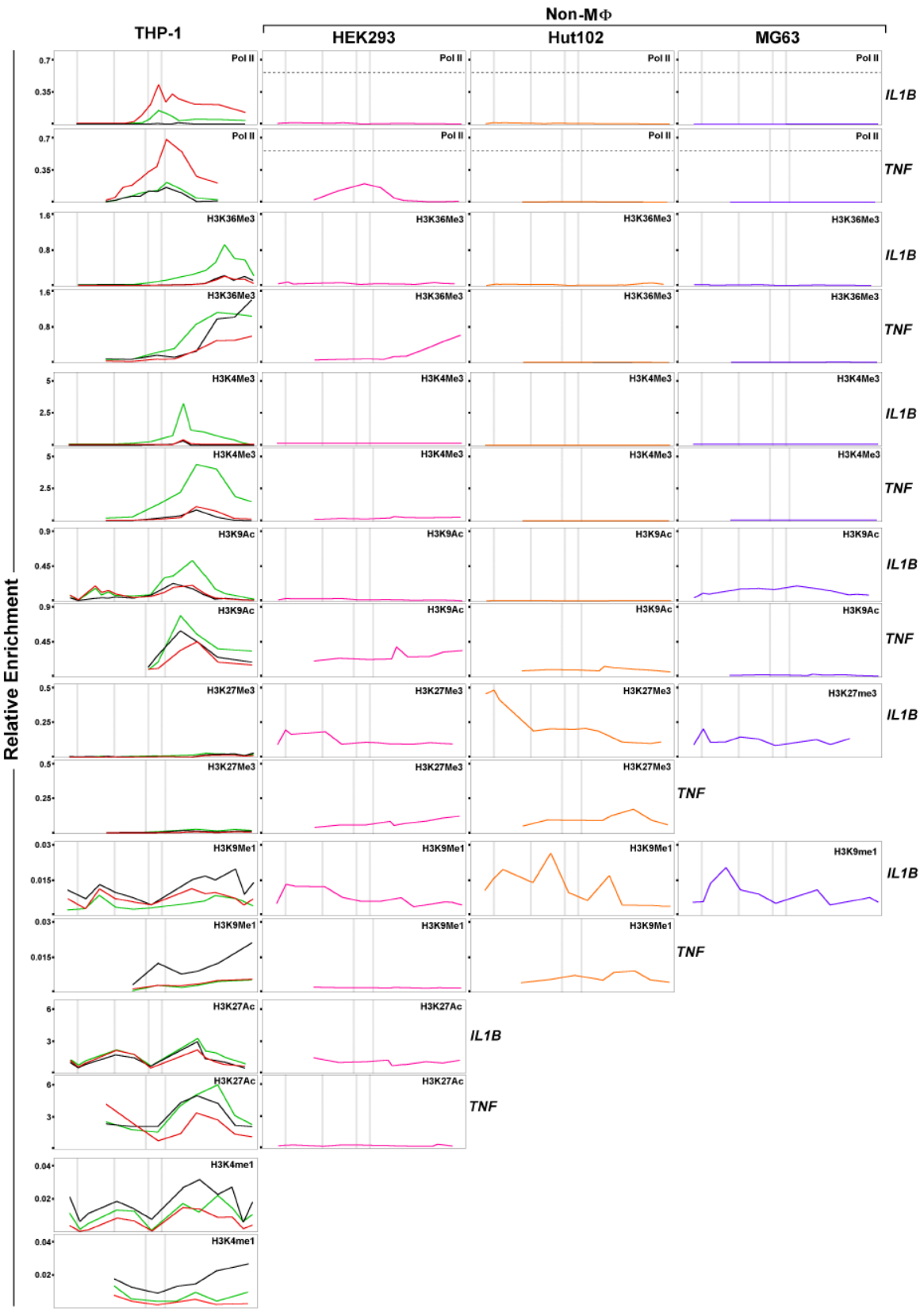
Non-MΦ
THP-1
HEK293
Hut102
MG63
Pol II
H3K36Me3
H3K4Me3
H3K9Ac
H3K27Me3
H3K9Me1
H3K27Ac
H3K4me1
IL1B
TNF
Relative Enrichment
Position Relative to TSS

Figure 33. Summary of the histone modification ChIP profiles for *IL1B* and *TNF* in THP-1, HEK 293, Hut102, and MG63 cells.

Illustrated are the summary profiles comparing nucleosome modifications for resting (black), 1h (red), and 5h (green) LPS-treated human THP-1 cells with untreated HEK293 pre-neuronal cells (pink line), Hut102 cutaneous T lymphocytes (orange line), and MG63 osteoblastic cells (blue line). Depicted are spatial and kinetic ChIP profiles for Pol II, H3K36me3, H3k4me3, H3K9ac, and H3K27me3, H3K9me1, H3K27ac, and H3K4me1 for *IL1B* and *TNF*. All panels are similarly scaled with respect to spatial distribution along each gene, permitting comparative localization. Data used for generation of this Figure are presented in **Appendix G**.

Active chromatin marks and levels of Pol lI in MG 63 cells largely differ from those of THP-1 monocytes. The inhibitory chromatin marks H3K9me1 and H3K27me3 (Kouzarides, 2007) are prevalently distributed along the *IL1B* locus, further confirming its transcriptional suppression in MG 63 cell line.

Lastly, the comparison of chromatin levels among the different cell lines enabled us to confirm that H3K9me1 is a likely indicator of transcriptional inactivation. Since *IL1B* and *TNF* are repressed in resting monocytes, I inquired whether H3K9me1 contributed to the regulation of induction or the switching-down/off of these IEs. I observed that the high levels of H3K9me1 distributed throughout *IL1B* and *TNF* in resting monocytes were rapidly lost following LPS treatment and remained low even during the transcriptional shut-down, which was opposite to the kinetic pattern of H3K9ac ChIP (**Figure 33**). I conclude that the TLR4 dependent activation of *IL1B* and *TNF* caused replacement of the repressive H3K9me1 mark with a transcriptionally permissive acetylation (Gomes and Espinosa, 2010), likely contributing to the expression of both genes.

Spi1 Mediates Monocyte-specific *IL1B* Expression

The regulatory sequences driving *IL1B* and *TNF* expression contain numerous binding sites for various transcription factors that cooperatively contribute to the precise temporal and cell-type specific expression. Evaluation of the spatial-temporal distribution of selected transcription factors revealed that *IL1B* is dependent upon a different set of regulators than *TNF*. A major factor involved in genome-wide maintenance of the macrophage lineage is the ETS domain DNA binding factor Spi1 (Lawrence and Natoli, 2011). In particular, recent genome-wide studies revealed a constitutive association of

Spi1, often with other signal inducible factors, at LPS responsive enhancers in murine macrophages (Ghisletti et al., 2010; Heinz et al., 2010).

Inducible *IL1B* transcription depends on a poised monocyte-specific enhancer that requires cooperative association of Interferon regulatory factor 8 (IRF8), Spi1, and non-tyrosine phosphorylated (NTP)-Stat1 (Unlu et al., 2007). In addition, Spi1 binding is also required at the *IL1B* promoter (Kominato et al., 1995). Consistent with earlier studies, ChIP revealed a robust constitutive association of Spi1 at the *IL1B* promoter and enhancer that persisted for an extended time post induction (**Figure 34**). In contrast, Spi1 was significantly less abundant at the *TNF* promoter (**Figure 34**).

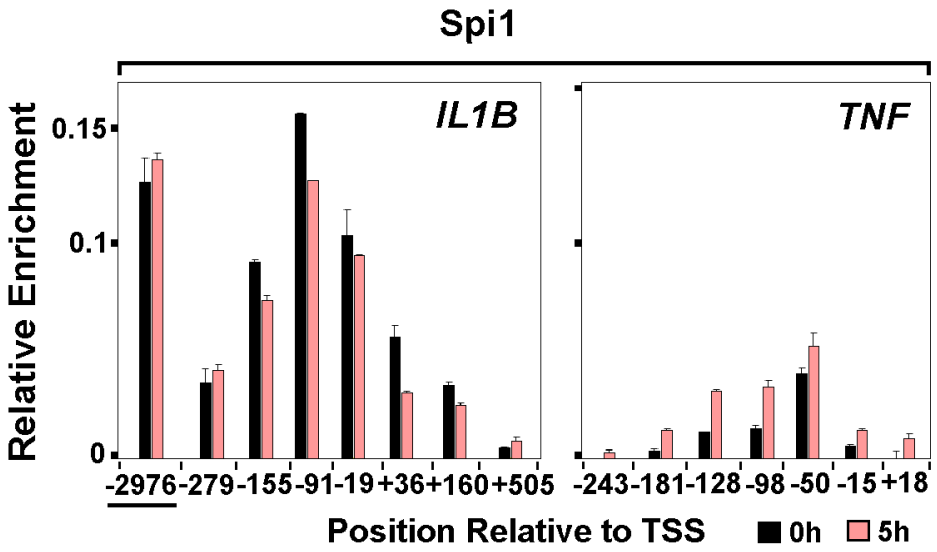

Figure 34. ChIP analysis of Spi1 binding to the *IL1B* promoter and enhancer regions.

Spi1 is constitutively present at the *IL1B* promoter (peaking at position -91) and enhancer (as measured at position -2976) regulatory regions (black bars). Its binding persists for up to 5 hours post LPS stimulation (pink bars). Spi1 is significantly less abundant at the *TNF* promoter.

I hypothesized that in addition to its role priming enhancers, Spi1 binding at the *IL1B* promoter mediates the cell-type restricted transcriptional competency of this

pro-inflammatory gene. To examine the role of this "pioneer factor" during *IL1B* induction, transient transfection studies were carried out in HEK293 cells, which do not transcribe *IL1B*. Initial screens for transcription factor expression levels revealed the absence of Spi1 in these cells, as compared to THP-1 monocytes (**Figure 35A**). Since HEK293 do not express LPS-sensing TLR4 receptor, co-transfection of TNF receptor-associated factor 6 (TRAF6) was used as a dominant-positive LPS surrogate in these cells (**Figure 35B**, illustration) (Wang et al., 2006).

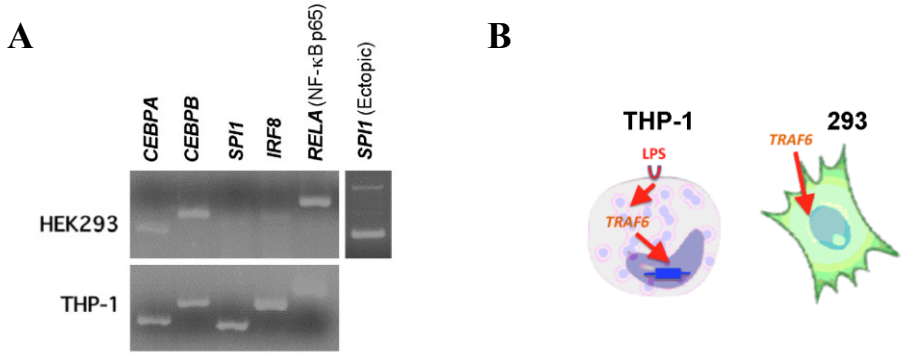

Figure 35. RT-PCR analysis of the transcription factor expression levels in HEK 293 cells.

(A) The 3% agarose gel showing the RT-PCR products for transcription factors in HEK293 and THP-1 cells. The monocyte specific factors Spi1 and IRF8 are not expressed in HEK 293 cells. An additional panel displays ectopic expression of Spi1 in transfected HEK293. **(B)** Compariative Illustrations showing ectopic transfection of TRAF6 being used as a surrogate to induce the signaling, resembling LPS activation of monocytes. TRAF6 is a signal transducer, which acts downstream of the TLR4 receptor signaling pathway.

Figure 36 shows that an *IL1B* reporter vector (XT-Luc) was potently up-regulated by Spi1 in combination with IRF8, a factor important for full *IL1B* activity in monocytes (Unlu et al., 2007) that is absent in HEK293, and dominant-positive TRAF6.

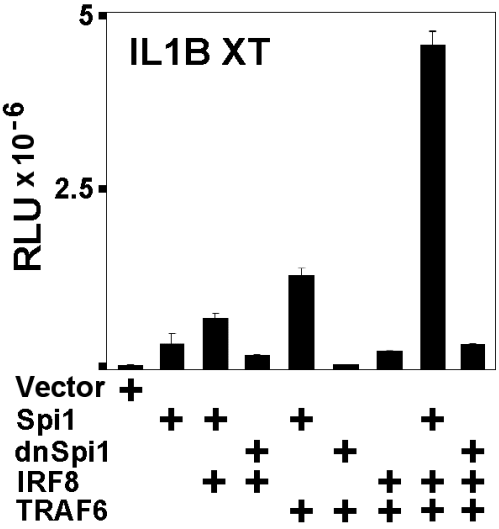

Figure 36. Spi1 is critical for IL1BXT-Luc reporter activity in HEK293 cells.

Transcription factors associated with *IL1B* activation were ectopically transfected into HEK 293 cells together with IL1BXT Luciferase reporter. Binding of the ectopically transfected transcription factors causes activation of IL1BXT-luc reporter, which is represented as RLU (relative luciferase units). The effect of individual and combined transcription factors is compared to an empty vector pCDNA3.1 (vector) transfected samples. The dnSpi1 denotes a dominant negative Spi1 deletion protein lacking a critical N-terminal trans-activation domain. The amount of the total transfected DNA was equal in all wells. The data are representative of three independent experiments.

Spi1 function requires the integrity of its N-terminal TBP Binding Domain (TBD), as revealed in transient transfection using HeLa cells (Kominato et al., 1995). In agreement, ectopic expression of a dominant-negative Spi1 mutant (dn/Spi1), containing only the Spi1 DNA binding domain, reduced XT-Luc activity to background levels. Analysis of the endogenous *IL1B* mRNA by RT-PCR (**Figure 37A, B**) as well as qPCR (**Figure 38A, B**) in HEK293 transfected with the same factors supported the luciferase results as well as the critical role of Spi1 for *IL1B* induction (**Figure 38**).

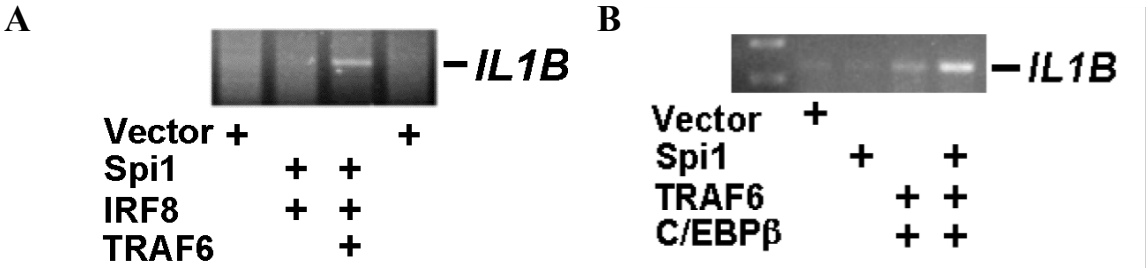

Figure 37. Ectopically transfected transcription factors induce endogenous *IL1B* expression in HEK 293 cells.

Represented are the *IL1B* RT-PCR products isolated from HEK 293 cells that were ectopically transfected with combinations of transcription factors Spi1 and IRF8 **(A)** and Spi1and C/EBPβ **(B)** co-transfected with the LPS surrogate TRAF6. *IL1B* RT-PCR products analyzed by 3% agarose gel electrophoresis. The amount of the total transfected DNA is equal in all wells. The data are representative of three independent experiments.

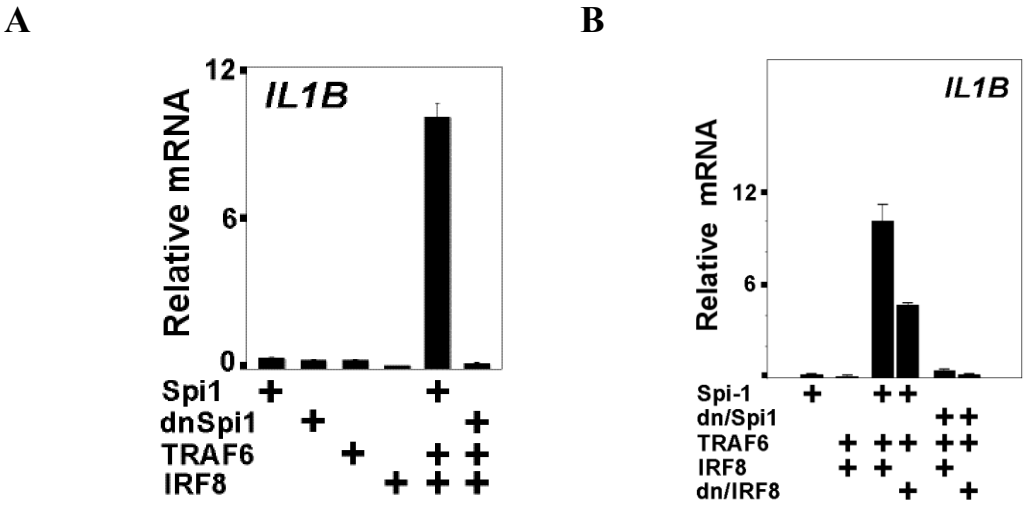

Figure 38. Spi1, IRF8, and TRAF6 induce endogenous *IL1B* mRNA levels in HEK293 cells.

(A) Shown are qPCR experiments detecting the *IL1B* mRNA in HEK293 cells that were ectopically transfected with wild type or dominant negative Spi1 and IRF8 co-transfected with the LPS surrogate TRAF6. Figure **(B)** shows *IL1B* mRNA levels in 293 cells transfected with above mentioned factors as well as a mutated IRF8 (IRF8Y211F). The data are normalized to the endogenous 18srRNA expression levels. The amount of the total transfected DNA is equal in all wells. The data are representative of three independent experiments.

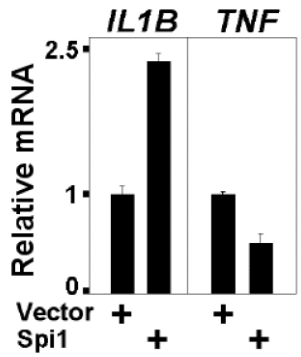

Figure 39. Spi1 does not affect the endogenous levels of *TNF* mRNA in HEK293 cells.

Represented is a qPCR analysis of the *IL1B* and *TNF* mRNA in HEK293 cells that were ectopically transfected with Spi1. The data are normalized to the endogenous 18srRNA expression levels.

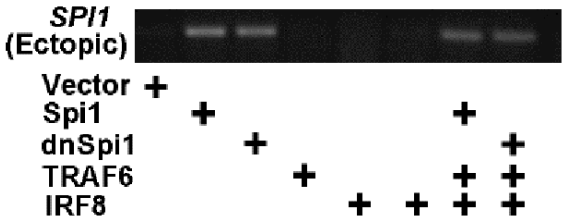

Figure 40. Detection of ectopically expressed Spi1 mRNA in HEK293 cells.

Shown is a 3% agarose gel of the Spi1 RT-PCR products from HEK293 cells transfected with various combinations of transcription factors and signaling molecules. Only HEK293 cells that express the ectopically transfected Spi1 reveal a positive RT-PCR band.

The basal level of *IL1B* transcription in cells transfected only with Spi1 was radically increased by addition of IRF8 and TRAF6. IRF8 and TRAF6 alone (**Figure 38A**) or in combination (**Figure 38B**) are insufficient for *IL1B* activation. Substitution of wild type with dn/Spi1 abolished *IL1B* expression. As **Figure 38B** demonstrates, *IL1B* message was reduced to a lesser degree in cells transfected with dominant negative IRF8 (dn/IRF8), as previously reported (Unlu et al., 2007). In addition, *TNF* expression in Spi1

transfected HEK293 was not affected (**Figure 39**). Control RT-PCR data revealed that both, the wild type and dn/Spi1 are expressed in ectopically transfected 293 cells (**Figure 40**).

Since the N-terminal activation domain of Spi1 has been shown to directly interact with TBP (Hagemeier et al., 1993), I wondered whether Spi1 plays a role in recruitment of TBP to the *IL1B* promoter. To test this hypothesis, ChIP of *IL1B* was carried out in HEK293 transfected with either wild type or dn/Spi1 in combination with IRF8 and TRAF6. As shown in **Figure 41**, transfection of Spi1 and the auxiliary factors increased occupancy of TBP at *IL1B* TATA box. In agreement with an increase in *IL1B* transcription, I observed recruitment of Pol II to *IL1B* downstream of TSS, resembling a paused polymerase, as well as to the transcribed region of the gene, consistent with elongation. Enrichment signals for TBP and Pol II occupancy in HEK293 transfected with dn/Spi1 were dramatically reduced (**Figure 41**). Transfection-induced *IL1B* activation was also associated with depletion of promoter-proximal phased nucleosomes. **Figure 42** shows that full length Spi1 in combination with TRAF6 and IRF8 is necessary for nucleosome depletion at the *IL1B* promoter. These data suggest that Spi1 plays a critical role at the *IL1B*, but not the *TNF* promoter. In addition to facilitating *IL1B* promoter accessibility (Marecki et al., 2004)**,** the N-terminal TBD of Spi1 may play an additional role in the recruitment of the general transcription machinery *via* TBP. Its constitutive association at the promoter in a macrophage-restricted setting mediates *IL1B* transcriptional competency as well as stimulus-responsive selective activation.

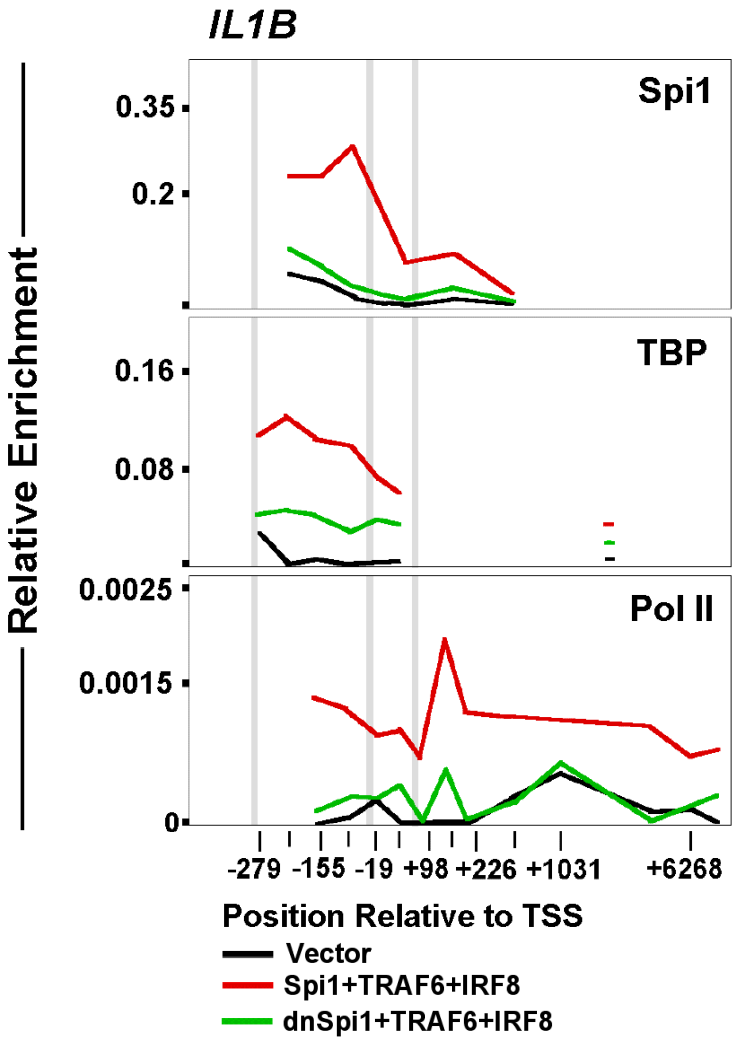

Figure 41. The N-terminal domain of Spi1 is critical for the recruitment of TBP and Pol II to the endogenous *IL1B* promoter in HEK293 cells.

Depicted are ChIP data for the ectopically expressed binding of Spi1 (top panel) along with the endogenous binding of TBP and Pol II. HEK 293 cells were transfected with an empty vector plasmid DNA (black line) or combination of wild type (red line) or mutant Spi1 (green line) co-transfected with IRF8 and TRAF6. The broader distribution of the TBP enrichment peak, as compared to the THP-1 experiments (**Figure** 17), is a result of a broader specificity for the antibody TFIID (TBP) sc-273, which was used for this experiment.

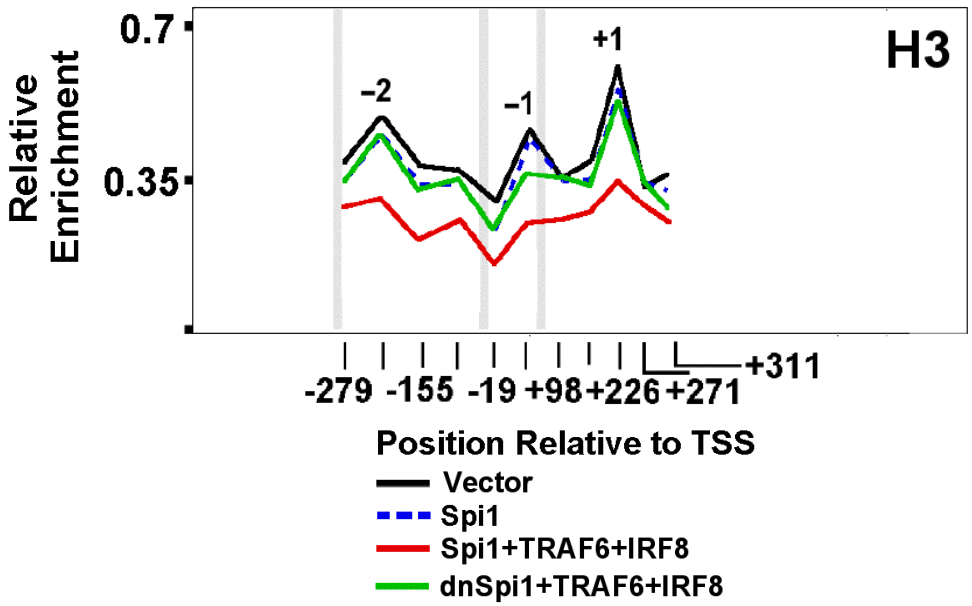

Figure 42. Spi1, co-transfected with IRF8 and TRAF6, mediates nucleosome eviction from the *IL1B* gene promoter.

Shown are ChIP data for the spatial distribution of the core histone 3 (H3) along the *IL1B* gene promoter. HEK 293 cells were transfected with an empty vector plasmid DNA (black line), Spi1 alone (dotted blue line), or combination of wild type (red line) or mutant Spi1 (green line) co-transfected with IRF8 and TRAF6. Data used for generation of this figure are presented in **Appendix F**.

C/EBPβ interaction with Spi1 mediates the LPS inducible induction of *IL1B*

It has been postulated that the lineage-determining factor Spi1 facilitates formation of NFR, exposing binding sites for LPS-responsive transcription factors in activated monocytes (Natoli, 2012). Endotoxin dependent binding of NF-κB, an IE transducer of numerous pro-inflammatory genes, has been shown to play an important role during coordinate induction of *IL1B* and *TNF* in monocytes (Hiscott et al., 1993);

(Collart et al., 1990). Our kinetic ChIP analyses revealed transient binding of NF-κB to both genes as early as 30 minutes post LPS treatment (**Figure 35**).

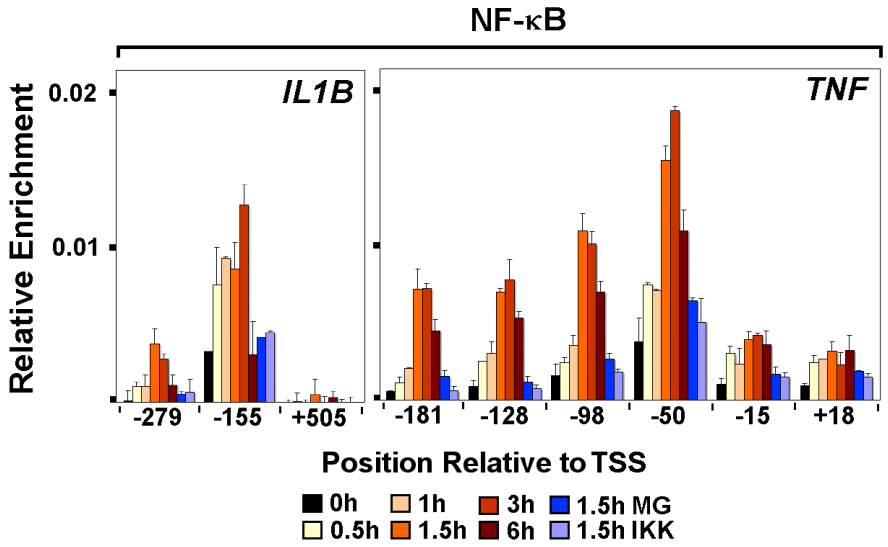

Figure 43. Kinetic binding of NF-κB to *IL1B* and *TNF* in THP-1 cells.

Shown is the ChIP analysis for the kinetics of NF-κB binding to the *IL1B* and *TNF* gene promoters. The time points for LPS treatments are indicated above. Pre-treatment of the THP-1 cells with MG132 (1.5h MG) and BMS-345541 (1.5h IKK) inhibitors reduced the NF-κB binding to both genes. The inhibitors were applied 2 hours prior to the 1.5-hour LPS stimulations of the THP-1 cells.

Pre-treatment of THP-1 cells with NF-κB-targeted inhibitors MG132 (proteasome inhibitor) and BMS-345541 (IκB kinase inhibitor) diminished NF-κB binding to both genes (**Figure 43**). Consistent with the decreased NF-κB binding, the mRNA levels of both genes were significantly reduced. The mRNA expression was tested in both THP-1 as well murine RAW cells (**Figure 44, 47**). The precise control of cell-permeable inhibitor addition to cells is suitable for conducting time sensitive kinetic experiments. Earlier studies used various *in vitro* assays in order to demonstrate the involvement of C/EBPβ during *IL1B* regulation (Auron and Webb, 1994; Tsukada et al., 1994).

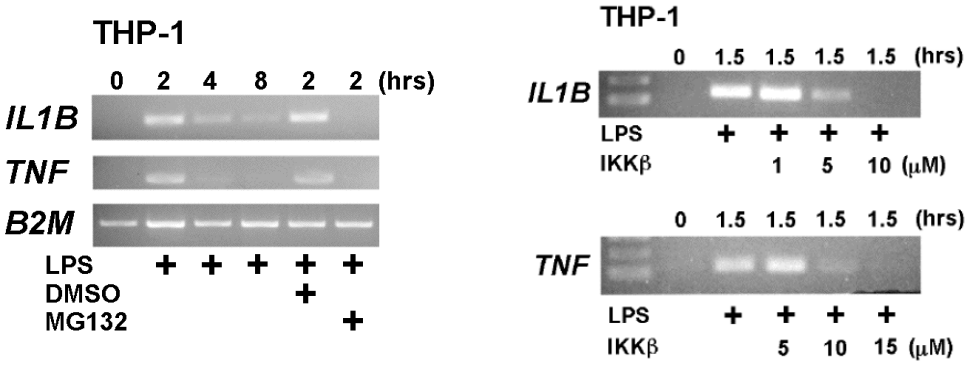

Figure 44. NF-κB is necessary for the LPS induction of *IL1B* and *TNF* genes in THP-1 cells.

The 3% agarose gels reveal RT-PCR data for *IL1B* and *TNF* mRNA expression in THP-1 cells. DMSO, used to resuspend the MG132 inhibitor, has no effect on the *IL1B* and *TNF* gene activation. Inhibitor was applied 2 hours prior to LPS treatments (time points for LPS addition are indicated above the gel images).

However, ChIP permits evaluation of the *in vivo* binding profile for C/EBPβ at *IL1B* and *TNF* regulatory regions in LPS stimulated cells. Kinetic analysis illustrates LPS-mediated recruitment of C/EBPβ to the *IL1B,* but not to the *TNF* promoter (**Figure 45**). Inhibitor U0126 was chosen in order to selectively target the MEK1/2 pathway that is involved in activation of C/EBPβ. LPS activated monocytes pre-treated with U0126 revealed decreased *IL1B* transcription (**Figure 46, 47)**, consistent with reduced C/EBPβ binding. *TNF* expression was unaffected by U0126 treatment (**Figure 46, 47**).

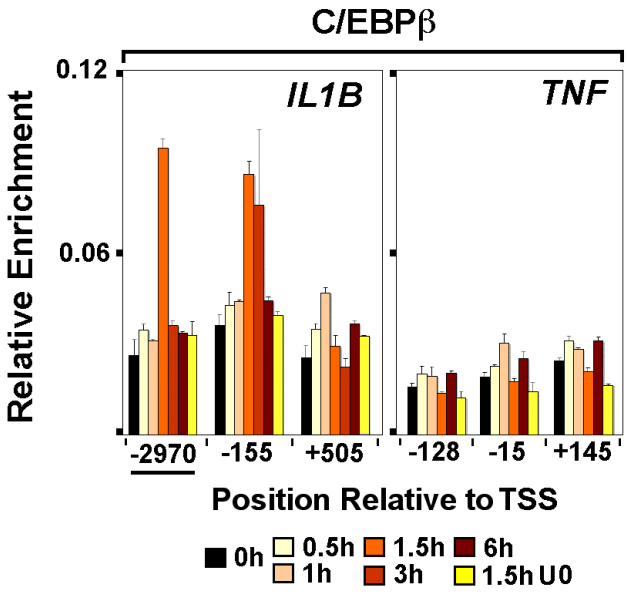

Figure 45. LPS inducible binding of C/EBPβ to *IL1B* in THP-1 cells.

Shown is the ChIP analysis for the kinetics of C/EBPβ binding to the *IL1B* and *TNF* gene promoters. The time points for LPS treatments are indicated above. Pre-treatment of the THP-1 cells with the inhibitor U0126 for 2 hours was used in order to inhibit the C/EBPβ activity.

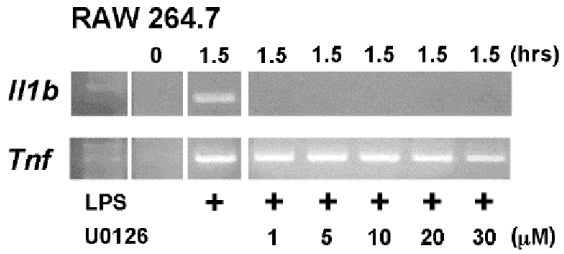

Figure 46. C/EBPβ inhibition decreases *IL1B* mRNA expression in RAW264.7 cells.

An RT-PCR analysis shows that selective targeting of MEK1/2 pathway leads to inhibition of *IL1B* and not *TNF* mRNA expression. RAW264.7 cells were pre-treated with various concentrations of U0126 for 2 hours and mRNA levels were analyzed 1.5-hour post LPS treatment. The RT-PCR products were resolved using 3 % agarose gel.

Transient transfection of the 293 cells was carried out in order to better define the role of these inducible transcription factors. NF-κB and C/EBPβ were not effective *IL1B* inducers when transfected alone into 293 cells.

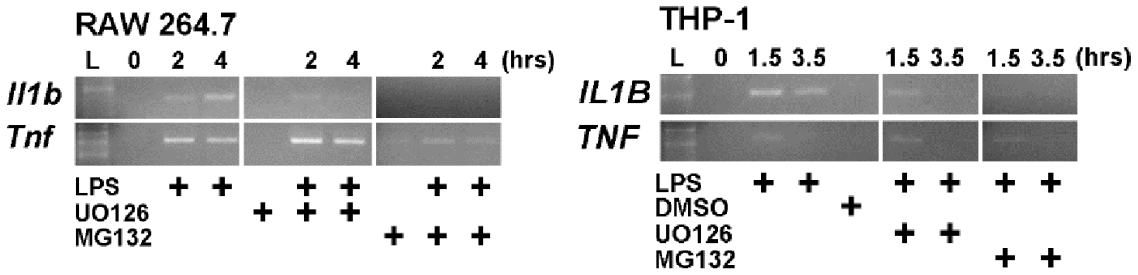

Figure 47. The effects of NF-κB and C/EBPβ inhibition on *IL1B* and *TNF* mRNA expression in RAW264.7 and THP-1 cells.

Shown are 3% agarose gels used for RT-PCR analysis of *IL1B* and *TNF* mRNA in RAW264.7 and THP-1 cells. The cell cultures were pre-treated with NF-κB (MG132) and C/EBPβ (U0126) inhibitors 2 hours prior to addition of LPS.

Significant activation of *IL1B* was observed when the factors were transfected in combination with Spi1. Co-expression with TRAF6 showed the strongest *IL1B*XT-Luc activity (**Figure 48**).

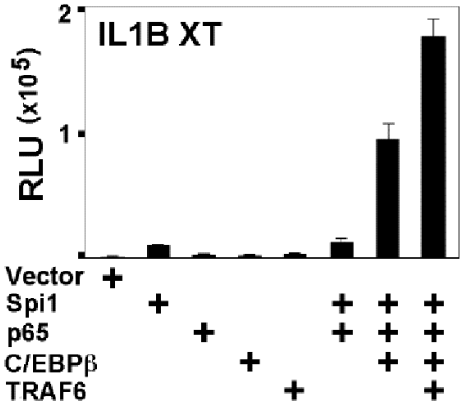

Figure 48. NF-κB and C/EBPβ cooperatively induce the *ILB*XT-Luc activity.

Sown are relative luciferase data for *IL1B*XT-Luc reporter activity in HEK293 cells ectopically transfected with indicated factors. The effect of individual and combined transcription factors is compared to an empty vector pCDNA3.1 (Vector) transfected samples. The amount of the total transfected DNA is equal in all wells. The data are representative of three independent experiments.

Overexpression of an IκBα super repressor (IκBαSR), (Van Antwerp et al., 1996) considerably reduced, but did not completely abolish, *IL1B* activity in 293 cells transfected with Spi1, TRAF6, and C/EBPβ (**Figure 49A**). This argues that in the absence of NF-κB, transcription of *IL1B* may continue due to the presence of C/EBPβ.

Experiments in RAW 264.7 cells further demonstrate that IκBαSR fully eliminates NF-κB activity without completely inactivating *IL1B*XT-Luc (**Figure 49B**).

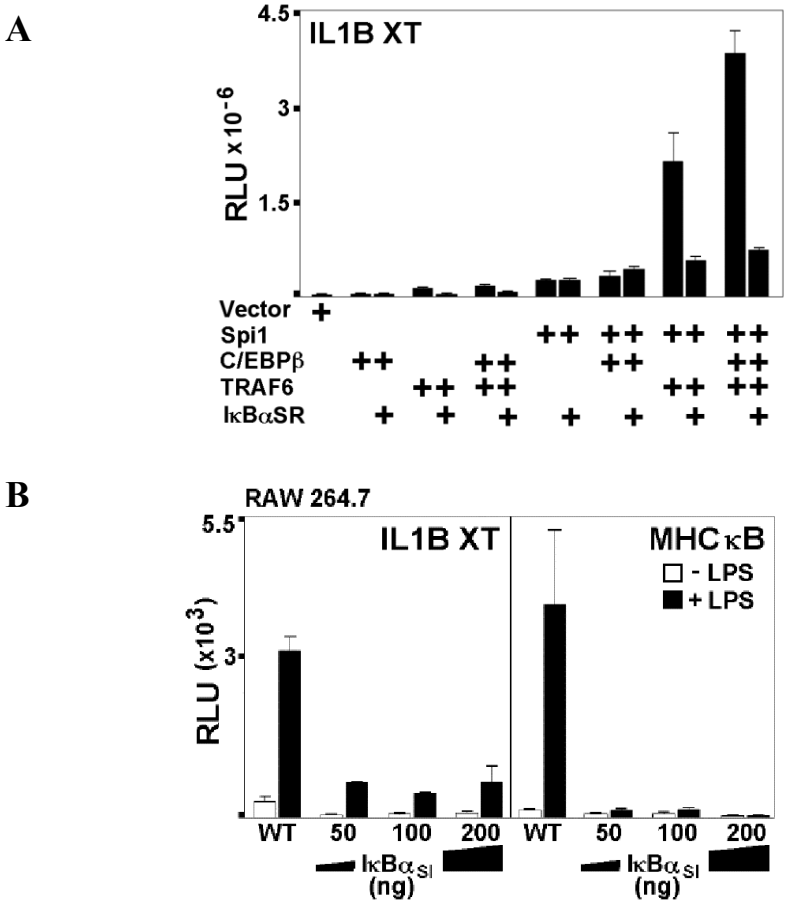

Figure 49. Inhibition of NF-κB activity does not completely abolish *IL1B*XT-Luc activity.

(A) Ectopic expression of IκBα super repressor (IκBαSR) in HEK293 co-transfected with indicated factors. **(B)** *IL1B*XT-Luc and MHCκB reporter activity in RAW264.7 transfected with IκBα super repressor (IκBαSR). The amount of the total transfected DNA is equal in all wells. The data are representative of three independent experiments.

In addition, titration of truncated, dn/C/EBPβ, (Tsukada et al., 1994) in 293 cells, confirmed a dose dependent inhibition of *IL1B* reporter expression (**Figure 50**).

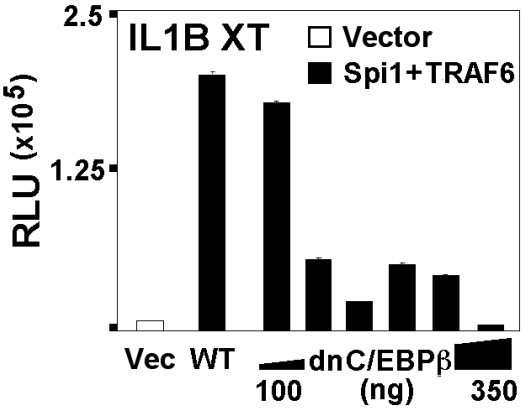

Figure 50. Ectopic transfection of dnC/EBPβ abolishes *IL1B*XT-Luc reporter activity in HEK293. Shown are relative luciferase data for IL1BXT-Luc reporter activity in HEK293 cells ectopically expressing wild type or indicated amounts of the dominant negative (dn) C/EBPβ co-transfected with Spi1 and TRAF6. The amount of the total transfected DNA is equal in all wells. The empty vector pCDNA3.1 was used to balance the amount DNA transfected across the samples. The data are representative of three independent experiments.

To further demonstrate the importance of NF-κB and C/EBPβ for *IL1B* induction, RAW264.7 cells were transiently transfected with modified *IL1B*XT-Luc reporter harboring mutations within the essential NF-κB (-300) and C/EBPβ (I-Region/Enhancer) binding sites. As depicted in **Figure 51**, disrupted binding of these two factors severely reduced responsiveness of the *IL1B* reporter to LPS. Lastly, siRNA for NF-κB and C/EBPβ in 293 cells revealed significant reduction of *IL1B*XT-Luc activity (**Figure 52**). *IL1B* expression was somewhat more sensitive to NF-κB inhibition, as

compared to that of C/EBPβ. In agreement with our previous results, depletion of Spi1 caused severe reduction of the *IL1B* reporter activity (**Figure 52**).

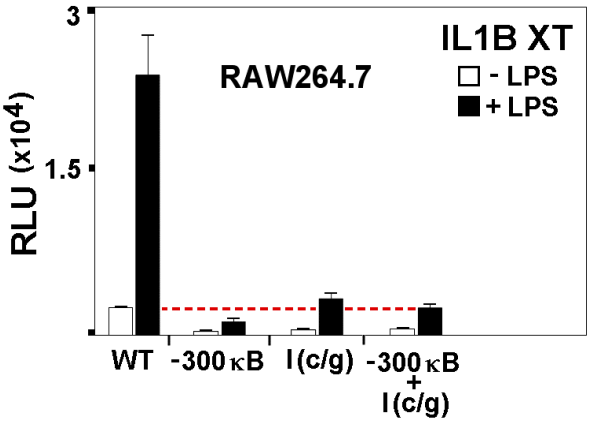

Figure 51. Mutation of the critical C/EBPβ and NF-κB binding sites reduces *IL1B*XT-Luc reporter activity.

Shown are relative luciferase data for *IL1B*XT-Luc reporter activity in RAW264.7 cells ectopically transfected with the modified *IL1B*XT-Luc reporter harboring mutations within the essential NF-κB (-300 κB) and C/EBPβ (I c/g) binding sites. The amount of the total transfected DNA is equal in all wells.

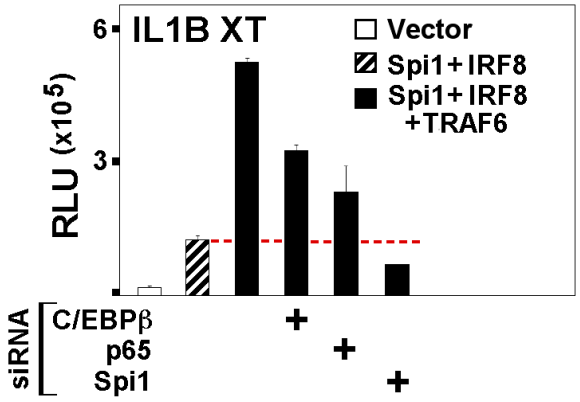

Figure 52. siRNA mediated inhibition of C/EBPβ, NF-κB, and Spi1 reduced *IL1B*XT-Luc reporter activity in HEK293.

Shown are relative luciferase data for *IL1B*XT-Luc reporter activity in HEK293 cells ectopically expressing Spi1, IRF8, and/or TRAF6. The indicated transcription factors (C/EBPβ, NF-κB, and Spi1) were depleted

using siRNA, which was transfected into HEK293 cells 24 hours prior to addition of Spi1, IRF8, and/or TRAF6.

The data presented here challenge the popular notion that NF-κB is the only critical factor affecting *IL1B* induction. It appears that NF-κB and C/EBPβ cooperatively regulate LPS induced transcription of *IL1B*, while expression of *TNF* appears influenced primarily by NF-κB.

I next explored the relationship between the factors and the dynamics of the release of paused Pol II during transcription of *IL1B* and *TNF*. To address this question, P-TEFb ChIP was conducted on LPS stimulated THP-1 cells pre-treated with inhibitors targeting selected transcription factors. As shown in **Figure 53**, inhibition of NF-κB resulted in significant depletion of P-TEFb recruitment to both genes. This observation is consistent with reports indicating that NF-κB phosphorylated at serine 276 interacts with the active P-TEFb complex consisting of bromodomain protein 4 (BRD4) and cyclin-dependent kinase 9 (CDK9) (Brasier et al., 2011). Signal dependent binding of NF-κB in conjunction with histone acetylation (Hargreaves et al., 2009; Zippo et al., 2009) mediates the recruitment of BRD4 to the vicinity of gene promoters with the associated activity of CDK9, which induces the release of paused polymerases (Ai et al., 2011). *TNF* promoter ChIP revealed a rapid-transient recruitment of BRD4 within 30 minutes of LPS stimulation, whereas occupancy of BRD4 at the *IL1B* promoter was less prominent (**Figure 54**).

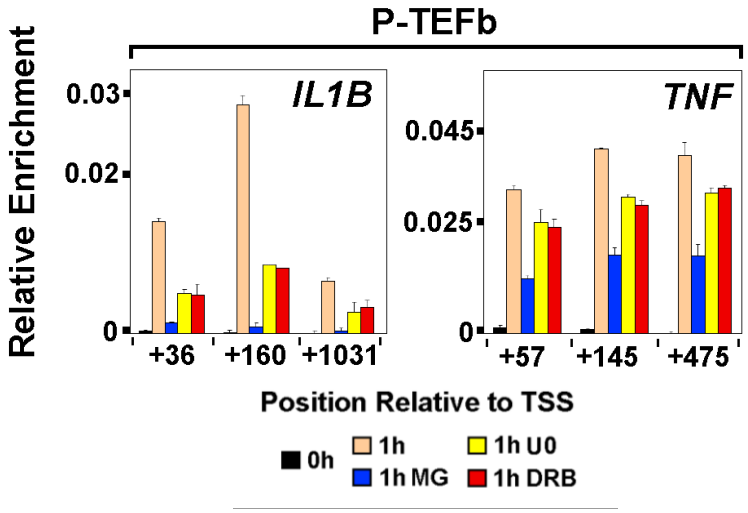

Figure 53. Effect of various inhibitors on P-TEFb binding to *IL1B* and *TNF* in THP-1 cells.

Shown is a ChIP analysis of the P-TEFb binding in 1-hour stimulated THP-1 cells, pre-treated with the transcription factor inhibitors MG132 (blue bars) and U0126 (yellow bars), as well as the elongation factor P-TEFb inhibitor DRB (red bars). The data are indicative of at least 2 independent experiments.

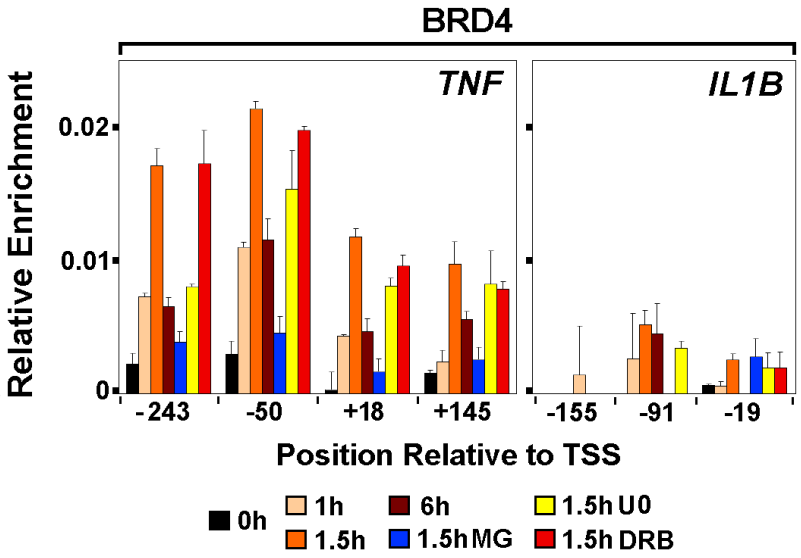

Figure 54. The effect of inhibitors on BRD4 binding to *IL1B* and *TNF* in THP-1 cells.

Shown is the ChIP analysis for the kinetics of BRD4 binding to the *IL1B* and *TNF* gene promoters. The time points for LPS treatments are indicated above. The inhibitors (MG132, U0126, and DRB) were

applied 2 hours prior to the 1.5-hour LPS stimulations of the THP-1 cells. The data are indicative of at least 2 independent experiments.

My analysis revealed that binding of BRD4 to *TNF* is unaffected in DRB treated cells (**Figure 54**). In agreement, only slight inhibition of P-TEFb association at the *TNF* promoter was observed. In contrast, P-TEFb binding upon DRB treatment to *IL1B* was significantly depleted (**Figure 53**). Consistent with these results, both transcription (**Figure 22**, *lower panels*) and serine 2 CTD phosphorylation along the coding region (**Figure 55**) were affected more significantly for *IL1B* than for *TNF*.

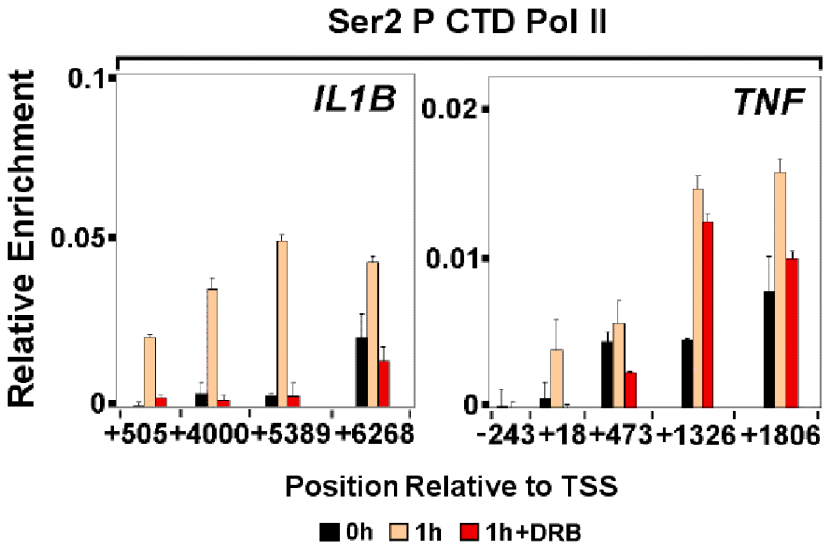

Figure 55. DRB differentially affects the S2P CTD Pol II occupancy on *IL1B* and *TNF* genes THP-1 cells.

Shown is a ChIP analysis of the S2P CTD Pol II occupancy in resting and 1-hour stimulated THP-1 cells. THP-1 cells were also pre-treated with the elongation factor P-TEFb inhibitor DRB (red bars) for 2 hours prior to LPS treatments.

I argue that the differential association of P-TEFb on promoters for these genes in DRB treated cells is mediated by gene-specific BRD4 recruitment. P-TEFb recruitment to

IL1B seems to be less dependent upon BRD4 than *TNF*. In contrast, inhibition of C/EBPβ activation had a dramatic effect on P-TEFb binding to *IL1B* (**Figure 53**). This result suggests a possible novel role for C/EBPβ as an adaptor mediating the recruitment of P-TEFb to the *IL1B* promoter. As expected, only minor changes in P-TEFb occupancy at the *TNF* promoter was observed in U0126 exposed cells.

Transcription Factor Mediated Looping Between the *IL1B* Distal Enhancer and Promoter

Previous reports have identified distal far-upstream enhancers, positioned -3000 bp upstream from the TSS for human and -2200 for mouse, critical for robust *IL1B* induction (Godambe et al., 1995; Shirakawa et al., 1993). Recent genome-wide studies in murine macrophages demonstrated that LPS responsive enhancers have common features marked by inducible p300 binding and H3K4me1 modification (Ghisletti et al., 2010; Heinz et al., 2010). This analysis of H3K4me1 revealed significant enrichment of this mark throughout the transcribed regions of *IL1B* and *TNF*, as well as at the -3000 bp upstream *IL1B* enhancer **(Figure 56)**.

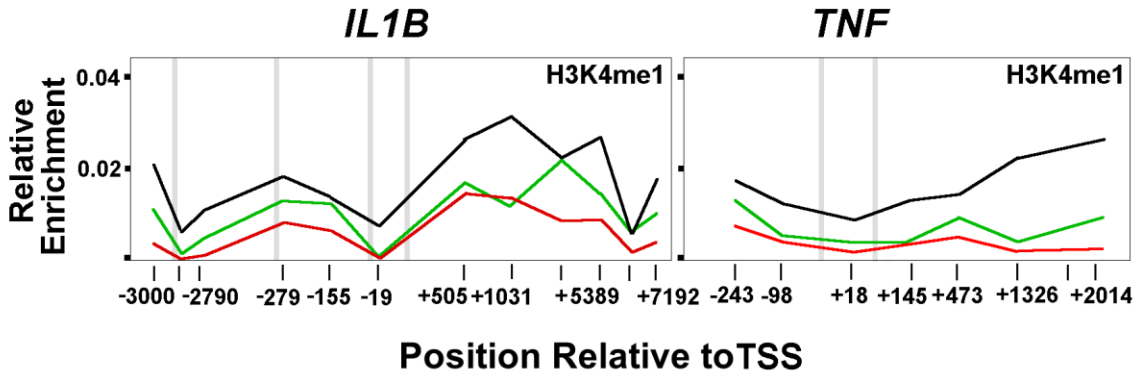

Figure 56. H3K4me1 is present throughout *IL1B* and *TNF* in THP-1 cells.

ChIP data revealing H3K4me1 spatial-temporal distribution along the *IL1B* and *TNF* loci in resting (black line) 1 hour (red line) and 5 hour (green line) stimulated THP-1 cells. Averaged profiles derived from data shown in **Appendix G**.

Chromosomal interactions between distal regulatory elements have been implicated in regulating gene expression (Dekker, 2006). The dynamic association of enhancers and promoters is often mediated by protein-protein and protein-DNA interactions among transcription factors and chromatin modifiers, ultimately leading to an enhanced transcription initiation (Deng et al., 2012). On the basis of *in vitro* studies, functional cooperation between enhancer bound C/EBPβ and promoter bound Spi1 DNA looping has previously been proposed as a mechanism for *IL1B* induction (Listman et al., 2005; Yang et al., 2000). In collaboration with Dr. Kent Z.Q. Wang in our laboratory, I used chromatin conformation capture (3C) to examine LPS-dependent *in vivo* long-range chromosomal interactions between the *IL1B* enhancer and promoter. **Figure 57B** reveals LPS-dependent physical association between the *IL1B* distal and proximal regulatory elements.

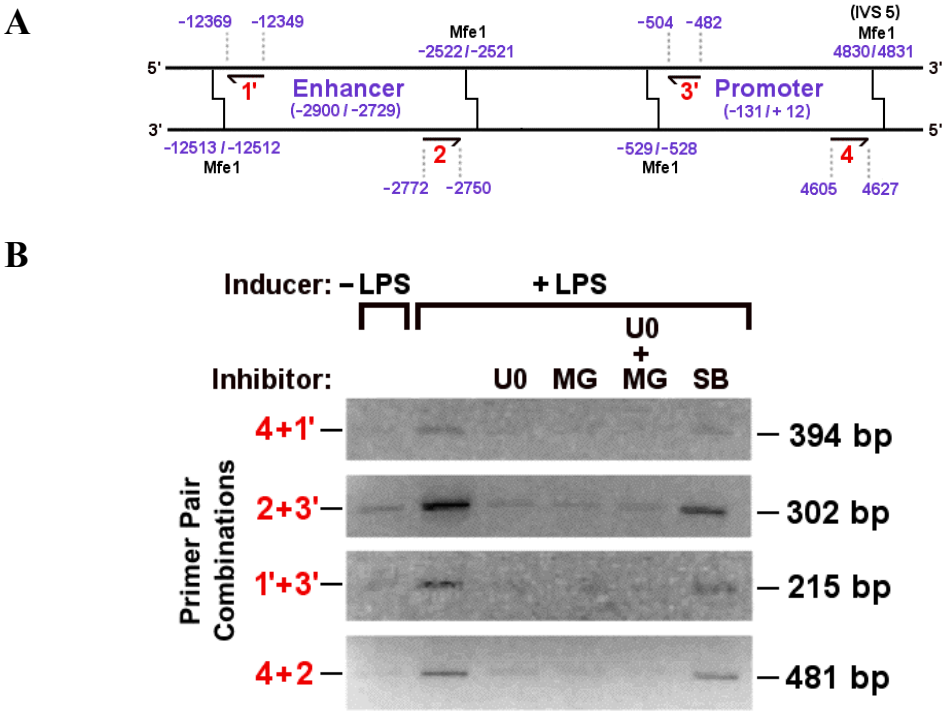

Figure 57. LPS induced chromatin looping regulates *IL1B* expression.

(A) Schematic representation of PCR primer pairs used for evaluating 3C ligation products. The four primers used for 3C analysis are indicated as 1', 2, 3', and 4 in the diagram.

(B) 2% agarose gel was used for the PCR assessment of 3C ligation (restriction fragment) products from resting, 1 hour stimulated, and inhibitor treated THP-1 cells. One hour stimulated THP-1 cells were pre-treated with the indicated transcription factor inhibitors MG132 (NF-κB inhibitor), U0126 (C/EBPβ inhibitor) and additional C/EBPβ inhibitor SB 202190.

The NF-κB and C/EBPβ inhibitors abolished LPS dependent chromosome loop formation (**Figure 57B**), transcription (**Figure 44, 46, 47**), nucleosome depletion (**Figure 28**), and Pol II recruitment to the *IL1B* promoter (**Figure 58**).

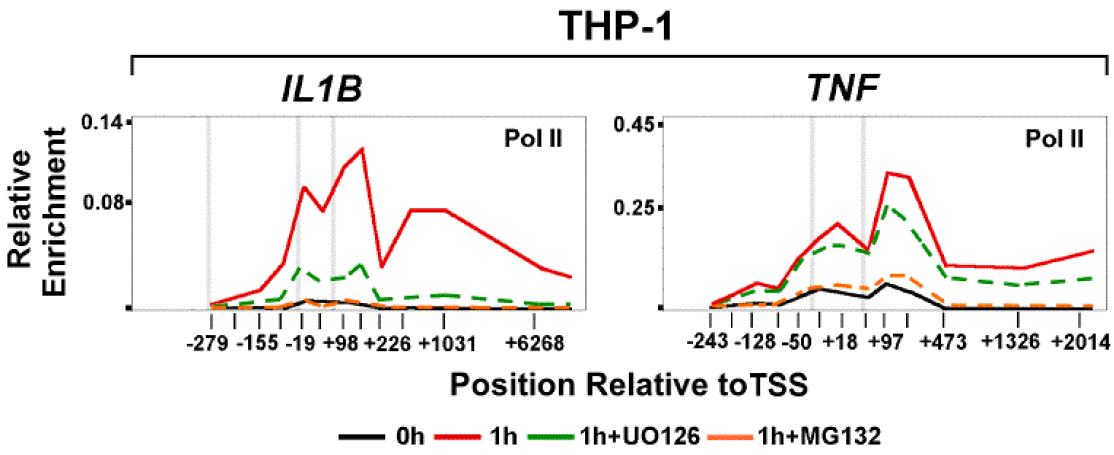

Figure 58. Effects of U0126 and MG132 on Pol II ChIP for *IL1B* and *TNF*.

Shown is the ChIP analysis for the spatial-temporal distribution of Pol II throughout the *IL1B* and *TNF* genes. The time points for LPS treatments are indicated above. The inhibitors MG132 (NF-κB inhibitor) and U0126 (C/EBPβ inhibitor) were applied 2 hours prior to the 1 hour LPS stimulations of the THP-1 cells. The data are indicative of at least 2 independent experiments.

My data reveal that the chromosome looping correlates with the binding of C/EBPβ to the enhancer and Spi1 to the promoter of *Il1B*. In addition to interacting with C/EBPβ, the DNA binding domain of Spi1 was shown to physically associate *in vitro* with NF-κB (Nawarat Wara-aswapati and Philip E. Auron, unpublished data).

These data suggest that endotoxin activation of both C/EBPβ and NF-κB may contribute to the dynamic juxtapositioning of the distal regulatory elements of *IL1B* by common association with two critical Spi1 binding sites previously mapped to the IL1B promoter (Kominato et al., 1995), resulting in the formation of a chromatin complex favorable for gene induction.

Metabolic Effects on Transcriptional Regulation of *Il1b* and *Tnf*

Since P-TEFb recruitment to *IL1B*, in contrast to *TNF*, appears to be less dependent upon BRD4 and more dependent upon C/EBPβ, other activation pathways for P-TEFb activation, by release from the inhibited 7SK/HEXIM1 complex, were considered. One of these is the possible involvement of PI3K/Akt, which has been reported to directly phosphorylate and inactivate HEXIM1 on the HIV promoter (Contreras et al., 2007). **Figure 59** reveals that the PI3K inhibitor LY-294002 has a greater effect on P-TEFb recruitment to *Il1b* than to *Tnf* in LPS-treated RAW264.7 cells.

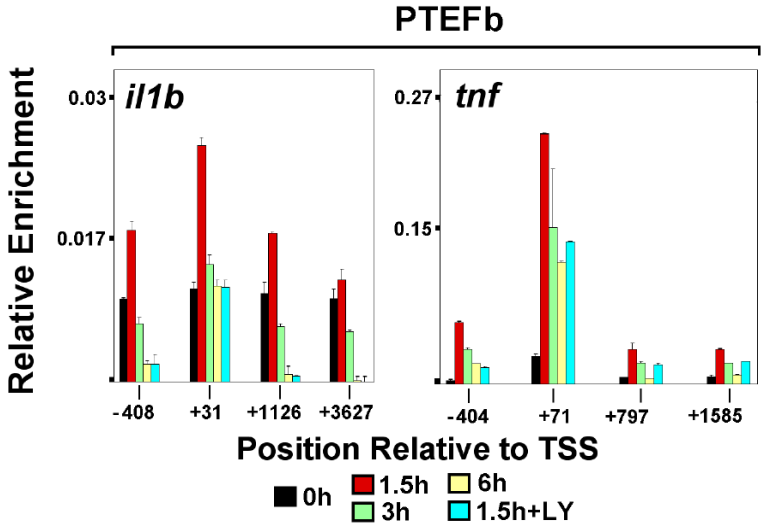

Figure 59. The effect of PI3K inhibition on P-TEFb recruitment to *Il1b* in RAW264.7 cells.

Shown is ChIP analysis of P-TEFb binding to *Il1b* and *Tnf* in the presence of the PI3K inhibitor LY-294002 in RAW264.7 cells. The inhibitor LY-294002 was applied 1 hour prior to LPS stimulations.

Since increased synthesis of PI3K results in phosphorylation and activation of Akt/PKB, which can counteract the inhibitory effect of AMPK (low ATP) on mTorc1, I wondered whether there is a connection between *Il1b* gene activation and cellular metabolism. The non-metabolizable glucose analogue and hexokinase inhibitor 2-deoxyglucose (2-DG) (Kang and Hwang, 2006) has been used to metabolically challenge cells by directly inhibiting glycolysis and ATP synthesis. I observed significantly higher levels of Pol II, S2P CTD, p-TEFb, and H3K36me3 on *Tnf* than on *Il1b* for 2-DG treated BMDM (**Figure 60**). In contrast to *Il1b*, the levels of S5P CTD at *Tnf* were not affected by 2DG. This is in agreement with experiments analyzing total Pol II levels, in which *Il1b* is more affected by treatment with 2DG (**Figure 60)**. These results are consistent with a greater metabolic sensitivity for *Il1b* that may relate to the distinct mechanism of P-TEFb activation. Interestingly, ligand-mediated activation of both TLR and IL1R receptors not only induces *IL1B* transcription, but also directly recruits and activates PI3K (Marmiroli et al., 1998; Sarkar et al., 2004), consistent with the proposed role for PI3K/Akt in P-TEFb activated induction.

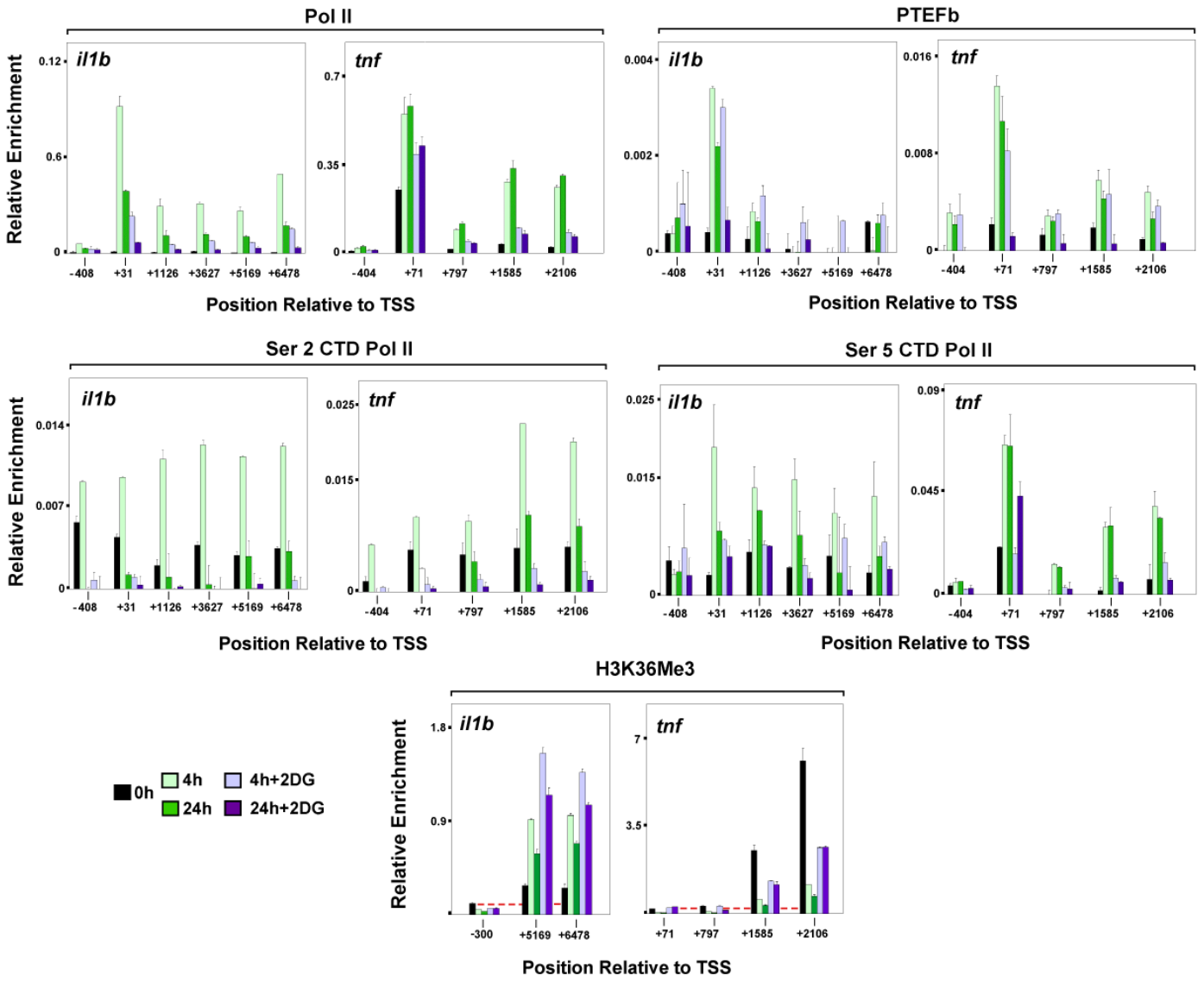
Pol II
PTEFb
Ser 2 CTD Pol II
Ser 5 CTD Pol II
H3K36Me3
il1b
tnf
Relative Enrichment
Position Relative to TSS
0h
4h
4h+2DG
24h
24h+2DG
-408
+31
+1126
+3627
+5169
+6478
-404
+71
+797
+1585
+2106
-300

Figure 60. Distinct metabolic sensitivity for transcription elongation on *Il1b* and *Tnf* in murine bone marrow-derived monocytes.

ChIP for factors related to Pol II initiation and elongation at *Il1b* and *Tnf* loci were measured in resting (black), 4h (light green) and 24h (light blue) LPS stimulated *ex vivo*-differentiated mouse BMDM. Enrichment profiles for Pol II, PTEFb, S2P CTD Pol II, S5P CTD Pol II, and H3K36me3 are shown. The BMDM were stimulated for indicated times with LPS ± 3 h pretreatment with 2-DG. The BMDM samples were provided by Luke O' Neill, Trinity Collage of Dublin, Ireland.

HIF-1α plays an important role in regulation of the pro-inflammatory genes that are activatied in the TLR4 stimulated macrophages (Tannahill and O'Neill, 2011). Our analysis of the murine *Ilib* locus revealed a putative HRE element known to bind HIF-1α (Kimura et al., 2000), which is adjacent to a previously reported NF-κB site (Hiscott et al., 1993) (**Figure 61**).

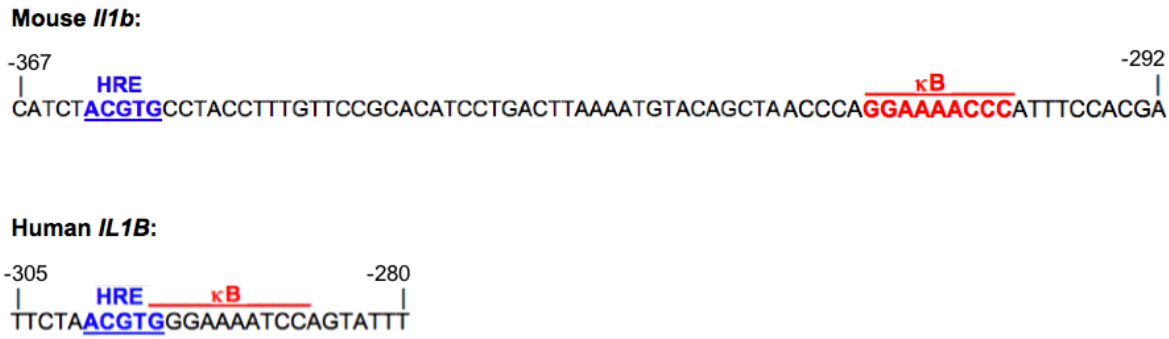

Figure 61. A schematic representation of putative HIF1α binding site upstream of the *il1b* gene promoter.

Our group has located a putative HIF1α response element (HRE) binding sequence in the vicinity of the *Il1b* promoter, 360 bp upstream of the TSS. Shown is a comparison of human and mouse putative HIF-1α binding site (Blue). The NF-κB binding site (red) is positioned further downstream in the mouse as compared to a human *IL1B*. Additional experiments revealed that mutations in the HRE reduced the expression of the IL1B-luciferase reporter (Tannahill GM, 2013).

ChIP analysis in BMDM revealed a delayed LPS inducible binding of HIF-1α to the putative murine HRE. The most prominent binding of HIF-1α to this promoter-proximal regulatory site is observed at 12 and 24 hours. This experiment is part of a collaborative study that has additional evidence of HIF-1α involvement in *Il1b* gene

regulation (Tannahill GM, 2013). Both 2DG and α-KG reduced the HIF-1α binding to the HRE (**Figure 62**). The *Tlr4* gene was used as a positive control (Kim et al., 2010). Our results reveal that HIF-1α is recruited to the *Il1b* promoter in LPS stimulated BMDM.

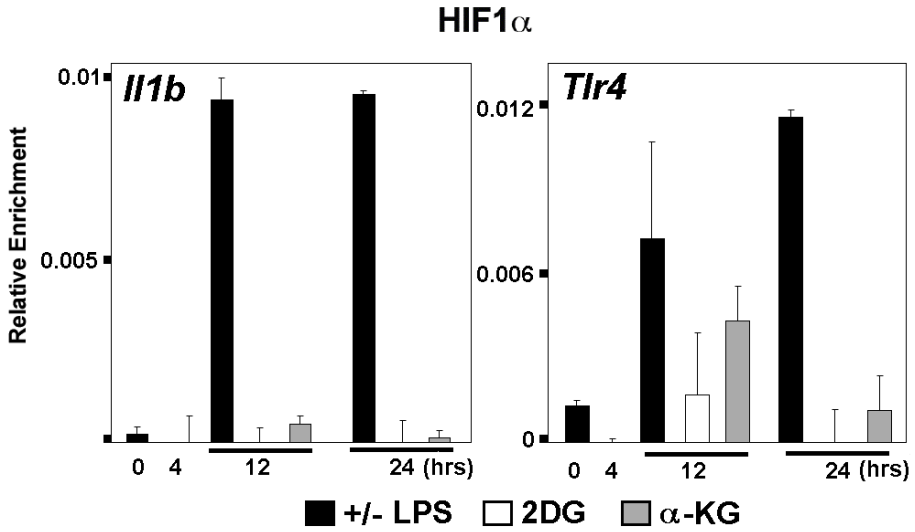

Figure 62. HIF-1α is recruited to the *Il1b* and *Tlr4* genes in LPS treated BMDM.

ChIP for HIF-1α binding to the *Il1b* and *Tlr4* proposed binding sites was measured in resting 4h, 12h, and 24h LPS stimulated *ex vivo*-differentiated mouse BMDM. The BMDM were stimulated for indicated times with LPS and/or pre-treated for 3h with the non-metabolizable glucose analogue and hexokinase inhibitor 2-deoxyglucose (2-DG) (Kang and Hwang, 2006), or the HIF1α inhibitor α-ketoglutarate (α-KG) (Gottlieb and Tomlinson, 2005). The BMDM samples were provided by Luke O' Neill, Trinity Collage of Dublin, Ireland.

IL-1 Family members are coordinately expressed in LPS stimulated THP-1 monocytes.

Since *IL1B* is a member of a family of 11 genes (Dinarello, 2009), I have investigated their LPS inducible expression in THP-1 monocytes. Our results reveal that 9 gene members are coordinately expressed with the transcription levels peaking at 2

hours post LPS treatment. Interestingly, *IL1F6* is constitutively expressed and LPS treatment dose not activate it. The expression of *IL1F10* was not detected in THP-1 cells. Since *IL1B* is potently expressed in THP-1 cells, additional qPCR plots were generated in order to better resolve the kinetic expression pattern of the other inducible gene members (**Figure 63**).

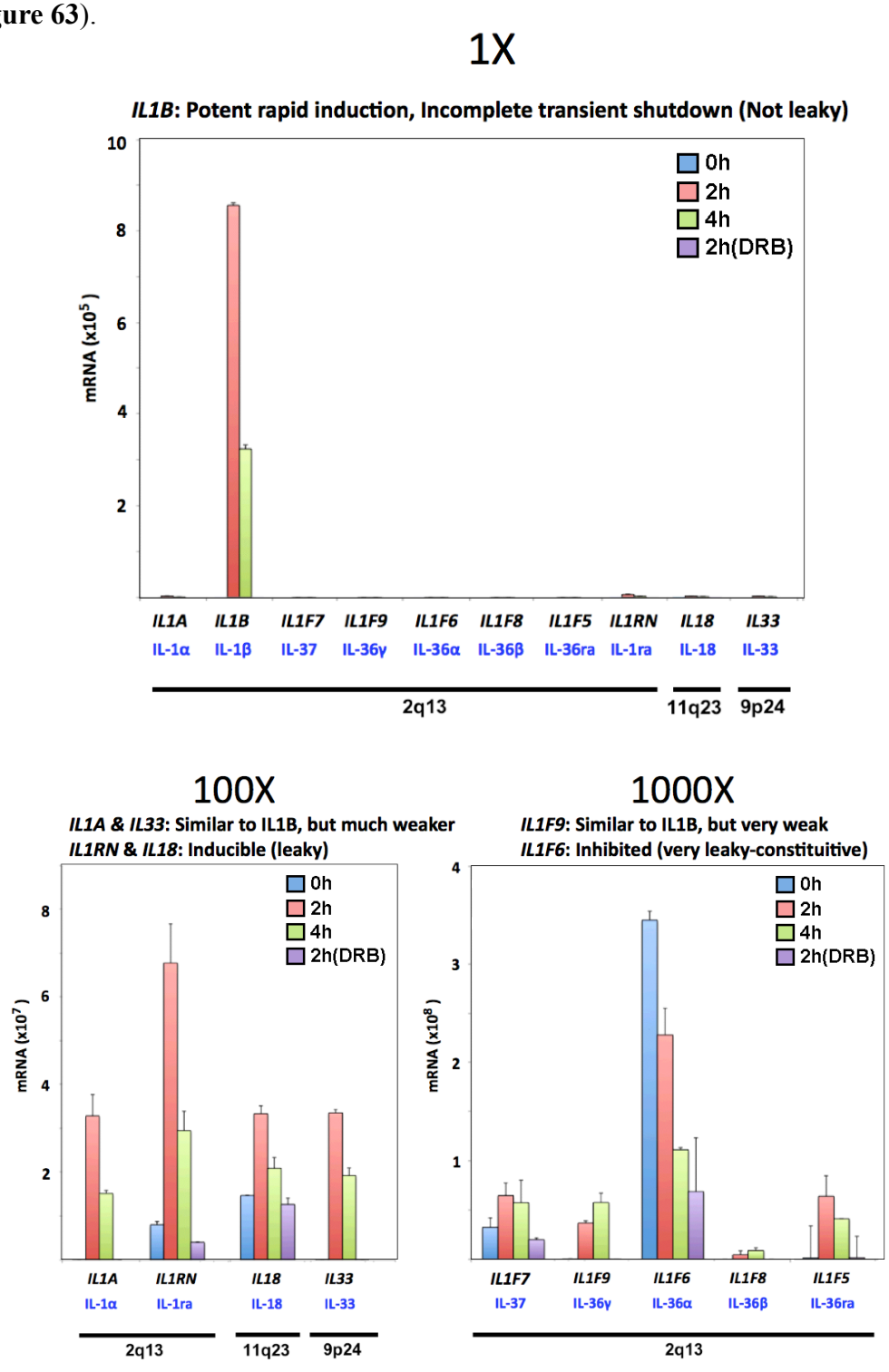

Figure 63. Coordinate expression of the IL-1 gene family members.

Shown are kinetic qPCR data for the various IL-1 family members in LPS stimulated THP-1 cells. LPS treatment time points are indicated. THP-1 cells were also pre-treated with the elongation factor P-TEFb inhibitor DRB (red bars) for 2 hours prior to LPS treatments. Since the expression of *IL1B* is extremely high, data presented in the bottom diagrams were re-scaled (100x, and 1000x) in order to visualize the expression kinetics for the less abundant family members.

DISCUSSION

The induction of pro-inflammatory IE genes *IL1B* and *TNF* involves stringently regulated sequences of events triggered by TLR4 mediated detection of the LPS component of bacterial cell walls. My detailed kinetic analyses of the mRNA profiles of these immune genes provide novel insights into changes associated with their induction, switch down and reactivation. I was able to recapitulate previous observations (Fenton et al., 1988) demonstrating the expression pattern for *IL1B* and compare it to that of another coordinately expressed IE gene, *TNF*. Temporal profiles of steady-state mRNA levels revealed that both genes undergo a rapid transient induction, but differ in their transcriptional shut down. While *TNF* fits the transient IE gene model and is completely switched-off at 4 hours, elevated expression of *IL1B* continues for up to 24 hours post-stimulation (**Figure 6, 7**). Because they code for potent inflammatory molecules, posttranscriptional degradation serves as a means to prevent their uncontrolled accumulation (Chen et al., 1994; Fenton et al., 1988). This explains the transient nature of these genes and argues that the observed sustained expression for *IL1B* is due to continuous transcription instead of message stabilization. Although *IL1B* sustained expression is relatively decreased, it is physiologically significant due to the potent biological activity of this cytokine (Dinarello, 2010) and the extremely high overall transcription level (Webb et al., 1985). Additionally, analysis of steady state mRNA levels in unstimulated THP-1 monocytes revealed the presence of low levels of un-spliced *TNF* mRNA transcripts in comparison to undetectable *IL1B*. It has been hypothesized that low levels of constitutive transcription for primary response genes favors accessible chromatin and transcriptional competence important for their activation

(Hargreaves et al., 2009). Previous reports indicate that activation of IE genes resides at the level of pre-assembled components of transcription machinery at their promoters (Adelman et al., 2009; Hargreaves et al., 2009). Engaged, but paused, Pol II complexes and an euchromatic nucleosome architecture favors the immediate response to an appropriate stimulus causing transition into a state of processive elongation (Escoubet-Lozach et al., 2011). Utilizing various molecular techniques I have analyzed the binding of specific signal-responsive transcription factors, general factors involved in Pol II regulation, and chromatin modifications in order to provide insights into mechanisms influencing the observed distinct expression profiles of *IL1B* and *TNF*. Although both mediators are classified as IE responders in TLR4-dependent stimulated cells, this study using human and murine monocytes reveals transcriptional and epigenetic differences during their expression cycle.

In unstimulated cells, the *TNF* promoter proximal region contains a significant amount of pre-bound Pol II, which is consistent with studies in murine macrophages (Adelman et al., 2009; Escoubet-Lozach et al., 2011; Hargreaves et al., 2009). A collection of antibodies recognizing various modifications of the Pol II CTD was used to characterize the nature of this pre-assembled Pol II complex. ChIP analysis revealed the presence of S5P modified CTD co-localized with the observed total Pol II enrichment peak (**Figure 17)**, which indicates that the observed Pol II has initiated transcription (Saunders et al., 2006), but paused nearly 57 bp beyond TSS. Additionally, I observed a high level of pre-bound TBP, a component necessary for accurate transcription initiation (Thomas and Chiang, 2006), at the expected *TNF* TATA box, further confirming the

presence of suitably engaged Pol II. I hypothesize that the pre-assembled components of the transcription machinery contribute to the low constitutive transcriptional leakiness of the *TNF* gene, keeping it primed for rapid activation. Under basal conditions, quiescent *IL1B* is more stringently regulated, containing only slight levels of Pol II engaged at the promoter and minimal TBP binding. I hypothesized that a recruitment of Pol II machinery to the *IL1B* promoter requires an additional step in the form of TLR4 dependent recruitment of effector proteins and/or changes in chromatin accessibility. LPS stimulation triggered a transient increase of Pol II at the proposed *TNF* pause site as well as throughout the body of the gene (corresponding to elongating Pol II), but the levels of TBP did not significantly change. On the other hand, the induction of *IL1B* was primarily dependent on *de novo* recruitment of Pol II complexes, which paused shortly after resuming initiation in the vicinity of the TSS. As expected, binding of TBP paralleled the LPS dependent increase of Pol II at the *IL1B* locus. These results suggest a presence of two gene specific induction mechanisms with different rate-limiting properties. While the rate-limiting step in *IL1B* activation depends on *de novo* recruitment of Pol II, *TNF* induction is mediated by a release of existing promoter bound Pol II complexes. These differences likely contribute to the observed transcriptional delay for *IL1B* as measured by steady state mRNA and Pol II kinetic occupancy assays (**Figure 8B)**. Analyses of NELF occupancy, a factor potentiating Pol II stalling (Core and Lis, 2008), revealed high binding levels at *TNF* in unstimulated cells followed by a decrease upon LPS treatment. An observed decline of NELF following stimulus is consistent with LPS dependent binding of P-TEFb, which induces phosphorylation of NELF (Gilmour, 2009) and alleviates the paused Pol II, transitioning it to elongation. At 5 hours post stimulation,

when message levels decline, P-TEFb is depleted from the promoter region and NELF occupancy returns to original levels, likely explaining gene shut down. In contrast to *TNF*, P-TEFb recruitment to *IL1B* is prolonged (although decreased) and present at 5 hours post stimulation. This provides a plausible explanation for the delayed/sustained phase of *IL1B* expression as compared to that of *TNF*. The data argue for a kinetic interplay between positive (P-TEFb) and negative (NELF) pausing factors that may contribute to the differential post-induction decrease and shutdown of these two IE genes.

A presence of paused polymerase, as indicated by increased enrichment signal at the promoter as compared to the structural gene, was detected at *TNF* and *IL1B* promoters in LPS stimulated monocytes. Interestingly, two paused Pol II complexes were detected at *IL1B* while only one primary complex was present at the *TNF* promoter (**Figure 11**). Analysis of the RNA intermediates revealed that the first Pol II peak at both genes was associated with short transcripts whose levels correlated with the temporal binding of Pol II and were selectively sensitive to inhibitor treatments (**Figure 22**). Global genome sequencing analysis revealed that such transcripts are actually nascent RNA intermediates emerging from stalling polymerases (Churchman and Weissman, 2011). Detection of RNA intermediates was limited only to the regions beyond the TSS of both genes, which further confirmed that the observed transcripts are specific to processive polymerase, and not aberrant byproducts of cDNA synthesis. A total of five antibodies (Pol II, S5P CTD Pol II, NELF and P-TEFb) from independent ChIP experiments collectively revealed two pausing sites near the *IL1B* gene promoter. I hypothesize that the second Pol II complex at the *IL1B* locus represents a second paused polymerase. The progression of these complexes is delayed due to several plausible

factors. Since nucleosomes have been indicated in posing as a physical barrier to transcribing polymerases (Petesch and Lis, 2012), the presence of a downstream +1 positioned nucleosome might be responsible for halting Pol II movement. An additional explanation for the Pol II resting can stem from the presence of a long 5' untranslated region (UTR) encompassing the first 505 bp of the *IL1B* gene. A recent study proposed a "complex interaction" model between core promoter elements and initiating and paused Pol II complexes, which can often accumulate at the intron-exon splicing junctions, as well as upstream of nucleosomes (Kwak et al., 2013). Such gathering of Pol II enzymes creates a dispersed Pol II enrichment signal at the transcription initiation site and beyond the TSS (Kwak et al., 2013). These observations further support the possibility that the 5' UTR and +1 nucleosome present at the *IL1B* dictate pausing for transcribing/elongating Pol II. Additionally there are indications that the length of a 5'UTR can influence gene expression levels (Cenik et al., 2010). Since mRNA splicing can occur co-transcriptionally (Goldstrohm et al., 2001), the augmented recruitment of splicing factors to the vicinity of 5'UTR can play a potential role in slowing down Pol II progression. In fact, studies suggest that a slower Pol II rate favors precise assembly of splicing factors for propter intron removal (de la Mata et al., 2010). I speculate that the second Pol II pause might serve as an additional regulatory checkpoint for ensuring proper *IL1B* transcription elongation.

Here I show that LPS inducible binding of NF-κB facilitates the recruitment of BRD4 and the subsequent recruitment of P-TEFb to human *TNF*. My data revealed that the inhibition of NF-κB binding resulted in significant depletion of P-TEFb recruitment

to both genes (**Figure 53**). This observation is consistent with reports indicating that NF-κB phosphorylated at Serine 276 interacts with the active P-TEFb complex consisting of bromodomain protein 4 (BRD4) and cyclin-dependent kinase 9 (CDK9) (Brasier et al., 2011). Signal dependent binding of NF-κB in conjunction with histone acetylation (Hargreaves et al., 2009; Zippo et al., 2009) mediates the recruitment of BRD4 to the vicinity of gene promoters with the associated activity of CDK9, which induces the release of paused polymerases (Ai et al., 2011). Accordingly, I detected a transient recruitment of BRD4 to the *TNF* gene. ChIP enrichment for BRD4 at the *IL1B* promoter was much less prominent (**Figure 54**), suggesting that P-TEFb is not brought to the *IL1B* promoter independently of BRD4. Cell permeable inhibitor DRB was used in this study to block action of P-TEFb and show that blockade of this factor causes freezing of Pol II throughout the *IL1B* and *TNF* gene loci (**Figure 17)** and reduction of transcript accumulation (**Figure 22**). In addition to selectively inhibiting CDK9 activity (Baumli et al., 2010), DRB has been also shown to alleviate the inactive 7SK/HEXIM1 sequestered P-TEFb to an active BRD4-bound state (Biglione et al., 2007; Nguyen et al., 2001; Yik et al., 2003). In this way DRB increased recruitment of BRD4 and P-TEFb to the viral C promoter in Burkitt's lymphoma cell lines (Palermo et al., 2011). My analysis revealed that binding of BRD4 to *TNF* is unaffected in DRB treated cells (**Figure 54**). In agreement, only slight inhibition of P-TEFb association at the *TNF* promoter was observed. In contrast, P-TEFb binding upon DRB treatment to *IL1B* was significantly depleted (**Figure 53**). Consistent with these results, both transcription (**Figure 22***, lower panels*) and S2P CTD along the coding region (**Figure 55**) were affected more significantly for *IL1B* than for *TNF*. I argue that the differential association of P-TEFb on

promoters for these genes in DRB treated cells is mediated by gene-specific BRD4 recruitment. The LPS inducible P-TEFb binding to *IL1B* seems to be less dependent upon BRD4 than is *TNF*. In contrast, inhibition of C/EBPβ activation had a dramatic effect on P-TEFb binding to *IL1B* (**Figure 53)**. This result indicates a likely novel role for C/EBPβ as an adaptor mediating the recruitment of P-TEFb to the *IL1B* promoter. As expected, only minor changes in P-TEFb occupancy at the *TNF* promoter were observed in cells depleted of active C/EBPβ by the usage of selective inhibitor U0126 (**Figure 53**). Additionally, I argue that PI3K/Akt mediated rescue of P-TEFb from inhibitory 7SK/HEXIM1 complex can selectively contribute to the elongation state of *Il1b* in murine macrophages (**Figure 59**). Since it has been shown that a metabolic imbalance of cells affects the PI3K/Akt transduction pathway, a disruption of glucose availability in stimulated BMDMs caused selective inhibition of *Il1b* transcription as compared to *TNF*, as shown in **Figure 60**.

Macrophage metabolism plays an important role regulating transcriptional control of pro-inflammatory cytokines (Murdoch et al., 2005). My collaborative work with the laboratory of Professor Luke O'Neill using murine macrophages revealed a novel role of the oxygen sensing effector protein HIF1α in controlling *Il1b* transcription. Our group has located a putative HIF1α response element (HRE) binding sequence in the vicinity of the *Il1b* promoter, 360 bp upstream of the TSS (Tannahill GM, 2013). TLR4 dependent stimulation of macrophages caused HIF1α binding to the HRE at 4 h with increasing levels by 24 hours (**Figure 62**). The functional role of HIF1α was further established by the addition of cell permeable α-KG, which abolished its LPS mediated recruitment to *Il1b*. It was shown that α-KG induces HIF1α degradation (Gottlieb and Tomlinson,

2005) and prevents its nuclear translocation. Additionally, treatment of cells with the non-metabolizable glucose analogue 2DG (Kang and Hwang, 2006) also prevented HIF1α binding. I postulate that 2DG mediated disruption of macrophage metabolism and down-regulated activity of HIF1α, leading to decreased *Il1b* expression. The *Tnf* gene was not susceptible to 2DG treatment, as revealed by mRNA and Pol II ChIP analysis (**Figure 62**). My kinetic ChIP analysis suggests that HIF1α recruitment to *Il1b* is delayed and follows the binding of the rapidly induced factors NF-κB and C/EBPβ. I speculate that HIF1α plays a role in mediating the sustained phase of *il1b* expression. This is distinct from *Tnf*, which lacks a putative HRE in the vicinity of its promoter. **Figure 64** summarizes the key observations and differences in the regulation of the *il1b* and *tnf* gene transcription.

Previous reports argued that *il1b* and *tnf* genes are refractory to reactivation due to a plethora of intrinsic immuno-protective mechanisms commonly recognized as endotoxin tolerance (Chan et al., 2005; Foster and Medzhitov, 2009). Endotoxin tolerance results in a decreased responsiveness of certain rapidly-induced monocyte genes to repeated LPS stimulation. In agreement with the previous studies, our data indicate that once activated, *TNF* cannot be re-expressed upon secondary stimulation (**Figure 7**). In addition, the reduced responsiveness of *TNF* cannot be reversed with increased concentration of LPS used for subsequent reactivation (**Figure 13**). Prior attempts to explain this phenomenon by transcription suppression have failed to note that expression profiles for these genes are highly transient. If transcription following secondary stimulation is not analyzed within a short time frame, the re-stimulation properties can be overlooked. The endotoxin tolerance study by Foster *et al.,* (Hargreaves

et al., 2009) used ten-fold less secondary LPS stimulant than the primary dose. I argue that the usage of inconsistent doses of secondary LPS throughout the studies skews the experimental results. In my reactivation experiments, cell cultures were re-stimulated with an equal dose of secondary LPS.

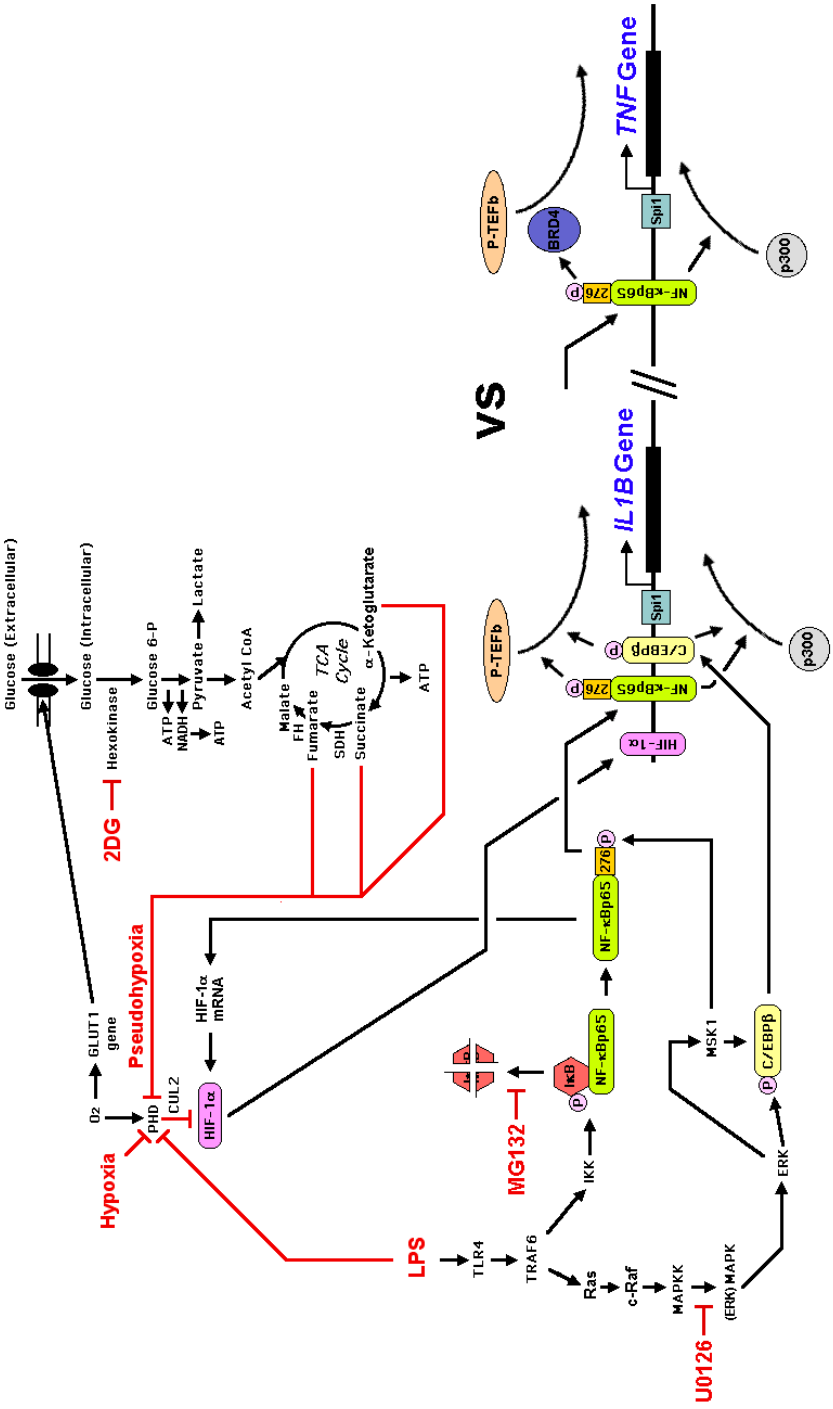

Figure 64. Metabolic and TLR4 dependent pathways differentially regulate transcription of *il1b* and *tnf*. Several findings of this work are represented in this figure. Depicted are LPS sensing TLR4 pathways leading to activation, nuclear translocation and DNA binding of the transcription factors NF-κB and C/EBPβ. While the induction of *TNF* is primarily dependent on NF-κB, *IL1B* requires both, NF-κB and C/EBPβ for its proper activation. This figure illustrates the connections between the metabolic pathways and the regulation of HIF1α stability. Hypoxia, LPS treatments, and various metabolites affect the presence of HIF1α in cells. These conditions inhibit the action of the enzyme prolyl hydroxylase (PHD), which causes the ubiquitin-mediated degradation of HIF-1α. Stabilized HIF-1α translocates into nucleus where it binds to the hypoxia-response element located upstream of *il1b*.

In addition, the washing of cells between primary and secondary endotoxin challenge may result in experimental variability and induce physiological stress to the highly sensitive cells. Here I show that the washing of cells caused dramatic reduction of *IL1B* expression (**Figure 27**). In contrast, *IL1B* transcription is not desensitized in un-washed cell cultures (**Figure 7, 13**). This indicates that secondary LPS addition after washing cells is ineffective and does not properly activate the transduction pathway leading to transcriptional induction of *IL1B*. I hypothesize that washing cells with PBS or media lacking fetal bovine serum (FBS) prior to secondary challenge may deprive the cells of important soluble components such as LPS-binding protein (LPB) and CD14 that are vital for proper TLR4 signaling (Aderem and Ulevitch, 2000).

My data provide evidence that IE gene promoters contained paused pol II complexes after their initial transient transcription burst for up to 25 hours. This work reveals that upon secondary stimulation, P-TEFb is re-recruited to the *IL1B* promoter, resulting in the resumption and maintenance of transcriptional elongation by Pol II. This is in contrast to tolerized *TNF*, in which secondary recruitment of P-TEFb and S2P are absent (**Figure 24, 25**). As described in the introduction, P-TEFb mediated phosphorylation of serine 2 within the CTD of elongating Pol II promotes recruitment of various splicing factors to ensure proper nascent mRNA processing (Buratowski, 2003; Egloff and Murphy, 2008). The fact that P-TEFb is recruited to *IL1B* and not *TNF* during secondary LPS exposures, prompted me to examine the integrity of transcripts produced in reactivated THP-1 cells. The analysis of a random primer (instead of polyA) generated cDNA products, which revealed a minor increase of *TNF* mRNA in secondary stimulated monocytes (**Figure 26**). These messages likely represent incompletely processed primary

TNF transcripts that are generated by the low levels of P-TEFb-deficient transcribing Pol II. I propose that the gene specific recruitment of P-TEFb serves as a regulatory step mediating the escape form endotoxin tolerance. This mechanism ensures proper *IL1B* mRNA polyadenylation and processing, which is deficient during the re-stimulation of the *TNF* gene. My results indicate that the low levels of sustained *IL1B* expression may maintain the gene sufficiently competent for secondary re-induction. Collectively my mRNA and protein analyses argue that secondary induction of *IL1B* is a physiologically significant phenomenon that further distinguishes it from *TNF*.

Nucleosome positioning is intimately linked to gene regulation by controlling the accessibility of gene promoter sequences (Bai and Morozov, 2010). I have mapped the nucleosome distribution (as measured by the spatial distribution of the nucleosome core protein histone 3) in the vicinity of the promoter proximal regions as well as the temporal changes associated with their LPS inducible evictions and differential re-assembly at the end of the transient *vs*. sustained phase of *TNF* and *IL1B* transcription, respectively. My data reveal a cell type specific NFR located upstream of the strongly phased +1 nucleosome at both genes (**Figure 28**). Analysis of HEK 293 cells, which do not transcribe *IL1B*, revealed the presence of a highly phased -1 nucleosome within the NFR that was also prominent in the inhibitor treated THP-1 cells (**Figure 28**). Transfection of Spi1 with IRF8 and TRAF6 (acting as an LPS surrogate) induces displacement of this -1 nucleosome. I hypothesize that this highly transiently positioned nucleosome serves as a control checkpoint mediating a cell type and stimulus selective accession of transcription machinery to the *IL1B* core promoter elements. Inhibition of transcription factor activation/recruitment to gene promoters in THP-1 cells similarly abolished LPS induced

nucleosome clearance in a gene specific manner (**Figure 58**). While the inhibition of NF-κB had a pronounced effect on both *IL1B* and *TNF,* C/EBPβ inhibition only affected nucleosomes on the *IL1B* promoter (**Figure 58**). This data provides a functional link between transcription factor activation and nucleosome clearance from these LPS-induced IE promoters. A temporary clash between the -1 nucleosome and Pol II binding could be responsible for the quiescent behavior of *IL1B* prior to its induction, contributing to the observed transcriptional delay, as shown by Pol II ChIP and mRNA kinetic studies (**Figure 12**). Spatial-temporal analysis of the chromatin modifications throughout the *TNF* and *IL1B* IE gene loci reveal monocyte-specific presence of low levels of active marks such as H3K4me3 and H3K9ac in unstimulated cells. To my surprise these marks did not significantly increase in 1 hour stimulated cells but significant elevation in their enrichment was observed during the switch off of the genes (**Figure 30, 33**). I argue that high levels of transcribing polymerases impede nucleosome deposition and modification throughout the structural part of the genes. At the end of the transient transcription burst, nucleosomes are re-deposited into their original positions and become subject to histone modifiers. Strikingly, my results revealed an opposite pattern for H3K9me1 levels distributed throughout *IL1B* and *TNF* in resting monocytes. This mark was high in resting cells, but rapidly lost following LPS treatment and remained low even during transcriptional shut-down. A methylated H3K9 commonly associated with repressive heterochromatin, was shown to play a role in repression of selected inflammatory genes in monocytes (Kouzarides, 2007; Saccani and Natoli, 2002). Although the antibody used in the study by Saccani and Natoli was not specific enough to distinguish mono-, di-, or tri-methylated lysine at H3, based on the spatial distribution of

H3K9me1 in *IL1B* non-expressing cell lines (**Figure 33**), the H3K9me1 can likely be the methylated form inducing a facultative heterochromatin. I observed that LPS replaced repressive H3K9Me1 marks with transcriptionally permissive acetylation, likely contributing to the enhanced gene expression of *IL1B* and *TNF* (Gomes and Espinosa, 2010). It is possible that monocytes package the *IL1B* and *TNF* genes with H3K9Me1 to form repressed, but poised, chromatin conformations for keeping these IE genes from exhibiting high transcriptional activity. The inhibitory mark H3K27me3 was virtually absent from the gene loci, but its level was increased in cell types that do not transcribe these IE genes (**Figure 30, 33**). *TNF* in Hut 102 cells reveals significant levels of both H3K4me3 and H3K27me3, the so-called "bivalent" mark (Akkers et al., 2009), indicative of developmental, rather than transient IE induction, possibly responsible for the constitutive expression of this gene in these HTLV-1 infected malignant T cells (**Figure 30, 33**). HEK293 cells do not show positive indicators for either gene, exhibiting non-bivalent inhibitory H3K27me3 on both. The inhibitory H3K27me3 extends throughout the entirety of both genes, but appears to be more focused over the coding region of *TNF*. In contrast, *IL1B* reveals a greater level of H3K27me3 far upstream over the potent LPS enhancer near -3000, which binds C/EBPβ (Shirakawa et al., 1993) (**Figure 30, 33**). The suppressive effect of the polycomb group proteins mediated by H3K27me3 directed transcriptional silencing is reversed by the H3K27 specific demethylase JMJD3 during macrophage inflammatory responses (De Santa et al., 2007). Loss of this repressive chromatin mark in *Drosophila* and embryonic stem cells, was shown to result in an increase in H3K27 acetylation, which was mediated by the histone acetyltransferase (HAT) activity of p300 and CBP (Pasini et al., 2010; Tie et al., 2009). My observations

of depleted levels of H3K27Me3 in THP-1 cells encouraged us to examine the kinetic changes in H3K27Ac deposition and binding patterns of p300 on *IL1B* and *TNF*. As revealed in **Figure 31**, acetylation at lysine 27 was associated with LPS-dependent increase at the -2 nucleosomes, while, transient decrease in H3K27Ac on downstream nucleosomes was observed. In agreement with these changes, p300 was transiently recruited upstream of *IL1B* and *TNF* promoters by LPS (**Figure 32**).

My data reveal that the cell type restricted expression of *IL1B* is due to the presence of the monocyte-specific differentiation factor Spi1/PU.1 (Spi1), which binds constitutively to the *IL1B* promoter and enhancer in resting THP-1 (**Figure 34**) and poises the gene for induction. The question of macrophage and B-cell restricted gene regulation was addressed in previous studies that revealed that Spi1 binding corresponded to nucleosome depleted regions and mediated local deposition of H3K4me1 as novel LPS inducible enhancer mark (Ghisletti et al., 2010; Heinz et al., 2010). Additionally my data show that Spi1 plays a critical role in poising and proper activation of the *IL1B* gene promoter. As a pioneer factor, Spi1 may have a unique capability of binding a properly oriented nucleosome wrapped DNA (Ghisletti et al., 2010; Smale, 2010). I provided evidence that ectopic expression of Spi1 facilitated the recruitment of TBP *via* its N-terminal binding domain (**Figure 41, 42**). In resting monocyes the *IL1B* core promoter was depleted of nucleosomes, but TBP recruitment was evident only upon LPS activation (**Figure 41**). I postulate that the binding of Spi1 is necessary, but insufficient, for LPS-mediated induction in THP-1 cells, as well as in HEK293 cells for which Spi1 in the absence of surrogate stimulation (co-expression of IRF8 and TRAF6) does not cause strong nucleosome clearance (**Figure 42**). I hypothesize that stimulation-dependent

binding of NF-κB and C/EBPβ to the DNA loop-mediated proximity of constitutively bound Spi1, facilitates induction of *IL1B via* nucleosome remodeling. Both of these factors bind transiently to specific promoter sites and cooperatively regulate the Pol II dynamics at this gene (**Figure 43, 45, 58**). The Spi1-mediated nucleosome eviction is especially true for the -1 nucleosome, which appears to occlude TSS-proximal binding of TBP (**Figure 28, 42)**. This contrasts with *TNF*, in which the -1 nucleosome resides further upstream, permitting TBP access (**Figure 28**). The mechanism by which this occurs could depend upon the observed stimulation-dependent recruitment of p300 histone acetyltransferase (**Figure 32**) and the SNF2β/BRG1 SWI/SNF chromatin remodeling enzyme (**Figure 29**) by activated transcription factors. Both NF-κB (Hottiger et al., 1998; Tando et al., 2010) C/EBPβ (Kowenz-Leutz and Leutz, 1999; Mink et al., 1997) as well as HIF-1α (Kenneth et al., 2009) have been reported to directly recruit both SWI/SNF remodelers and p300 histone acetyltransferases. This would enable the nucleosome clearance required for Spi1-assisted recruitment of TBP to TATA box DNA. Regardless, as suggested by ectopic expression in HEK293 cells (**Figure 42**), nucleosome remodeling depends upon the integrity of the Spi1 N-terminal domain in concert with the activation of transcription factors, and appears to be necessary for TBP recruitment. These cooperative associations likely facilitate the subsequent assembly of the paused Pol II complex and regulate its release by P-TEFb in order to transition into productive transcription elongation. The presence of highly paused and rapidly transcribed Pol II further enhances the open promoter by competing with nucleosome re-deposition (Core and Lis, 2009).

Additionally, it was postulated that CK2 kinase may play a role as an LPS inducible switch for Spi1 bound at the *IL1B* enhancer mediating IRF4 recruitment and facilitating gene expression (Liang et al., 2006). In search of a mechanism for Spi1 activation, I hypothesized that CK2 can potentially act as an LPS dependent Spi1 activator mediating recruitment of TBP. My ChIP analyses did not reveal the presence of LPS induced CK2 binding to the *IL1B* promoter. On the other hand, Spi1-mediated TBP recruitment can be suppressed by an inhibitory factor in unstimulated monocytes. For example, Translocated in liposarcoma (TLS), an RNA binding protein was shown to bind Spi1 *in vivo* and suppress its transcriptional activity (Hallier et al., 1998). RNA binding properties of TLS were also associated with noncoding RNA (ncRNA) mediated CBP/p300 inhibition and transcriptional repression of *CCDN1* gene upon DNA damage signals (Wang et al., 2008). I speculate a potential role for TLS or a similar inhibitory factor acting as a repressive control switch at the *IL1B* promoter that is alleviated in a TLR4 dependent manner. Interestingly a preliminary screen for LPS induced non-coding RNA in THP-1 cells has revealed a candidate ncRNA with TLS binding site (J. Adamik, unpublished data) located at approximately -300 bp upstream of the *IL1B* TSS. **Figure 65** depicts a model for Spi1 mediated TBP recruitment as well as the recruitment of two paused complexes to *IL1B* gene.

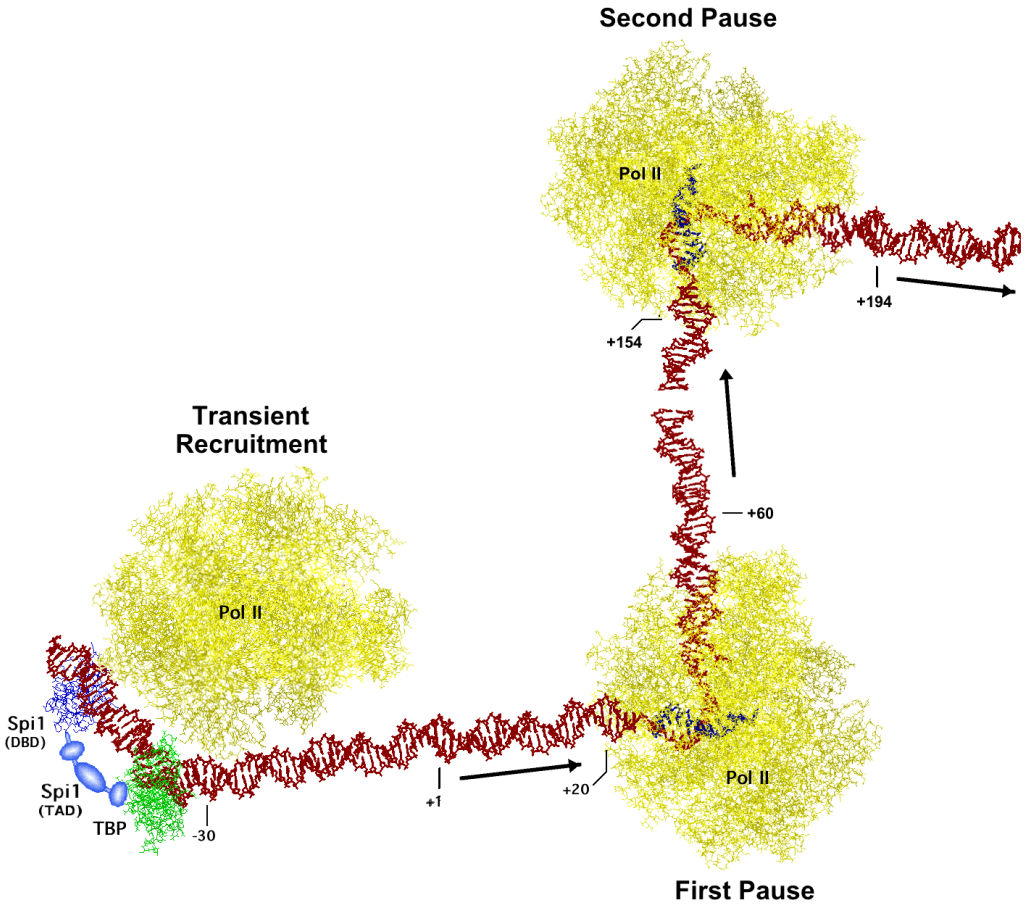

Figure 65. Model depicting a possible spatial configuration for the *IL1B* promoter sequence (Courtesy of Philip E. Auron).

The model is derived from the published X-ray structures using coordinates provide by the RCSB Protein Data Bank (PDB): Spi1 DNA binding ETS domain (1PUE) (Kodandapani, R., et al., 1996); TBP (1YTB) (Kim, J.L., et al, 1993); and Pol II (1EN0) (Gnatt et al., 2001) DNA complexes. The PDB coordinates for the above structures were positioned as independent DNA complexes in pseudo 3D-space, connected by appropriate lengths (Kominato et al., 1995) of B-form DNA in accordance with the theoretical interaction reported for the association of Pol II with TBP (Bushnell et al., 2004) using RasMac 2.7.3 molecular graphics visualization software. The location and nature of the cartoon extension representing the amino, extra-ETS domain, regions of the Spi1 transactivation region is positioned in contact with TBP, as supported by an earlier report (Hagemeier et al., 1993).

Finally I show, that the orchestrated recruitment of transcription factors to the *IL1B* enhancer and promoter mediate their proximal chromosomal interactions (**Figure 57**). Since NF-κB and C/EBPβ are necessary for induction of the chromatin loop and were shown to physically associate with Spi1 (Nawarat Wara-aswapati and Philip E. Auron, unpublished data) (Listman et al., 2005), I postulate that such interactions may mediate activation of Spi1 leading to recruitment of TBP and Pol II, resulting in gene transcription. Interestingly, the 3C results demonstrating the existence of a chromatin loop, consistently revealed the prevalence of one PCR product in unstimulated monocytes. This PCR band, which represents a primary recombination product in unstimulated monocytes, suggests the possibility of a preferred conformational proximity for the upstream and downstream *IL1B* sequences prior to LPS induction (**Figure 57**). Such preformed chromatin architecture has been observed for cells at specific developmental stages (Meaburn and Misteli, 2007).

Analysis of the temporal expression patterns of the IL-1 family genes revealed LPS inducible coordinate expression for several members (**Figure 63**). The most abundantly expressed member of the cytokine family in the THP-1 cells is *IL1B*. *IL1A*, *IL1RN*, *IL18*, and *IL33* are expressed with similar kinetics, but their expression is weaker. The last group of genes including: *IL1F7*, *IL1F9*, *IL1F8*, and *IL1F5* also correspond to the LPS inducible expression pattern with the weakest detection level. I did not detect expression of *IL1F10* in LPS stimulated THP-1 monocytes. Interestingly, *IL1F6* was constitutively expressed and its expression was actually down regulated with LPS treatment. A significant level of constitutive expression was also detected for the members: *IL1RN*, *IL18*, and *ILF7*. Strikingly DRB treatment abolished the expression of

all the members suggesting that they are transcribed by paused polymerases and that P-TEFb recruitment serves as an important regulatory step during their activation. Members that were constitutively active were reduced to a lesser degree when treated with DRB. This suggests that some of their accumulated transcripts produced in resting cells were present even though their LPS inducible transcription was halted due to the lack of active P-TEFb. The eukaryotic nucleus is organized into distinct transcriptional units that contain preformed Pol II machineries called "transcription factories". These clusters of transcription complexes and coactivators bound to gene regulatory regions are tethered *via* DNA loops and are able to efficiently coordinate the transcription of several gene units (Cook, 2010; Papantonis and Cook, 2010). Since the IL-1 family members are transcribed with similar kinetics, and most of them are located on the same chromosome, it is possible that they are part of a larger 3D transcription unit. I speculate that the 3kb chromatin loop observed for the *IL1B* promoter and enhancer might be part of a higher order clustered gene family conformation. The paused polymerases present at the promoters might likely facilitate the assembly of chromatin domains that bring the gene members into proximity.

In summary, *IL1B* and *TNF* differ in the initial state of their promoters in unstimulated cells. Strikingly, during maximal initial expression (1 h) the chromatin architecture of the two genes looks quite similar. However, at later times (5 h) distinct new architectures are established, resulting in the tolerizing of *TNF*. Importantly, I observe that the *IL1B* and *TNF* genes, although both dependent upon the activation of NF-κB, reveal numerous distinctions (**Figure 66**) that may be reflective of the known differences that exist for the cell source range and functions of their gene products. IL-1β

expression is known to be more restricted to monocytes than is TNFα (Kronke et al., 1988), likely dependent upon the requirement for Spi1. The distinct functions of the two proteins is supported by the recent advent of specific therapeutic blockers, which reveal that there are various diseases in which protein blockade results in asymmetric efficacy, and occasionally asymmetric contraindication (Argiles et al., 2011; Dinarello, 2011a, b). Consequently, it is reasonable that such functional differences might require a degree of differential regulation for two similar, but non-identical immune effectors.

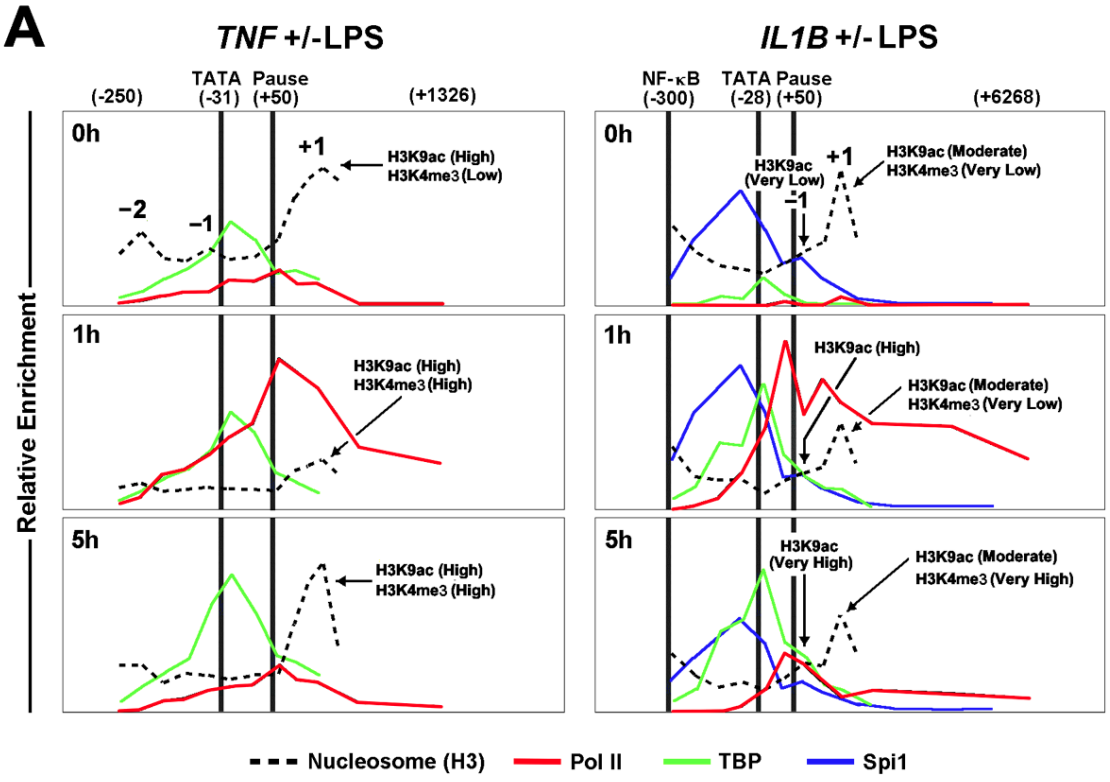

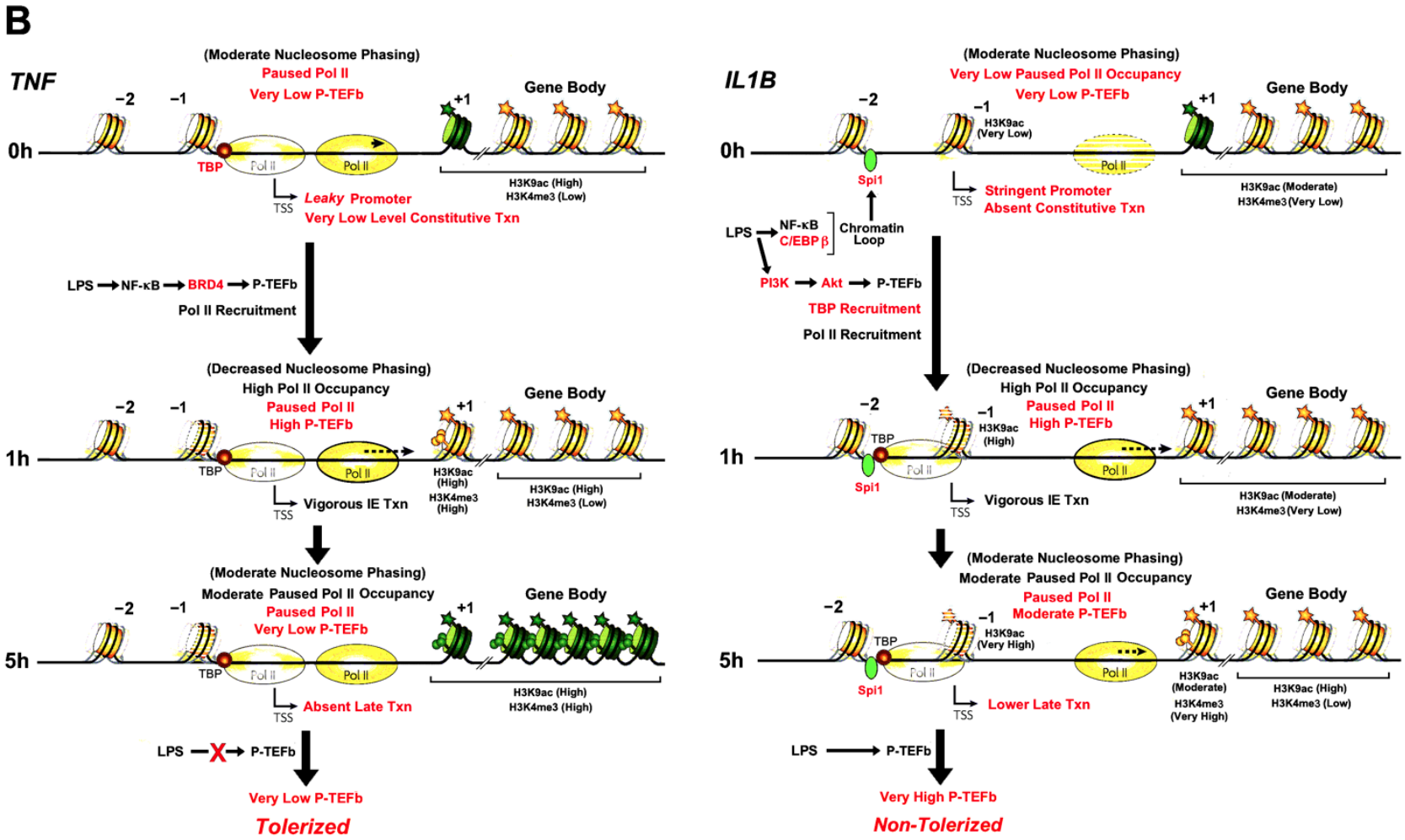
B
TNF
(Moderate Nucleosome Phasing)
Paused Pol II
Very Low P-TEFb
Gene Body
0h
TBP
Pol II
Leaky Promoter
Very Low Level Constitutive Txn
H3K9ac (High)
H3K4me3 (Low)
LPS → NF-κB → BRD4 → P-TEFb
Pol II Recruitment
(Decreased Nucleosome Phasing)
High Pol II Occupancy
Paused Pol II
High P-TEFb
1h
Vigorous IE Txn
H3K9ac (High)
H3K4me3 (High)
(Moderate Nucleosome Phasing)
Moderate Paused Pol II Occupancy
Paused Pol II
Very Low P-TEFb
5h
Absent Late Txn
LPS — X → P-TEFb
Very Low P-TEFb
Tolerized
IL1B
(Moderate Nucleosome Phasing)
Very Low Paused Pol II Occupancy
Very Low P-TEFb
H3K9ac (Very Low)
Spi1
Stringent Promoter
Absent Constitutive Txn
H3K9ac (Moderate)
H3K4me3 (Very Low)
LPS → NF-κB / C/EBP β
Chromatin Loop
PI3K → Akt → P-TEFb
TBP Recruitment
Pol II Recruitment
(Decreased Nucleosome Phasing)
High Pol II Occupancy
Paused Pol II
High P-TEFb
H3K9ac (High)
Vigorous IE Txn
(Moderate Nucleosome Phasing)
Moderate Paused Pol II Occupancy
Paused Pol II
Moderate P-TEFb
H3K9ac (Very High)
Lower Late Txn
H3K9ac (Moderate)
H3K4me3 (Very High)
LPS → P-TEFb
Very High P-TEFb
Non-Tolerized

Figure 66. Proposed Mechanism for LPS mediated induction of *IL1B* and *TNF* in monocytes (Courtesy of Philip E. Auron).

(A) Summary of ChIP kinetics for some key features of *IL1B* and *TNF* in THP-1 monocytes. Pol II, TBP and Spi1 are as indicated. Histone modifications at specific locations detailed in the text are labeled. Key nucleosomes are designated by position relative to the TSS (-2, -1, +1). **(B)** Models for *IL1B* and *TNF* gene regulation. Red text highlights important distinctions between the two genes along the induction kinetic. Nucleosomes are marked with stars (acetylation) and spheres (trimethylation) representative of significant increases in modification. Darkly colored nucleosomes are phased and likely to be less dynamic, and suggestive of impediments to gene expression. The indicated locations of Pol II are represented by various levels of intensity, reflecting the relative degree of proposed dwelling on DNA. Arrowheads on Pol II represent the relative efficiency of elongation, as indicated by the length of the associated dotted line.

SUMMARY OF NOVEL FINDINGS AND FUTURE STUDIES

This dissertation significantly contributes to the understanding of immediate early (IE) gene induction for two important Toll-like receptor 4 (TLR4)-dependent genes coding for TNFα and IL-1β. The study of these two immune mediators can be applied to variety of other stimulus dependent immune and developmental genes. IE genes are almost instantaneously induced in response to extracellular signaling events due to gene poising, a process that is thought to involve a paused, pre-recruited, RNA polymerase (Pol II). I have investigated the mechanisms of endotoxin induction, shutdown and endotoxin tolerance for these genes. This study reveals major distinctions that correlate with the transcription factor requirement, dynamics of Pol II pausing, nucleosomal promoter architecture, and epigenetic signatures. The kinetic approach used in this study focuses on the resting state, prompt transcription, and transient shut down, providing a novel understanding of the temporal resolution of IE gene regulation. An additional issue relates to the study of endotoxin tolerance, the phenomenon of desensitization of a TLR4 signal following recent prior signaling. Here I show that the IE genes have low levels of paused polymerases for up to 24 hours post-stimulation even though their transcription is absent or minimal. Upon subsequent LPS exposure, the tolerized *TNF* gene remains in a paused state, while the *IL1B* gene resumes additional transcription due to influence of the a positive elongation kinase P-TEFb. This work presents novel connections between macrophage metabolism and the regulation of pro-inflammatory genes. My additional collaborative study in murine macrophages revealed a novel role for the oxygen sensing effector protein HIF1α in controlling *Il1b* transcription. The genes coding for TNFα and IL-1β have long been associated with the activation of the NF-κB transcription factor,

which is important for vigorous expression. As a consequence of this dependence and similar expression kinetics, the assumption has been that these genes are similarly regulated. I have observed that in contrast to *TNF*, *IL1B* is continually expressed for long periods and is significantly less susceptible to the phenomenon of endotoxin tolerance, while being more sensitive to the metabolic state of the cell. My study shows that although I observe pre-induced *TNF* to behave as what is now classically referred to as a poised gene, by virtue of the presence of a paused pre-recruited RNA polymerase (Pol II) and TATA binding protein (TBP), the resting *IL1B* gene is generally devoid of TBP and Pol II. Therefore, *IL1B* appears to behave as a poised IE gene in the absence of the hallmarks that have been suggested to be critical for immediate early induction. I provide novel results demonstrating that complete NF-κB inhibition decreases, but does not completely eliminate, *IL1B* transcription, supporting the involvement of other factors which may play a critical role in regulating this potent gene. These include C/EBPβ for the IL-1β gene (*IL1B*), and the realization that the various new specific therapeutic blockers of TNFα and IL-1β often generate distinct asymmetric effects and contraindications, supporting evidence in favor of distinct roles and mechanisms for these molecules in homeostasis and disease. My C/EBPβ and NF-κB inhibition experiments suggest a distinct functional linkage between the transcription factors and the recruitment of Pol II machinery as well as the P-TEFb to these IE genes. A detailed analysis of the spatial-temporal distribution of chromatin marks in resting monocytes reveals that epigenetic modifications such as H3K4me3 and H3K9ac often resemble chromatin patterns of an actively transcribed gene as compared to non-monocytic cell lines. Here I provide new evidence that the differential gene shutdown observed between the two IE

genes is reflected by the nature of their chromatin modifications following the initial phase of rapid-transient transcription. My results extend beyond the previously reported Spi-1/Pu.1-mediated opening of pro-inflammatory gene enhancers and suggest a novel role for this pioneer factor at selected IE gene promoters. The findings of this work provide a new model for *IL1B* gene activation, which involves an inducible enhanceosome-like chromosomal looping and dynamic nucleosome transactions mediated by inducible transcription factor interactions.

Since the mechanisms associated with *IL1B* and *TNF* gene regulation are highly dynamic and complex, several unanswered questions remain to be determined. As hypothesized in the discussion, the mechanism responsible for the IE nature of the *IL1B* gene is intriguing because this functionally "poised" gene fails to exhibit the classic hallmark of a significant amount of pre-bound/paused Pol II, as has been suggested by others (Gilchrist et al., 2008; Guenther et al., 2007; Kininis et al., 2009; Muse et al., 2007; Rahl et al., 2010; Zeitlinger et al., 2007). However, many aspects of the *IL1B* promoter such as nucleosome phasing, constitutive transcription factor assembly, and the transcriptionally permissive chromatin marks suggest that the promoter is competent for Pol II recruitment. Yet, one striking difference is the relatively low level of pre-recruited TBP. In this way, *IL1B* does not fit the model of an IE gene. One possible explanation is that the *IL1B* promoter is repressed in a way that prevents its basal transcription, perhaps inhibiting TBP recruitment by Spi1. Studies of the *CCND1* gene, which codes for cyclin D1, revealed that its expression is down-regulated by an upstream series of inhibitory ncRNA. By associating with the TLS (translocated in liposarcoma) protein, ncRNA mediates inhibition of p300 histone acetyltransferase activity leading to gene shut down

(Wang et al., 2008). Interestingly, my preliminary examination of the *IL1B* locus revealed a TLS consensus binding sequence approximately 300 bp upstream of the *IL1B* promoter. An initial screening using non-quantitative PCR revealed the existence of several LPS-dependent upstream transcripts, one of which contained the TLS consensus. A kinetic ChIP, targeting TLS in resting and LPS treated monocytes could provide an indication of its connection to the expressed ncRNA. If a correlation is observed, siRNA mediated inhibition of TLS can be performed in order to reverse the potential repressive effects associated with its association with the *IL1B* promoter. Additionally, one could design antisense probes (shRNA) to target potential ncRNA, potentially abolishing any ncRNA inhibitory effect on *IL1B* in resting monocytes, observing whether this results a low level of basal transcription and Pol II recruitment to the gene.

Another issue beyond the initial repression of *IL1B* is the mechanism responsible for both its extended expression and re-induction (i.e., its resistance to endotoxin tolerance). One possible model is that this process is dependent upon a distinct means of late induction. An obvious candidate is the late LPS-dependent binding of HIF-1α (Figure 61). This could be approached by using inhibitors, such as α-ketoglutarate or HIF-1α siRNA to determine whether a reduction in HIF-1α can convert the induction profile for *IL1B* into one similar to that exhibited by *TNF*.

The IL-1 family gene members are another topic that could be explored in more detail. Since the preliminary mRNA study revealed a coordinate expression of these genes (Figure 64), Pol II ChIP can be performed to further define the transcriptional responsiveness of these genes. Additionally, a circularized chromatin conformation capture (4C) (Simonis et al., 2007), which can capture numerous long-range interactions,

could be a valuable tool to assess physical chromatin associations at the 180 kbp IL-1 gene family locus on human chromosome 2.

REFERENCES CITED

Adelman, K., Kennedy, M.A., Nechaev, S., Gilchrist, D.A., Muse, G.W., Chinenov, Y., and Rogatsky, I. (2009). Immediate mediators of the inflammatory response are poised for gene activation through RNA polymerase II stalling. Proc Natl Acad Sci U S A *106*, 18207-18212.

Aderem, A., and Ulevitch, R.J. (2000). Toll-like receptors in the induction of the innate immune response. Nature *406*, 782-787.

Ai, N., Hu, X., Ding, F., Yu, B., Wang, H., Lu, X., Zhang, K., Li, Y., Han, A., Lin, W.*, et al.* (2011). Signal-induced Brd4 release from chromatin is essential for its role transition from chromatin targeting to transcriptional regulation. Nucleic Acids Res *39*, 9592-9604.

Aida, M., Chen, Y., Nakajima, K., Yamaguchi, Y., Wada, T., and Handa, H. (2006). Transcriptional pausing caused by NELF plays a dual role in regulating immediate-early expression of the junB gene. Mol Cell Biol *26*, 6094-6104.

Akira, S., Takeda, K., and Kaisho, T. (2001). Toll-like receptors: critical proteins linking innate and acquired immunity. Nat Immunol *2*, 675-680.

Akkers, R.C., van Heeringen, S.J., Jacobi, U.G., Janssen-Megens, E.M., Francoijs, K.J., Stunnenberg, H.G., and Veenstra, G.J. (2009). A hierarchy of H3K4me3 and H3K27me3 acquisition in spatial gene regulation in Xenopus embryos. Dev Cell *17*, 425-434.

Arbibe, L., and Sansonetti, P.J. (2007). Epigenetic regulation of host response to LPS: causing tolerance while avoiding Toll errancy. Cell Host Microbe *1*, 244-246.

Argiles, J.M., Busquets, S., and Lopez-Soriano, F.J. (2011). Anti-inflammatory therapies in cancer cachexia. Eur J Pharmacol *668 Suppl 1*, S81-86.

Armant, M.A., and Fenton, M.J. (2002). Toll-like receptors: a family of pattern-recognition receptors in mammals. Genome Biol *3*, REVIEWS3011.

Auffray, C., Sieweke, M.H., and Geissmann, F. (2009). Blood monocytes: development, heterogeneity, and relationship with dendritic cells. Annu Rev Immunol *27*, 669-692.

Auron, P.E., and Webb, A.C. (1994). Interleukin-1: a gene expression system regulated at multiple levels. Eur Cytokine Netw *5*, 573-592.

Auwerx, J. (1991). The human leukemia cell line, THP-1: a multifacetted model for the study of monocyte-macrophage differentiation. Experientia *47*, 22-31.

Bai, L., and Morozov, A.V. (2010). Gene regulation by nucleosome positioning. Trends Genet *26*, 476-483.

Baldassare, J.J., Bi, Y., and Bellone, C.J. (1999). The role of p38 mitogen-activated kinase in IL-1b transcription. J Immunol *162*, 5367-5373.

Baumli, S., Endicott, J.A., and Johnson, L.N. (2010). Halogen bonds form the basis for selective P-TEFb inhibition by DRB. Chem Biol *17*, 931-936.

Beeson, P.B. (1947a). Tolerance to Bacterial Pyrogens : I. Factors Influencing Its Development. J Exp Med *86*, 29-38.

Beeson, P.B. (1947b). Tolerance to Bacterial Pyrogens : Ii. Role of the Reticulo-Endothelial System. J Exp Med *86*, 39-44.

Bianchi, M.E. (2007). DAMPs, PAMPs and alarmins: all we need to know about danger. J Leukoc Biol *81*, 1-5.

Biglione, S., Byers, S.A., Price, J.P., Nguyen, V.T., Bensaude, O., Price, D.H., and Maury, W. (2007). Inhibition of HIV-1 replication by P-TEFb inhibitors DRB, seliciclib and flavopiridol correlates with release of free P-TEFb from the large, inactive form of the complex. Retrovirology *4*, 47.

Brasier, A.R., Tian, B., Jamaluddin, M., Kalita, M.K., Garofalo, R.P., and Lu, M. (2011). RelA Ser276 phosphorylation-coupled Lys310 acetylation controls transcriptional elongation of inflammatory cytokines in respiratory syncytial virus infection. J Virol *85*, 11752-11769.

Bres, V., Yoh, S.M., and Jones, K.A. (2008). The multi-tasking P-TEFb complex. Curr Opin Cell Biol *20*, 334-340.

Brookes, E., and Pombo, A. (2009). Modifications of RNA polymerase II are pivotal in regulating gene expression states. EMBO Rep *10*, 1213-1219.

Buratowski, S. (2003). The CTD code. Nat Struct Biol *10*, 679-680.

Buratowski, S. (2009). Progression through the RNA polymerase II CTD cycle. Mol Cell *36*, 541-546.

Bushnell, D.A., Westover, K.D., Davis, R.E., and Kornberg, R.D. (2004). Structural basis of transcription: an RNA polymerase II-TFIIB cocrystal at 4.5 Angstroms. Science *303*, 983-988.

Cavaillon, J.M., Adrie, C., Fitting, C., and Adib-Conquy, M. (2003). Endotoxin tolerance: is there a clinical relevance? J Endotoxin Res *9*, 101-107.

Cenik, C., Derti, A., Mellor, J.C., Berriz, G.F., and Roth, F.P. (2010). Genome-wide functional analysis of human 5' untranslated region introns. Genome Biol *11*, R29.

Chan, C., Li, L., McCall, C.E., and Yoza, B.K. (2005). Endotoxin tolerance disrupts chromatin remodeling and NF-kappaB transactivation at the IL-1beta promoter. J Immunol *175*, 461-468.

Chandra, G., Cogswell, J.P., Miller, L.R., Godlevski, M.M., Stinnett, S.W., Noel, S.L., Kadwell, S.H., Kost, T.A., and Gray, J.G. (1995). Cyclic AMP signaling pathways are important in IL-1 beta transcriptional regulation. J Immunol *155*, 4535-4543.

Chen, C.-Y., Chen, T.-M., and Shyu, A.-B. (1994). Interplay of two functionally and structurally distinct domains of the c-*fos* AU-rich element specifies its mRNA-destabilizing function. Mol Cell Biol *14*, 416-426.

Chen, L.F., and Greene, W.C. (2004). Shaping the nuclear action of NF-kappaB. Nat Rev Mol Cell Biol *5*, 392-401.

Churchman, L.S., and Weissman, J.S. (2011). Nascent transcript sequencing visualizes transcription at nucleotide resolution. Nature *469*, 368-373.

Collart, M.A., Baeuerle, P., and Vassalli, P. (1990). Regulation of tumor necrosis factor alpha transcription in macrophages: involvement of four kappa B-like motifs and of constitutive and inducible forms of NF-kappa B. Mol Cell Biol *10*, 1498-1506.

Contreras, X., Barboric, M., Lenasi, T., and Peterlin, B.M. (2007). HMBA releases P-TEFb from HEXIM1 and 7SK snRNA via PI3K/Akt and activates HIV transcription. PLoS Pathog *3*, 1459-1469.

Cook, P.R. (2010). A model for all genomes: the role of transcription factories. J Mol Biol *395*, 1-10.

Core, L.J., and Lis, J.T. (2008). Transcription regulation through promoter-proximal pausing of RNA polymerase II. Science *319*, 1791-1792.

Core, L.J., and Lis, J.T. (2009). Paused Pol II captures enhancer activity and acts as a potent insulator. Genes Dev *23*, 1606-1612.

Coussens, L.M., and Werb, Z. (2002). Inflammation and cancer. Nature *420*, 860-867.

de la Mata, M., Lafaille, C., and Kornblihtt, A.R. (2010). First come, first served revisited: factors affecting the same alternative splicing event have different effects on the relative rates of intron removal. RNA *16*, 904-912.

De Santa, F., Totaro, M.G., Prosperini, E., Notarbartolo, S., Testa, G., and Natoli, G. (2007). The histone H3 lysine-27 demethylase Jmjd3 links inflammation to inhibition of polycomb-mediated gene silencing. Cell *130*, 1083-1094.

Dekker, J. (2006). The three 'C' s of chromosome conformation capture: controls, controls, controls. Nat Methods *3*, 17-21.

Deng, W., Lee, J., Wang, H., Miller, J., Reik, A., Gregory, P.D., Dean, A., and Blobel, G.A. (2012). Controlling long-range genomic interactions at a native locus by targeted tethering of a looping factor. Cell *149*, 1233-1244.

Dinarello, C.A. (1986). Multiple biological properties of recombinant human interleukin 1 (beta). Immunobiology *172*, 301-315.

Dinarello, C.A. (1994). The interleukin-1 family: 10 years of discovery. FASEB J *8*, 1314-1325.

Dinarello, C.A. (2009). Immunological and inflammatory functions of the interleukin-1 family. Annu Rev Immunol *27*, 519-550.

Dinarello, C.A. (2010). IL-1: discoveries, controversies and future directions. Eur J Immunol *40*, 599-606.

Dinarello, C.A. (2011a). A clinical perspective of IL-1beta as the gatekeeper of inflammation. Eur J Immunol *41*, 1203-1217.

Dinarello, C.A. (2011b). Interleukin-1 in the pathogenesis and treatment of inflammatory diseases. Blood *117*, 3720-3732.

Dunn, E., Sims, J.E., Nicklin, M.J., and O'Neill, L.A. (2001). Annotating genes with potential roles in the immune system: six new members of the IL-1 family. Trends Immunol *22*, 533-536.

Egloff, S. (2012). Role of Ser7 phosphorylation of the CTD during transcription of snRNA genes. RNA Biol *9*, 1033-1038.

Egloff, S., and Murphy, S. (2008). Cracking the RNA polymerase II CTD code. Trends Genet *24*, 280-288.

Egloff, S., Zaborowska, J., Laitem, C., Kiss, T., and Murphy, S. (2012). Ser7 phosphorylation of the CTD recruits the RPAP2 Ser5 phosphatase to snRNA genes. Mol Cell *45*, 111-122.

El Gazzar, M., Yoza, B.K., Hu, J.Y., Cousart, S.L., and McCall, C.E. (2007). Epigenetic silencing of tumor necrosis factor alpha during endotoxin tolerance. J Biol Chem *282*, 26857-26864.

Escoubet-Lozach, L., Benner, C., Kaikkonen, M.U., Lozach, J., Heinz, S., Spann, N.J., Crotti, A., Stender, J., Ghisletti, S., Reichart, D.*, et al.* (2011). Mechanisms establishing TLR4-responsive activation states of inflammatory response genes. PLoS Genet *7*, e1002401.

Fan, H., and Cook, J.A. (2004). Molecular mechanisms of endotoxin tolerance. J Endotoxin Res *10*, 71-84.

Fenton, M.J., Clark, B.D., Collins, K.L., Webb, A.C., Rich, A., and Auron, P.E. (1987). Transcriptional regulation of the human prointerleukin 1b gene. J Immunol *138*, 3972-3979.

Fenton, M.J., Vermeulen, M.W., Clark, B.D., Webb, A.C., and Auron, P.E. (1988). Human pro-IL-1b gene expression in monocytic cells is regulated by two distinct pathways. J Immunol *140*, 2267-2273.

Fish, R.N., and Kane, C.M. (2002). Promoting elongation with transcript cleavage stimulatory factors. Biochim Biophys Acta *1577*, 287-307.

Foster, S.L., Hargreaves, D.C., and Medzhitov, R. (2007). Gene-specific control of inflammation by TLR-induced chromatin modifications. Nature *447*, 972-978.

Foster, S.L., and Medzhitov, R. (2009). Gene-specific control of the TLR-induced inflammatory response. Clin Immunol *130*, 7-15.

Fuda, N.J., Ardehali, M.B., and Lis, J.T. (2009). Defining mechanisms that regulate RNA polymerase II transcription in vivo. Nature *461*, 186-192.

Fujita, T., Piuz, I., and Schlegel, W. (2009). The transcription elongation factors NELF, DSIF and P-TEFb control constitutive transcription in a gene-specific manner. FEBS Lett *583*, 2893-2898.

Galson, D.L., Hensold, J.O., Bishop, T.R., Schalling, M., D'Andrea, A.D., Jones, C., Auron, P.E., and Housman, D.E. (1993). Mouse b-globin DNA-binding protein B1 is identical to a proto-oncogene, the transcription factor Spi-1/PU.1, and is restricted in expression to hematopoietic cells and the testis. Mol Cell Biol *13*, 2929-2941.

Ghisletti, S., Barozzi, I., Mietton, F., Polletti, S., De Santa, F., Venturini, E., Gregory, L., Lonie, L., Chew, A., Wei, C.L.*, et al.* (2010). Identification and characterization of enhancers controlling the inflammatory gene expression program in macrophages. Immunity *32*, 317-328.

Gilchrist, D.A., and Adelman, K. (2012). Coupling polymerase pausing and chromatin landscapes for precise regulation of transcription. Biochim Biophys Acta.

Gilchrist, D.A., Dos Santos, G., Fargo, D.C., Xie, B., Gao, Y., Li, L., and Adelman, K. (2010). Pausing of RNA polymerase II disrupts DNA-specified nucleosome organization to enable precise gene regulation. Cell *143*, 540-551.

Gilchrist, D.A., Nechaev, S., Lee, C., Ghosh, S.K., Collins, J.B., Li, L., Gilmour, D.S., and Adelman, K. (2008). NELF-mediated stalling of Pol II can enhance gene expression by blocking promoter-proximal nucleosome assembly. Genes Dev *22*, 1921-1933.

Gilmore, T.D. (2006). Introduction to NF-kappaB: players, pathways, perspectives. Oncogene *25*, 6680-6684.

Gilmour, D.S. (2009). Promoter proximal pausing on genes in metazoans. Chromosoma *118*, 1-10.

Glover-Cutter, K., Kim, S., Espinosa, J., and Bentley, D.L. (2008). RNA polymerase II pauses and associates with pre-mRNA processing factors at both ends of genes. Nat Struct Mol Biol *15*, 71-78.

Gnatt, A.L., Cramer, P., Fu, J., Bushnell, D.A., and Kornberg, R.D. (2001). Structural basis of transcription: an RNA polymerase II elongation complex at 3.3 A resolution. Science *292*, 1876-1882.

Godambe, S.A., Chaplin, D.D., Takova, T., Read, L.M., and Bellone, C.J. (1995). A novel cis-acting element required for lipopolysaccharide-induced transcription of the murine interleukin-1 beta gene. Mol Cell Biol *15*, 112-119.

Goldstrohm, A.C., Greenleaf, A.L., and Garcia-Blanco, M.A. (2001). Co-transcriptional splicing of pre-messenger RNAs: considerations for the mechanism of alternative splicing. Gene *277*, 31-47.

Gomes, N.P., and Espinosa, J.M. (2010). Gene-specific repression of the p53 target gene PUMA via intragenic CTCF-Cohesin binding. Genes Dev *24*, 1022-1034.

Gordon, S., and Taylor, P.R. (2005). Monocyte and macrophage heterogeneity. Nat Rev Immunol *5*, 953-964.

Gottlieb, E., and Tomlinson, I.P. (2005). Mitochondrial tumour suppressors: a genetic and biochemical update. Nat Rev Cancer *5*, 857-866.

Greive, S.J., and von Hippel, P.H. (2005). Thinking quantitatively about transcriptional regulation. Nat Rev Mol Cell Biol *6*, 221-232.

Grondin, B., Lefrancois, M., Tremblay, M., Saint-Denis, M., Haman, A., Waga, K., Bedard, A., Tenen, D.G., and Hoang, T. (2007). c-Jun homodimers can function as a context-specific coactivator. Mol Cell Biol *27*, 2919-2933.

Guenther, M.G., Levine, S.S., Boyer, L.A., Jaenisch, R., and Young, R.A. (2007). A chromatin landmark and transcription initiation at most promoters in human cells. Cell *130*, 77-88.

Guha, M., and Mackman, N. (2001). LPS induction of gene expression in human monocytes. Cell Signal *13*, 85-94.

Hagemeier, C., Bannister, A.J., Cook, A., and Kouzarides, T. (1993). The activation domain of transcription factor PU.1 binds the retinoblastoma (RB) protein and the transcription factor TFIID *in vitro*: RB shows sequence similarity to TFIID and TFII. Proc Natl Acad Sci USA *90*, 1580-1584.

Hallier, M., Lerga, A., Barnache, S., Tavitian, A., and Moreau-Gachelin, F. (1998). The transcription factor Spi-1/PU.1 interacts with the potential splicing factor TLS. J Biol Chem *273*, 4838-4842.

Hargreaves, D.C., Horng, T., and Medzhitov, R. (2009). Control of inducible gene expression by signal-dependent transcriptional elongation. Cell *138*, 129-145.

Heinz, S., Benner, C., Spann, N., Bertolino, E., Lin, Y.C., Laslo, P., Cheng, J.X., Murre, C., Singh, H., and Glass, C.K. (2010). Simple combinations of lineage-determining transcription factors prime cis-regulatory elements required for macrophage and B cell identities. Mol Cell *38*, 576-589.

Henikoff, S. (2008). Nucleosome destabilization in the epigenetic regulation of gene expression. Nat Rev Genet *9*, 15-26.

Henikoff, S., and Shilatifard, A. (2011). Histone modification: cause or cog? Trends Genet *27*, 389-396.

Herschman, H.R. (1991). Primary response genes induced by growth factors and tumor promoters. Annu Rev Biochem *60*, 281-319.

Hiscott, J., Marois, J., Garoufalis, J., D'addario, M., Roulston, A., Kwan, I., Pepin, N., Lacoste, J., Nguyen, H., Bensi, G.*, et al.* (1993). Characterization of a functional NF-kB site in the human interleukin 1b promoter: Evidence for a positive autoregulatory loop. Mol Cell Biol *13*, 6231-6240.

Hooper, L.V., Littman, D.R., and Macpherson, A.J. (2012). Interactions between the microbiota and the immune system. Science *336*, 1268-1273.

Hottiger, M.O., Felzien, L.K., and Nabel, G.J. (1998). Modulation of cytokine-induced HIV gene expression by competitive binding of transcription factors to the coactivator p300. EMBO J *17*, 3124-3134.

Huang, Q., Liu, D., Majewski, P., Schulte, L.C., Korn, J.M., Young, R.A., Lander, E.S., and Hacohen, N. (2001). The plasticity of dendritic cell responses to pathogens and their components. Science *294*, 870-875.

Iwasaki, A., and Medzhitov, R. (2010). Regulation of adaptive immunity by the innate immune system. Science *327*, 291-295.

Jiang, C., and Pugh, B.F. (2009). Nucleosome positioning and gene regulation: advances through genomics. Nat Rev Genet *10*, 161-172.

Johnson, P.F. (2005). Molecular stop signs: regulation of cell-cycle arrest by C/EBP transcription factors. J Cell Sci *118*, 2545-2555.

Kang, H.T., and Hwang, E.S. (2006). 2-Deoxyglucose: an anticancer and antiviral therapeutic, but not any more a low glucose mimetic. Life Sci *78*, 1392-1399.

Kang, J.Y., and Lee, J.O. (2011). Structural biology of the Toll-like receptor family. Annu Rev Biochem *80*, 917-941.

Kastenbauer, S., and Ziegler-Heitbrock, H.W. (1999). NF-kappaB1 (p50) is upregulated in lipopolysaccharide tolerance and can block tumor necrosis factor gene expression. Infect Immun *67*, 1553-1559.

Kawai, T., and Akira, S. (2007). Signaling to NF-kappaB by Toll-like receptors. Trends Mol Med *13*, 460-469.

Kenneth, N.S., Mudie, S., van Uden, P., and Rocha, S. (2009). SWI/SNF regulates the cellular response to hypoxia. J Biol Chem *284*, 4123-4131.

Kim, S.Y., Choi, Y.J., Joung, S.M., Lee, B.H., Jung, Y.S., and Lee, J.Y. (2010). Hypoxic stress up-regulates the expression of Toll-like receptor 4 in macrophages via hypoxia-inducible factor. Immunology *129*, 516-524.

Kimura, H., Weisz, A., Kurashima, Y., Hashimoto, K., Ogura, T., D'Acquisto, F., Addeo, R., Makuuchi, M., and Esumi, H. (2000). Hypoxia response element of the human vascular endothelial growth factor gene mediates transcriptional regulation by nitric oxide: control of hypoxia-inducible factor-1 activity by nitric oxide. Blood *95*, 189-197.

Kininis, M., Isaacs, G.D., Core, L.J., Hah, N., and Kraus, W.L. (2009). Postrecruitment regulation of RNA polymerase II directs rapid signaling responses at the promoters of estrogen target genes. Mol Cell Biol *29*, 1123-1133.

Kominato, Y., Galson, D., Waterman, W.R., Webb, A.C., and Auron, P.E. (1995). Monocyte expression of the human prointerleukin 1 beta gene (IL1B) is dependent on promoter sequences which bind the hematopoietic transcription factor Spi-1/PU.1. Mol Cell Biol *15*, 58-68.

Kono, H., and Rock, K.L. (2008). How dying cells alert the immune system to danger. Nat Rev Immunol *8*, 279-289.

Kouzarides, T. (2007). Chromatin modifications and their function. Cell *128*, 693-705.

Kovacs, K.A., Steinmann, M., Magistretti, P.J., Halfon, O., and Cardinaux, J.R. (2003). CCAAT/enhancer-binding protein family members recruit the coactivator CREB-binding protein and trigger its phosphorylation. J Biol Chem *278*, 36959-36965.

Kowenz-Leutz, E., and Leutz, A. (1999). A C/EBP beta isoform recruits the SWI/SNF complex to activate myeloid genes. Mol Cell *4*, 735-743.

Kronke, M., Hensel, G., Schluter, C., Scheurich, P., Schutze, S., and Pfizenmaier, K. (1988). Tumor necrosis factor and lymphotoxin gene expression in human tumor cell lines. Cancer Res *48*, 5417-5421.

Kwak, H., Fuda, N.J., Core, L.J., and Lis, J.T. (2013). Precise maps of RNA polymerase reveal how promoters direct initiation and pausing. Science *339*, 950-953.

LaRue, K.E., and McCall, C.E. (1994). A labile transcriptional repressor modulates endotoxin tolerance. J Exp Med *180*, 2269-2275.

Lawrence, T., and Natoli, G. (2011). Transcriptional regulation of macrophage polarization: enabling diversity with identity. Nat Rev Immunol *11*, 750-761.

Lee, C.K., Shibata, Y., Rao, B., Strahl, B.D., and Lieb, J.D. (2004). Evidence for nucleosome depletion at active regulatory regions genome-wide. Nat Genet *36*, 900-905.

Liang, M.D., Zhang, Y., McDevit, D., Marecki, S., and Nikolajczyk, B.S. (2006). The interleukin-1beta gene is transcribed from a poised promoter architecture in monocytes. J Biol Chem *281*, 9227-9237.

Liew, F.Y., Pitman, N.I., and McInnes, I.B. (2010). Disease-associated functions of IL-33: the new kid in the IL-1 family. Nat Rev Immunol *10*, 103-110.

Listman, J.A., Wara-aswapati, N., Race, J.E., Blystone, L.W., Walker-Kopp, N., Yang, Z., and Auron, P.E. (2005). Conserved ETS domain arginines mediate DNA binding, nuclear localization, and a novel mode of bZIP interaction. J Biol Chem *280*, 41421-41428.

Marecki, S., McCarthy, K.M., and Nikolajczyk, B.S. (2004). PU.1 as a chromatin accessibility factor for immunoglobulin genes. Mol Immunol *40*, 723-731.

Marmiroli, S., Bavelloni, A., Faenza, I., Sirri, A., Ognibene, A., Cenni, V., Tsukada, J., Koyama, Y., Ruzzene, M., Ferri, A.*, et al.* (1998). Phosphatidylinositol 3-kinase is recruited to a specific site in the activated IL-1 receptor I. FEBS Lett *438*, 49-54.

Mavrich, T.N., Jiang, C., Ioshikhes, I.P., Li, X., Venters, B.J., Zanton, S.J., Tomsho, L.P., Qi, J., Glaser, R.L., Schuster, S.C.*, et al.* (2008). Nucleosome organization in the Drosophila genome. Nature *453*, 358-362.

Meaburn, K.J., and Misteli, T. (2007). Cell biology: chromosome territories. Nature *445*, 379-381.

Medzhitov, R. (2001). Toll-like receptors and innate immunity. Nat Rev Immunol *1*, 135-145.

Min, I.M., Waterfall, J.J., Core, L.J., Munroe, R.J., Schimenti, J., and Lis, J.T. (2011). Regulating RNA polymerase pausing and transcription elongation in embryonic stem cells. Genes Dev *25*, 742-754.

Mink, S., Haenig, B., and Klempnauer, K.H. (1997). Interaction and functional collaboration of p300 and C/EBPb. Mol Cell Biol *17*, 6609-6617.

Mitchell, T., and Sugden, B. (1995). Stimulation of NF-kappa B-mediated transcription by mutant derivatives of the latent membrane protein of Epstein-Barr virus. J Virol *69*, 2968-2976.

Mouri, F., Tsukada, J., Mizobe, T., Higashi, T., Yoshida, Y., Minami, Y., Izumi, H., Kominato, Y., Kohno, K., and Tanaka, Y. (2008). Intracellular HMGB1 transactivates the human IL1B gene promoter through association with an Ets transcription factor PU.1. Eur J Haematol *80*, 10-19.

Munoz, M.J., de la Mata, M., and Kornblihtt, A.R. (2010). The carboxy terminal domain of RNA polymerase II and alternative splicing. Trends Biochem Sci *35*, 497-504.

Murdoch, C., Muthana, M., and Lewis, C.E. (2005). Hypoxia regulates macrophage functions in inflammation. J Immunol *175*, 6257-6263.

Muse, G.W., Gilchrist, D.A., Nechaev, S., Shah, R., Parker, J.S., Grissom, S.F., Zeitlinger, J., and Adelman, K. (2007). RNA polymerase is poised for activation across the genome. Nat Genet *39*, 1507-1511.

Natoli, G. (2012). NF-kappaB and chromatin: ten years on the path from basic mechanisms to candidate drugs. Immunol Rev *246*, 183-192.

Naugler, W.E., and Karin, M. (2008). NF-kappaB and cancer-identifying targets and mechanisms. Curr Opin Genet Dev *18*, 19-26.

Nguyen, V.T., Kiss, T., Michels, A.A., and Bensaude, O. (2001). 7SK small nuclear RNA binds to and inhibits the activity of CDK9/cyclin T complexes. Nature *414*, 322-325.

Ni, Z., Saunders, A., Fuda, N.J., Yao, J., Suarez, J.R., Webb, W.W., and Lis, J.T. (2008). P-TEFb is critical for the maturation of RNA polymerase II into productive elongation in vivo. Mol Cell Biol *28*, 1161-1170.

Nishiyama, C., Nishiyama, M., Ito, T., Masaki, S., Masuoka, N., Yamane, H., Kitamura, T., Ogawa, H., and Okumura, K. (2004). Functional analysis of PU.1 domains in monocyte-specific gene regulation. FEBS Lett *561*, 63-68.

Nizet, V., and Johnson, R.S. (2009). Interdependence of hypoxic and innate immune responses. Nat Rev Immunol *9*, 609-617.

O'Neill, L.A. (2011). Plant science. Innate immunity in plants goes to the PUB. Science *332*, 1386-1387.

Owen-Hughes, T., and Gkikopoulos, T. (2012). Making sense of transcribing chromatin. Curr Opin Cell Biol *24*, 296-304.

Pahl, H.L., Scheibe, R.J., Zhang, D.-E., Chen, H.-M., Galson, D.L., Maki, R.A., and Tenen, D.G. (1993). The proto-oncogene PU.1 regulates expression of the myeloid-specific CD11b promoter. J Biol Chem *268*, 5014-5020.

Palermo, R.D., Webb, H.M., and West, M.J. (2011). RNA polymerase II stalling promotes nucleosome occlusion and pTEFb recruitment to drive immortalization by Epstein-Barr virus. PLoS Pathog *7*, e1002334.

Papantonis, A., and Cook, P.R. (2010). Genome architecture and the role of transcription. Curr Opin Cell Biol *22*, 271-276.

Pasini, D., Malatesta, M., Jung, H.R., Walfridsson, J., Willer, A., Olsson, L., Skotte, J., Wutz, A., Porse, B., Jensen, O.N.*, et al.* (2010). Characterization of an antagonistic switch between histone H3 lysine 27 methylation and acetylation in the transcriptional regulation of Polycomb group target genes. Nucleic Acids Res *38*, 4958-4969.

Petesch, S.J., and Lis, J.T. (2008). Rapid, transcription-independent loss of nucleosomes over a large chromatin domain at Hsp70 loci. Cell *134*, 74-84.

Petesch, S.J., and Lis, J.T. (2012). Overcoming the nucleosome barrier during transcript elongation. Trends Genet *28*, 285-294.

Pham, T.H., Langmann, S., Schwarzfischer, L., El Chartouni, C., Lichtinger, M., Klug, M., Krause, S.W., and Rehli, M. (2007). CCAAT enhancer-binding protein beta regulates constitutive gene expression during late stages of monocyte to macrophage differentiation. J Biol Chem *282*, 21924-21933.

Price, D.H. (2000). P-TEFb, a cyclin-dependent kinase controlling elongation by RNA polymerase II. Mol Cell Biol *20*, 2629-2634.

Radisky, D.C., and Bissell, M.J. (2007). NF-kappaB links oestrogen receptor signalling and EMT. Nat Cell Biol *9*, 361-363.

Radman-Livaja, M., and Rando, O.J. (2010). Nucleosome positioning: how is it established, and why does it matter? Dev Biol *339*, 258-266.

Rahl, P.B., Lin, C.Y., Seila, A.C., Flynn, R.A., McCuine, S., Burge, C.B., Sharp, P.A., and Young, R.A. (2010). c-Myc regulates transcriptional pause release. Cell *141*, 432-445.

Ramirez-Carrozzi, V.R., Braas, D., Bhatt, D.M., Cheng, C.S., Hong, C., Doty, K.R., Black, J.C., Hoffmann, A., Carey, M., and Smale, S.T. (2009). A unifying model for the selective regulation of inducible transcription by CpG islands and nucleosome remodeling. Cell *138*, 114-128.

Saccani, S., and Natoli, G. (2002). Dynamic changes in histone H3 Lys 9 methylation occurring at tightly regulated inducible inflammatory genes. Genes Dev *16*, 2219-2224.

Sarkar, S.N., Peters, K.L., Elco, C.P., Sakamoto, S., Pal, S., and Sen, G.C. (2004). Novel roles of TLR3 tyrosine phosphorylation and PI3 kinase in double-stranded RNA signaling. Nat Struct Mol Biol *11*, 1060-1067.

Saunders, A., Core, L.J., and Lis, J.T. (2006). Breaking barriers to transcription elongation. Nat Rev Mol Cell Biol *7*, 557-567.

Schones, D.E., Cui, K., Cuddapah, S., Roh, T.Y., Barski, A., Wang, Z., Wei, G., and Zhao, K. (2008). Dynamic regulation of nucleosome positioning in the human genome. Cell *132*, 887-898.

Semenza, G.L. (2003). Targeting HIF-1 for cancer therapy. Nat Rev Cancer *3*, 721-732.

Shaw, G., Morse, S., Ararat, M., and Graham, F.L. (2002). Preferential transformation of human neuronal cells by human adenoviruses and the origin of HEK 293 cells. FASEB J *16*, 869-871.

Shirakawa, F., Saito, K., Bonagura, C.A., Galson, D.L., Fenton, M.J., Webb, A.C., and Auron, P.E. (1993). The human prointerleukin 1b gene requires DNA sequences both proximal and distal to the transcription start site for tissue-specific induction. Mol Cell Biol *13*, 1332-1344.

Simonis, M., Kooren, J., and de Laat, W. (2007). An evaluation of 3C-based methods to capture DNA interactions. Nat Methods *4*, 895-901.

Smale, S.T. (2010). Selective transcription in response to an inflammatory stimulus. Cell *140*, 833-844.

Takeda, K., and Akira, S. (2005). Toll-like receptors in innate immunity. Int Immunol *17*, 1-14.

Tando, T., Ishizaka, A., Watanabe, H., Ito, T., Iida, S., Haraguchi, T., Mizutani, T., Izumi, T., Isobe, T., Akiyama, T.*, et al.* (2010). Requiem protein links RelB/p52 and the Brm-type SWI/SNF complex in a noncanonical NF-kappaB pathway. J Biol Chem *285*, 21951-21960.

Tannahill GM, C.A., Adamik J, Palsson-McDermott EM, Frezza C, Goel G, McGettrick AF, Bernard NJ, Zheng L, Kelly B, Gardet A, Clish C, Tong Z, Foley NH, Jany SS, Corr SC, Walmsley S, Beasley FC, Cummins E, Nizet V, Whyte M, Taylor CT, Masters SL, Lin H, Gottlieb E, Kelly V, Auron PE, Xavier RJ, and O'Neill LA (2013). Succinate is a danger signal from mitochondria that induces IL-1β transcription via HIF-1α. Nature, in press.

Tannahill, G.M., and O'Neill, L.A. (2011). The emerging role of metabolic regulation in the functioning of Toll-like receptors and the NOD-like receptor Nlrp3. FEBS Lett *585*, 1568-1572.

Thomas, M.C., and Chiang, C.M. (2006). The general transcription machinery and general cofactors. Crit Rev Biochem Mol Biol *41*, 105-178.

Tie, F., Banerjee, R., Stratton, C.A., Prasad-Sinha, J., Stepanik, V., Zlobin, A., Diaz, M.O., Scacheri, P.C., and Harte, P.J. (2009). CBP-mediated acetylation of histone H3 lysine 27 antagonizes Drosophila Polycomb silencing. Development *136*, 3131-3141.

Tsukada, J., Saito, K., Waterman, W.R., Webb, A.C., and Auron, P.E. (1994). Transcription factors NF-IL6 and CREB recognize a common essential site in the human prointerleukin 1 beta gene. Mol Cell Biol *14*, 7285-7297.

Tsukada, J., Yoshida, Y., Kominato, Y., and Auron, P.E. (2011). The CCAAT/enhancer (C/EBP) family of basic-leucine zipper (bZIP) transcription factors is a multifaceted highly-regulated system for gene regulation. Cytokine *54*, 6-19.

Unlu, S., Kumar, A., Waterman, W.R., Tsukada, J., Wang, K.Z., Galson, D.L., and Auron, P.E. (2007). Phosphorylation of IRF8 in a pre-associated complex with Spi-1/PU.1 and non-phosphorylated Stat1 is critical for LPS induction of the IL1B gene. Mol Immunol *44*, 3364-3379.

Van Antwerp, D.J., Martin, S.J., Kafri, T., Green, D.R., and Verma, I.M. (1996). Suppression of TNF-alpha-induced apoptosis by NF-kappaB. Science *274*, 787-789.

Wang, K.Z., Wara-Aswapati, N., Boch, J.A., Yoshida, Y., Hu, C.D., Galson, D.L., and Auron, P.E. (2006). TRAF6 activation of PI 3-kinase-dependent cytoskeletal changes is cooperative with Ras and is mediated by an interaction with cytoplasmic Src. J Cell Sci *119*, 1579-1591.

Wang, W., Deng, M., Liu, X., Ai, W., Tang, Q., and Hu, J. (2011). TLR4 activation induces nontolerant inflammatory response in endothelial cells. Inflammation *34*, 509-518.

Wang, X., Arai, S., Song, X., Reichart, D., Du, K., Pascual, G., Tempst, P., Rosenfeld, M.G., Glass, C.K., and Kurokawa, R. (2008). Induced ncRNAs allosterically modify RNA-binding proteins in cis to inhibit transcription. Nature *454*, 126-130.

Warburg, O., Wind, F., and Negelein, E. (1927). The Metabolism of Tumors in the Body. J Gen Physiol *8*, 519-530.

Weake, V.M., and Workman, J.L. (2010). Inducible gene expression: diverse regulatory mechanisms. Nat Rev Genet *11*, 426-437.

Webb, A.C., Auron, P.E., Rosenwasser, L.J., Mucci, S.F., Rich, A., Wolff, S.M., and Dinarello, C.A. (1985). Isolation and characterization of human interleukin-1 mRNA by molecular cloning. Brit J Rheum *24 (Suppl 1)*, 82-86.

Wu, C.H., Yamaguchi, Y., Benjamin, L.R., Horvat-Gordon, M., Washinsky, J., Enerly, E., Larsson, J., Lambertsson, A., Handa, H., and Gilmour, D. (2003). NELF and DSIF cause promoter proximal pausing on the hsp70 promoter in Drosophila. Genes Dev *17*, 1402-1414.

Wu, J.Q., and Snyder, M. (2008). RNA polymerase II stalling: loading at the start prepares genes for a sprint. Genome Biol *9*, doi:10.1186/gb-2008-1189-1185-1220.

Wu, X., and Brewer, G. (2012). The regulation of mRNA stability in mammalian cells: 2.0. Gene *500*, 10-21.

Xie, J., Crooke, P.S., McKinney, B.A., Soltman, J., and Brandt, S.J. (2008). A computational model of quantitative chromatin immunoprecipitation (ChIP) analysis. Cancer Inform *6*, 138-146.

Yamaguchi, Y., Inukai, N., Narita, T., Wada, T., and Handa, H. (2002). Evidence that negative elongation factor represses transcription elongation through binding to a DRB sensitivity-inducing factor/RNA polymerase II complex and RNA. Mol Cell Biol *22*, 2918-2927.

Yang, Z., Wara-Aswapati, N., Chen, C., Tsukada, J., and Auron, P.E. (2000). NF-IL6 (C/EBPbeta) vigorously activates il1b gene expression via a Spi-1 (PU.1) protein-protein tether. J Biol Chem *275*, 21272-21277.

Yik, J.H., Chen, R., Nishimura, R., Jennings, J.L., Link, A.J., and Zhou, Q. (2003). Inhibition of P-TEFb (CDK9/Cyclin T) kinase and RNA polymerase II transcription by the coordinated actions of HEXIM1 and 7SK snRNA. Mol Cell *12*, 971-982.

Yoshida, Y., Kumar, A., Koyama, Y., Peng, H., Arman, A., Boch, J.A., and Auron, P.E. (2004). Interleukin 1 Activates STAT3/Nuclear Factor-kB Cross-talk via a Unique TRAF6- and p65-dependent Mechanism. J Biol Chem *279*, 1768-1776.

Yoza, B.K., Hu, J.Y., and McCall, C.E. (2002). Inhibition of histone deacetylation enhances endotoxin-stimulated transcription but does not reverse endotoxin tolerance. J Endotoxin Res *8*, 109-114.

Zeitlinger, J., Stark, A., Kellis, M., Hong, J.W., Nechaev, S., Adelman, K., Levine, M., and Young, R.A. (2007). RNA polymerase stalling at developmental control genes in the Drosophila melanogaster embryo. Nat Genet *39*, 1512-1516.

Zhang, Y., Saccani, S., Shin, H., and Nikolajczyk, B.S. (2008). Dynamic protein associations define two phases of IL-1beta transcriptional activation. J Immunol *181*, 503-512.

Ziegler-Heitbrock, H.W., Wedel, A., Schraut, W., Strobel, M., Wendelgass, P., Sternsdorf, T., Bauerle, P.A., Haas, J.G., and Riethmuller, G. (1994). Tolerance to lipopolysaccharide involves mobilization of nuclear factor kappa B with predominance of p50 homodimers. J Biol Chem *269*, 17001-17004.

Zippo, A., Serafini, R., Rocchigiani, M., Pennacchini, S., Krepelova, A., and Oliviero, S. (2009). Histone crosstalk between H3S10ph and H4K16ac generates a histone code that mediates transcription elongation. Cell *138*, 1122-1136.

Zuckerman, S.H., Evans, G.F., and Butler, L.D. (1991). Endotoxin tolerance: independent regulation of interleukin-1 and tumor necrosis factor expression. Infect Immun *59*, 2774-2780.

APPENDICES

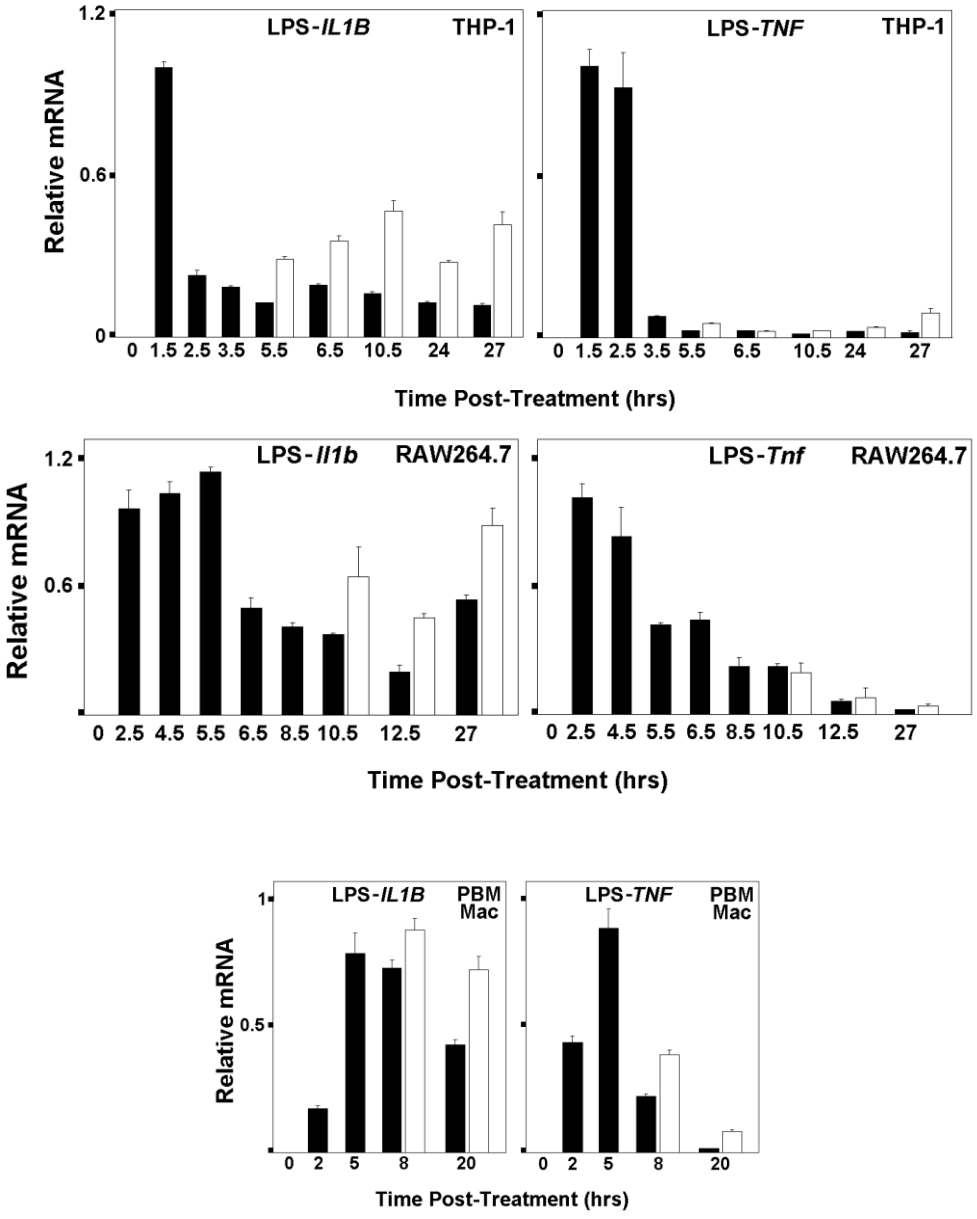

Appendix A. Comparison of *IL1B* and *TNF* Transcription in Monocytes

Steady-state mRNA kinetics for *IL1B* and *TNF* transcripts in LPS stimulated THP-1, RAW264.7, and hPBMCs. Transcript levels were normalized to beta 2-microtubulin (*B2M*), and then as ratio of amount in resting vs. LPS-treated cells. The mRNA dlevels for primary LPS challenge are represented as black bars. White bars show transcript levels following re-stimulation.

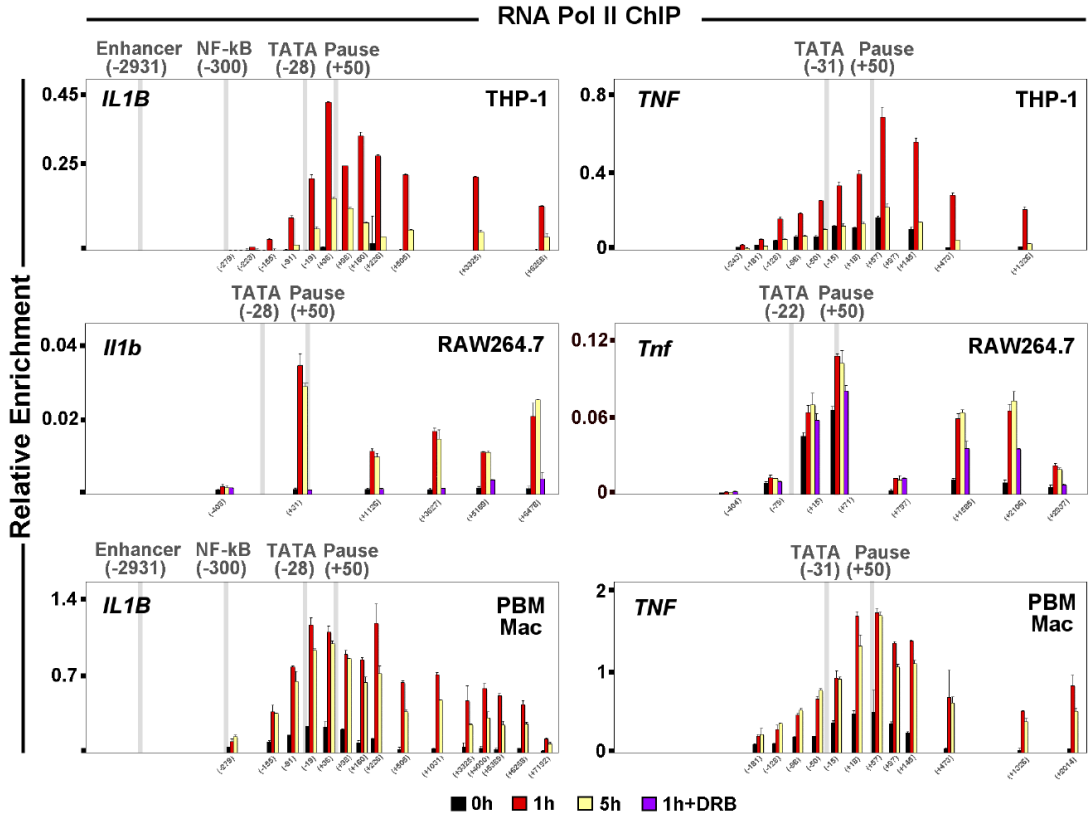

Appendix B. Pol II occupancy at the *il1b* and *tnf* loci.

Pol II ChIP throughout the *IL1B* and *TNF* loci in resting (black bars), 1h (red bars), and 5h (yellow bars) LPS stimulated THP-1, RAW264.7, and hPBMC cells. Vertical gray bars locate the positions of important gene *landmarks*. Numbers at the bottom of the figures denote positions relative to the TSS. These include TATA box and the canonical Pol II pause position (approximately 30 bp upstream and 50 bp downsteam of TSS, respectively).

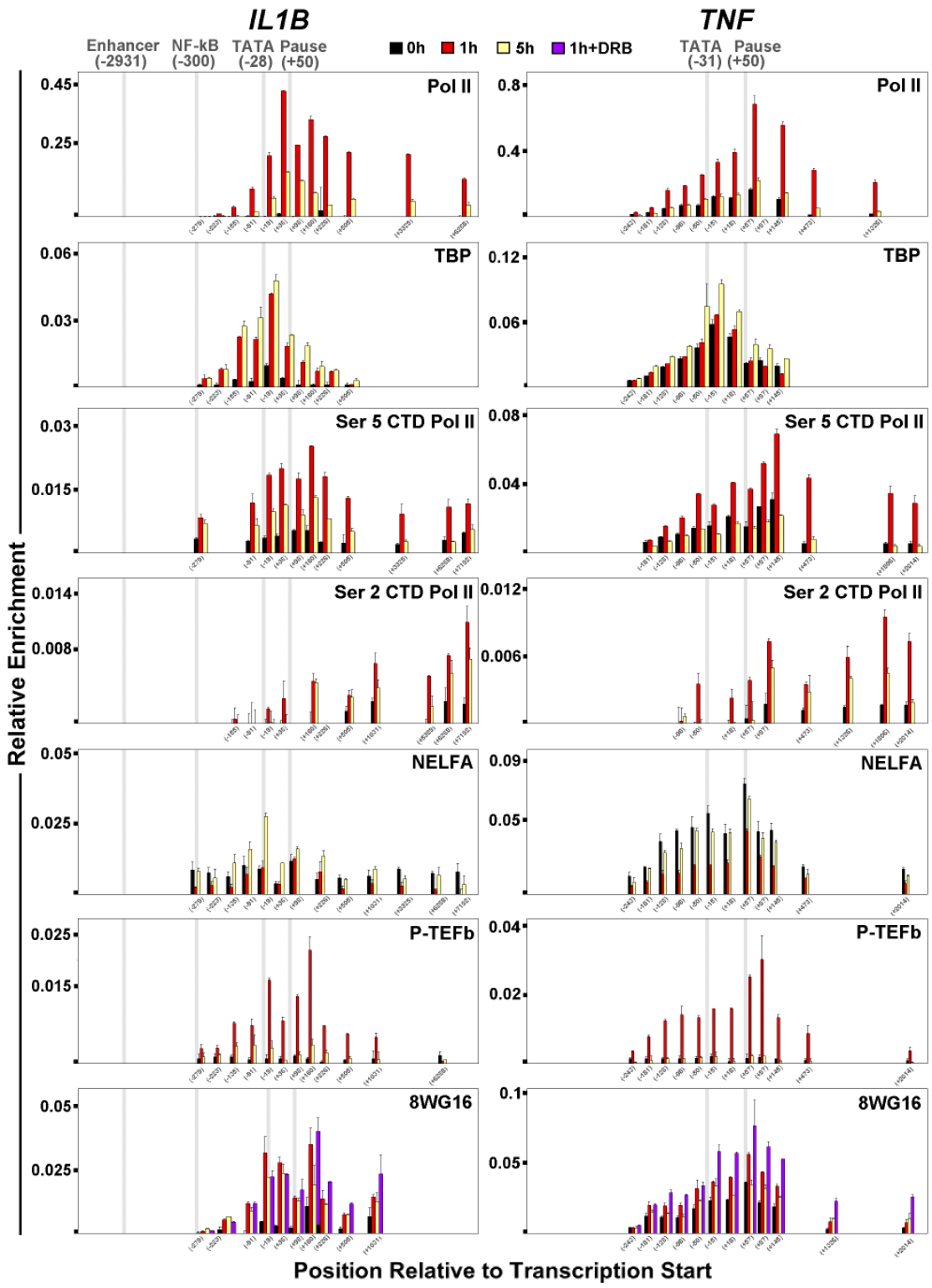

Appendix C. Distribution of factors relevant to differential transcriptional regulation.

ChIP for factors related to Pol II initiation and elongation at *IL1B* and *TNF* loci in THP-1 cells were measured at distinct time points in resting (black bars), 1h (red bars) and 5h (yellow bars) LPS stimulated THP-1 cells. Enrichment profiles for TBP, S5P CTD Pol II, S2P CTD Pol II, NELF, P-TEFb and Pol II (using alternative 8WG16 antibody) are shown. A purple bars in the 8WG16 (bottom panels) experiment represents a 1-hour time point, in which THP-1 cells were pre-treated with the P-TEFb inhibitor 5,6-dichloro-1-beta-D-ribofuranosylbenzimidazol (DRB) prior to stimulation with LPS.

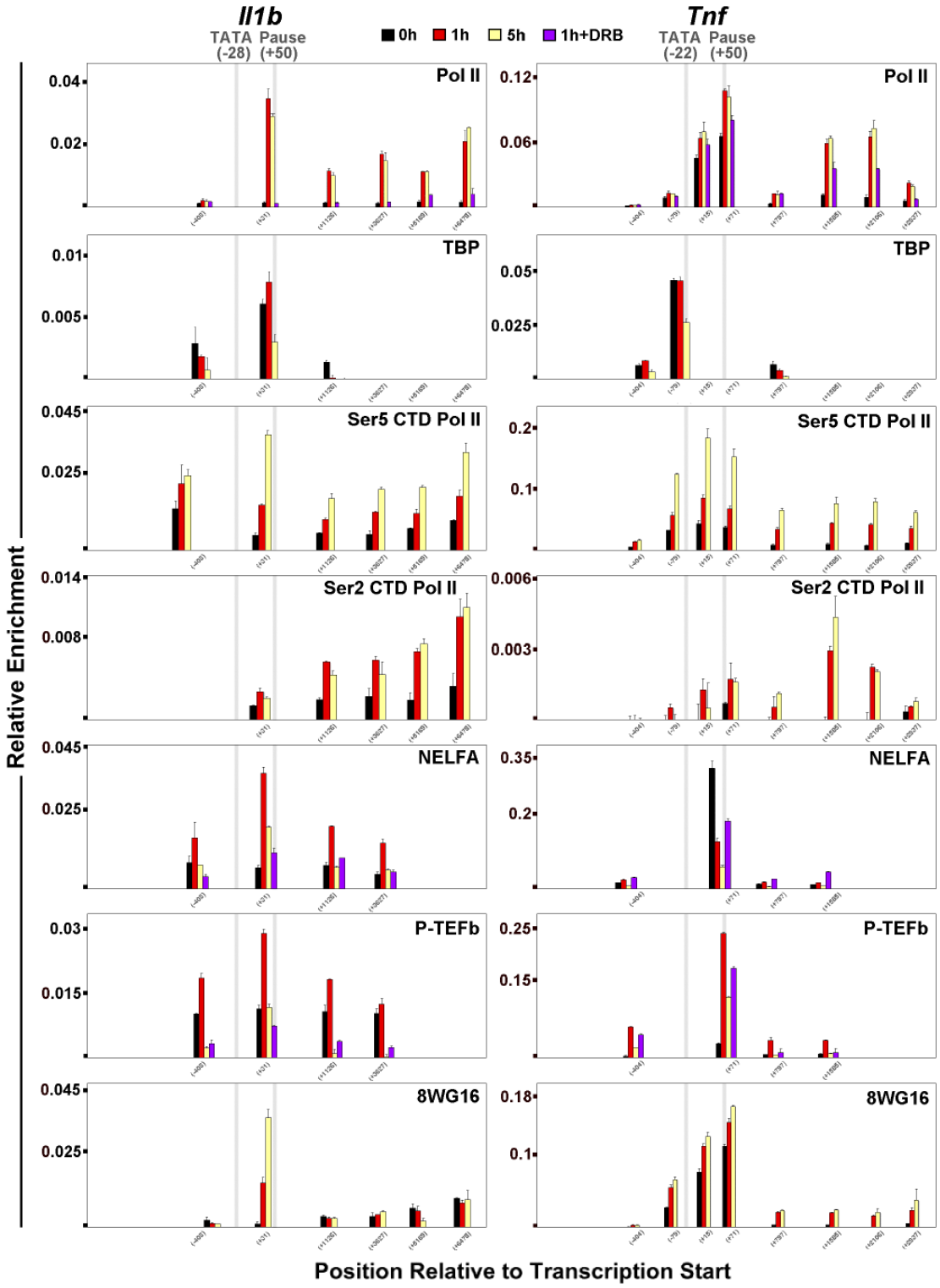
Il1b
TATA Pause
(-28) (+50)
0h
1h
5h
1h+DRB
Tnf
TATA Pause
(-22) (+50)
Pol II
TBP
Ser5 CTD Pol II
Ser2 CTD Pol II
NELFA
P-TEFb
8WG16
Relative Enrichment
Position Relative to Transcription Start

Appendix D. Average profiles of factors relevant to differential transcriptional regulation in LPS-treated RAW264.7 cells.

ChIP for factors related to Pol II initiation and elongation at *Il1b* and *Tnf* loci in RAW264.7 cells were measured at distinct time points in resting (black bars), 1h (red bars) and 5h (yellow bars) LPS stimulated THP-1, cells. Enrichment profiles for Pol II, TBP, S5P CTD Pol II, S2P CTD Pol II, NELF, P-TEFb and Pol II (using alternative 8WG16 antibody) are shown. A purple dotted line in the 8WG16 (bottom panels) experiment represents a 1-hour time point, in which RAW264.7 cells were pre-treated with the P-TEFb inhibitor 5,6-dichloro-1-beta-D-ribofuranosylbenzimidazol (DRB) prior to stimulation with LPS.

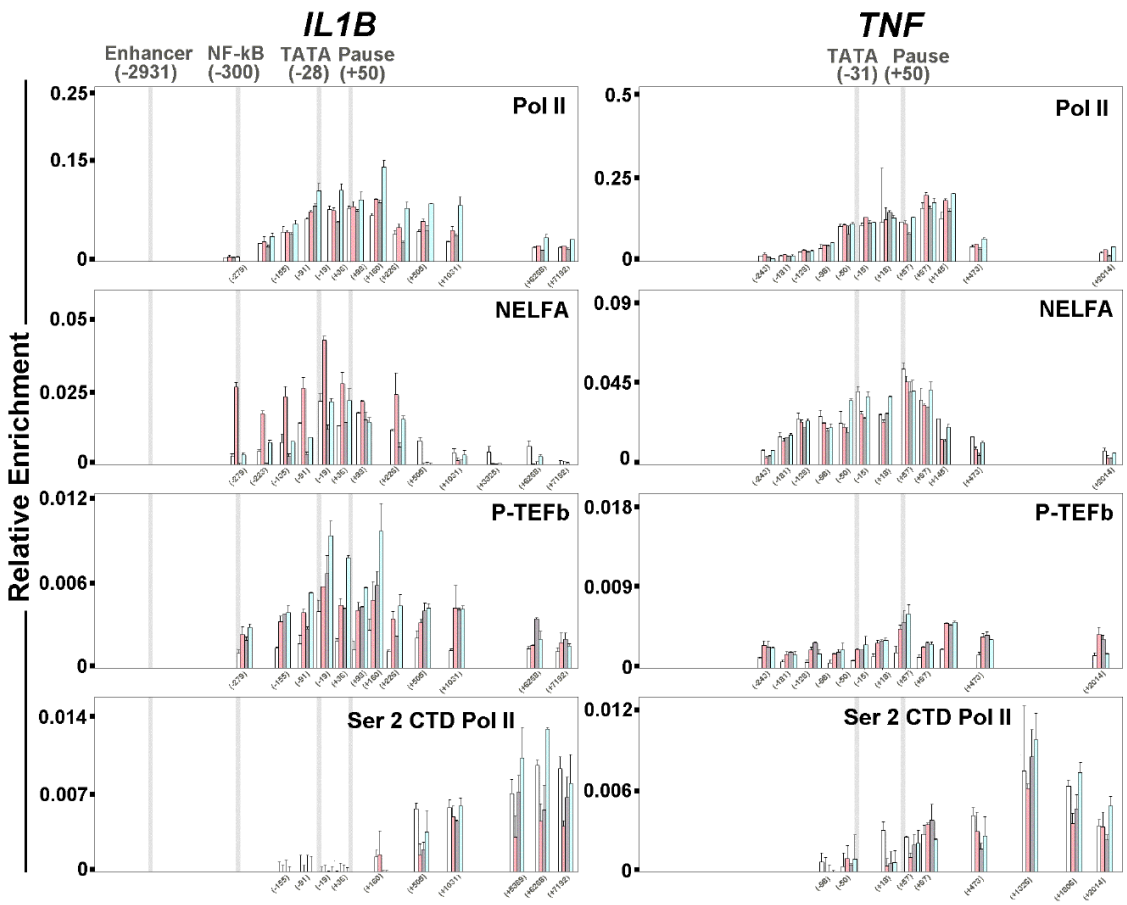

Appendix E. ChIP re-stimulation experiments at 25 hours.

ChIP for S2P CTD Pol II, NELF, P-TEFb, and Pol II at the *IL1B* and *TNF* during secondary LPS stimulation of THP-1 cells. The white and gray bars denote ChIP data for primary LPS challenge harvested at 13 and 25 hours post simulation respectively. The pink and light green bars show ChIP data for THP-1 cells that were initially treated for 13 and 24 hours respectively with LPS, and subjected to a re-stimulation for an hour prior to their fixation and harvest. Equal dosage of LPS (1 μg/ml) was used in both, primary and secondary stimulation experiments.

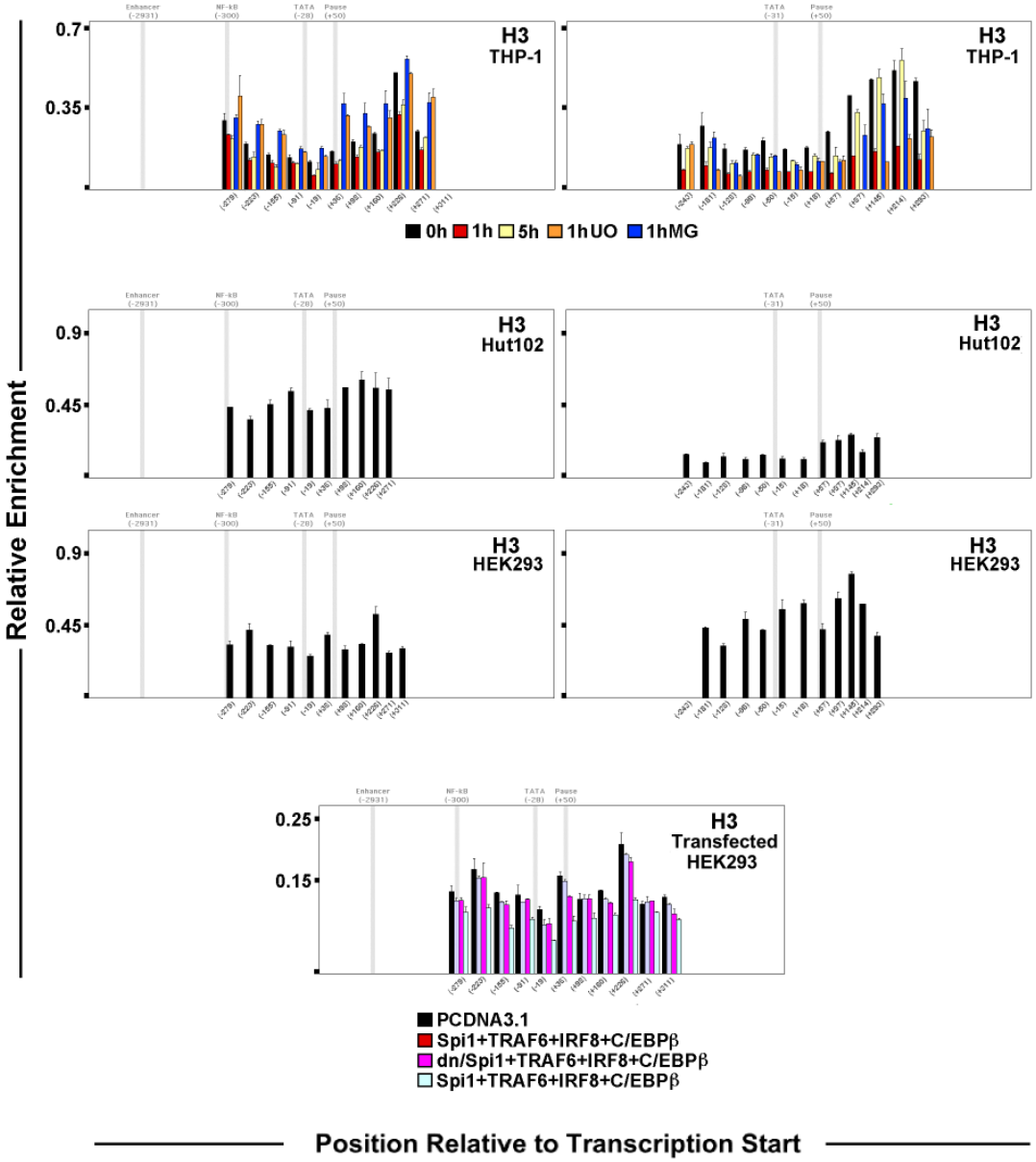

Appendix F. Nucleosome positioning dynamics during *IL1B* and *TNF* induction.

In the top panels are depicted spatial and kinetic histone 3 (H3) ChIP data for *IL1B* and *TNF* in resting (black bars), 1h (red bars), and 5h (yellow bars) stimulated THP-1 cells. The blue bars represent H3 ChIP for THP-1 cells pre-treated with the NF-κB inhibitor MG132 and the orange bars denote the U0126 (C/EBPβ inhibitor) treated THP-1 cell samples. The middle panels reveal H3 occupancy throughout the *IL1B* and *TNF* in Hut102 and HEK293 cells. Bottom panel indicates H3 ChIP for 293 cells transfected with indicated transcription factors.

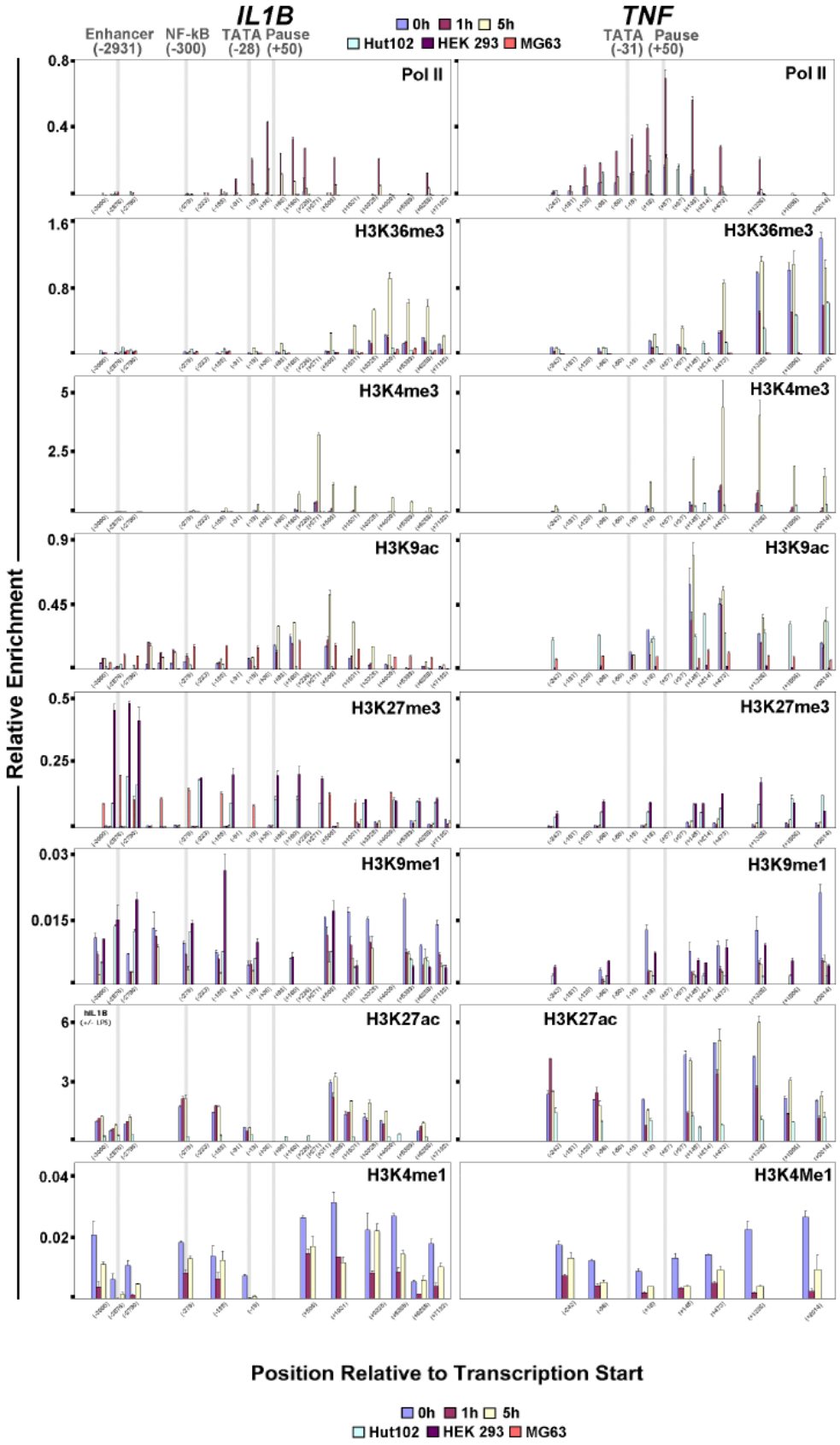
IL1B
Enhancer (-2931)
NF-kB (-300)
TATA (-28)
Pause (+50)
0h 1h 5h
Hut102 HEK 293 MG63
TNF
TATA (-31)
Pause (+50)
Pol II
H3K36me3
H3K4me3
H3K9ac
H3K27me3
H3K9me1
H3K27ac
H3K4me1
H3K4Me1
Relative Enrichment
Position Relative to Transcription Start

Appendix G. Summary of the histone modification ChIP profiles for *IL1B* and *TNF* in THP-1, HEK 293, Hut102, and MG63 cells.

Illustrated are the summary profiles comparing nucleosome modifications for resting (black bars), 1h (red bars), and 5h (yellow bars) LPS-treated human THP-1 cells with untreated HEK293 pre-neuronal cells (purple bars), Hut102 cutaneous T lymphocytes (light blue bars), and MG63 osteoblastic cells (orange bars). Depicted are spatial and kinetic ChIP profiles for Pol II, H3K36me3, H3k4me3, H3K9ac, and H3K27me3, H3K9me1, H3K27ac, and H3K4me1 for *IL1B* and *TNF*. All panels are similarly scaled with respect to spatial distribution along each gene, permitting comparative localization.